Morphology and ultrastructure of external sense organs of *Drosophila* larvae

Vincent Richter[1], Anna Rist[2], Georg Kislinger[2], Michael Laumann[3], Andreas Schoofs[4], Anton Miroschnikow[4], Michael Pankratz[4], Albert Cardona[5], Andreas S. Thum[1,2,6*]

[1] Department of Genetics, Leipzig University, Institute for Biology, Leipzig, Germany

[2] Department of Biology, University of Konstanz, Konstanz, Germany

[3] Electron Microscopy Center, University of Konstanz, Konstanz, Germany

[4] Department of Molecular Brain Physiology and Behavior, LIMES Institute,

University of Bonn, Bonn, Germany

[5] Department of Physiology, Development and Neuroscience, University of

Cambridge, Cambridge, United Kingdom

[6] German Centre for Integrative Biodiversity Research (iDiv) Halle-Jena-Leipzig, Leipzig, Germany

* corresponding author: andreas.thum@uni-leipzig.de

KEYWORDS

sensory system, sensillum, dorsal organ, ventral organ, labial organ, keilin's organ

ABSTRACT

Sensory perception is the ability through which an organism is able to process sensory stimuli from the environment. This stimulus is transmitted from the peripheral sensory organs to the central nervous system, where it is interpreted. *Drosophila melanogaster* larvae possess peripheral sense organs on their head, thoracic, and abdominal segments. These are specialized to receive diverse environmental information, such as olfactory, gustatory, temperature or mechanosensory signals. In this work, we complete the description of the morphology of external larval sensilla and provide a comprehensive map of the ultrastructure of the different types of sensilla that comprise them. This was achieved by 3D electron microscopic analysis of partial and whole body volumes, which contain high-resolution and complete three-dimensional data of the anatomy of the sensilla and adjacent ganglia.

Our analysis revealed three main types of sensilla on thoracic and abdominal segments: the papilla sensillum, the hair sensillum and the knob sensillum. They occur solitary or organized in compound sensilla such as the thoracic keilin's organ or the terminal sensory cones. We present a spatial map defining these sensilla by their position on thoracic and abdominal segments. Further, we identify and name the sensilla at the larval head and the last fused abdominal segments. We show that mechanosensation dominates in the larval peripheral nervous system, as most sensilla have corresponding structural properties. The result of this work, the construction of a complete structural and neuronal map of the external larval sensilla, provides the basis for following molecular

and functional studies to understand which sensory strategies the *Drosophila* larva employs to orient itself in its natural environment.

INTRODUCTION

Drosophila melanogaster larvae have become a favored model organism for studying the principles of sensory perception (reviewed in (Gerber und Stocker 2007; Melcher et al. 2007; Apostolopoulou et al. 2015; Joseph und Carlson 2015; Rimal und Lee 2018; Widmann et al. 2018; Thum und Gerber 2019)). It has been shown that larvae actively use sensory cues of different modalities to navigate through their environment. Thermo-, photo-, chemo-, and mechanosensory information is perceived and processed by the larvae's peripheral nervous system to optimize their behavior output for favorable conditions (e.g., to find food sources) and to avoid unpleasant or even harmful situations (e.g., predators and deterrent or toxic substances) (Tracey et al. 2003; Gomez-Marin und Louis 2012; Apostolopoulou et al. 2014; Klein et al. 2015; Ohyama et al. 2015; Scholz et al. 2015; Apostolopoulou et al. 2016; Choi et al. 2016; Croset et al. 2016; Ni et al. 2016; van Giesen et al. 2016; Humberg et al. 2018; Tastekin et al. 2015).

An increasing number of studies investigating the neuronal and molecular basis of larval sensory perception has even enabled the identification of the respective sensory cells and receptors for distinct stimuli. Among others, this includes a distinct set of olfactory receptors (Or) (Fishilevich et al. 2005; Kreher et al. 2005), gustatory receptors (Gr), ionotropic receptors (Ir), pickpocket receptors (ppk), transient receptor potential (TRP) channels and rhodopsins (Rh). Some receptor genes have been associated with specific sensory functions, for instance Gr43a (fructose) (Mishra et al. 2013), Gr28a (ribonucleosides and RNA) (Mishra et al. 2018), Gr33a, Gr66a and Gr97a (quinine) (Apostolopoulou et al. 2014), Gr33a, Gr66a and Gr93a (caffeine) (Apostolopoulou et al. 2016), Ir76b (amino acids) (Croset et al. 2016), Ir25a (denatonium) (van Giesen et al. 2016), ppk11 and ppk19 (low salt) (Liu et al. 2003; Alves et al. 2014), ppk23 and ppk29 (pheromones) (Mast et al. 2014), painless and ppk (noxious heat) (Tracey et al. 2003), ppk and piezo (noxious mechanical stimuli) (Zhong et al. 2010; Kim et al. 2012)), dCIRL and nompC (mechanosensation) (Scholz et al. 2015; Scholz et al. 2017; Yan et al. 2013), Ir68a, Ir93a, Ir25a, and Ir21a (temperature) (Klein et al. 2015; Ni et al. 2016; Hernandez-Nunez et al. 2021), and Rh5 and Rh6 (vision) (Humberg et al. 2018). This sensory description is complemented by a large-scale electron microscopic reconstruction of the larval brain (Winding et al. 2022). The reconstruction characterizes at the cellular and synaptic level the sensory inputs and initial information processing steps for the olfactory antennal lobe (Berck et al. 2016), the optic neuropil (Larderet et al. 2017), the gustatory subesophageal zone (Miroschnikow et al. 2018) and the nociceptive and mechanosensory brain centers (Ohyama et al. 2015; Jovanic et al. 2016; Takagi et al. 2017; Burgos et al. 2018; Jovanic et al. 2019; Masson et al. 2020).

Despite these advances, the structural basis of sensory perception in *Drosophila* larvae is far from fully elucidated because electron microscopic reconstruction is still limited to the central nervous system. A comparable analysis for the entire peripheral nervous system is not available.

Still, most knowledge on the ultrastructure of larval sensory organs and their sensilla derives from studies of different dipteran species carried out mostly during the 1970s and 1980s (Hertweck 1931; Thurm 1964; Chu und Axtell 1971; Chu-Wang und Axtell 1972a, 1972b; Zacharuk 1972; Denell und Frederick 1983; Campos-Ortega und Hartenstein 1985; Dambly-Chaudière und Ghysen 1986; Whittle et al. 1986; Honda und Ishikawa 1987; Lanfranchi und Belcari 1990; Keil 1997). Most of this work was done on different developmental stages of dipteran larvae using different methodical

approaches. Current attempts to understand the relationship between the structure and function of larval sensory organs of *Drosophila* are therefore hampered by an anatomical description that, on the one hand, is detailed for specific aspects and species but, on the other hand, has gaps for the *Drosophila* larva that are only indirectly addressed from anatomical results of different fly species.

To overcome this limitation and gain precise knowledge of peripheral sensory organ ultrastructure, we have recently analyzed the anatomy of the terminal organ (TO) of the *Drosophila* larva, its major external taste organ (Rist und Thum 2017). This was possible by taking advantage of technical improvements in volume electron microscopy. In particular, we used focused ion beam scanning electron microscopy (FIB-SEM) to gain precise, three-dimensional reconstructions of each of the 14 external sensilla of the TO. FIB-SEM can automatically generate serial images of ultrastructure with superior z-resolution compared to other common volume EM techniques. Extremely thin layers of the specimen are ablated by an ion beam and an image is taken by the SEM after each removed layer (Helmstaedter et al. 2011; Peddie und Collinson 2014). A more "classic" approach is serial section scanning transmission electron microscopy (ssTEM). In this approach, ultrathin sections of the complete sample are created and then scanned using transmission electron microscopy. These methods have increasingly been used to obtain 3D representations of cellular and even subcellular structures at high resolution (Peddie und Collinson 2014; Titze und Genoud 2016).

Using partial larval 3D volumes based on FIB-SEM and a full larval body volume established via the ssTEM technique (serial sections imaged with a TEM in scanning mode) (Schoofs et al. 2023), we have now analyzed the anatomy of the remaining three major head sensory organs, the dorsal organ (DO), the ventral organ (VO), and the labial organ (LO) at ultra-resolution. The three peripheral sensory organs are known to be formed by several sensilla (Hertweck 1931; Chu und Axtell 1971; Chu-Wang und Axtell 1972b; Kankel 1980; Singh und Singh 1984; Python und Stocker 2002). The DO was proven to be the primary larval olfactory organ based on anatomical, molecular and functional experiments (Chu und Axtell 1971; Singh und Singh 1984; Heimbeck et al. 1999; Oppliger et al. 2000; Python und Stocker 2002; Fishilevich et al. 2005; Kreher et al. 2005). Its prominent "dome" houses 21 olfactory receptor neurons organized in seven triplets that respond to different sets of odors. Less is known about the six peripheral sensory sensilla and their additional roles in thermosensation (Klein et al. 2015; Ni et al. 2016; Hernandez-Nunez et al. 2021) and putatively mechano- and taste sensation (Chu und Axtell 1971; Singh und Singh 1984; Python und Stocker 2002). The VO and the LO are comparatively small sensory organs and have been little noticed in larval anatomical or functional studies (Chu-Wang und Axtell 1972b; Python und Stocker 2002; Miroschnikow et al. 2018). They are assumed to serve a mechanosensory and/or gustatory function.

Another focus of our work was to describe the morphology and ultrastructure of the external sensory organs of the thoracic and abdominal segments. A comparatively simple organization was reported for these. The majority of them consisted of only one sensillum, which was described to be either of the campaniform, basiconic or trichoid type (Kankel 1980; Singh und Singh 1984; Campos-Ortega und Hartenstein 1985; Hartenstein 1988; Campos-Ortega und Hartenstein 1997). Other studies, however, called campaniform sensilla papilla or pit sensilla. Trichoid sensilla were also called hair sensilla. For the basiconic sensilla, the nomenclature is most diverse, as these are called koelbchen, knob, knob-in-pit, hair-type B, sensory papillae, dorsal or ventral pit, or black sensory organ (Hertweck 1931; Dambly-Chaudière und Ghysen 1986; Singh und Singh 1984; Rist und Thum 2017; Singh 1997; Kankel 1980; Lohs-Schardin et al. 1979; Hartenstein 1988; Sato und Denell 1985; Lewis 1978; Campos-Ortega und Hartenstein 1985). In addition, not all sensilla are described and named

in the fused first head and last abdominal segments (Schmidt-Ott et al. 1994; Courtney et al. 2000; Wipfler et al. 2013). Accurate classification and nomenclature of the different types of sensilla throughout the larval body – as applied in this work - will therefore be useful for future anatomical and functional studies.

RESULTS

Proper classification of sensilla requires investigation of their external and internal morphology. However, the ultrastructure of scattered and small insect sensilla, like that of *Drosophila* larvae, is challenging to investigate. Fortunately, recent advances in EM technique made it possible to image large regions of tissue, like the entire central nervous system of larval (Ohyama et al. 2015; Schlegel et al. 2016; Carreira-Rosario et al. 2018; Miroschnikow et al. 2018; Winding et al. 2022) and adult *Drosophila melanogaster* (Zheng et al. 2018; Scheffer et al. 2020; Schlegel et al. 2023), *Caenorhabditis elegans* (White et al. 1986; Cook et al. 2019), *Ciona intestinalis* (Ryan et al. 2016) and the larva of *Platynereis dumerilii* (Verasztó et al. 2020), as well as parts of the brain of P*ristionchus pacificus* (Bumbarger et al. 2013; Hong et al. 2019) and rodents (Denk und Horstmann 2004; Helmstaedter et al. 2013; Motta et al. 2019). In this data we reconstructed the external sensory sensilla in a full body first instar EM volume (Schoofs et al. 2023) and in volumes of single sensilla of third instar larvae obtained by FIB-SEM. For single sensilla imaging, accuracy and precision are required which are often difficult to realize technically. In order to achieve these technical demands, we took advantage of FIB-SEM in combination with an optimized preparation protocol. This allowed us to exactly target even the smallest sensilla on the larval body wall for subsequent serial slicing and imaging by FIB-SEM (for details, see supplementary Figure S1).

Structural organization of *Drosophila* larvae

The body of *Drosophila* larvae is divided into segments (Figure 1A): a pseudocephalon (Pce, from now on called "head", Figure 1A'), three thoracic (T1-T3) and nine abdominal (A1-A9) segments (Campos-Ortega und Hartenstein 1997). The head is the strongly reduced head capsule of the larva, dorsally fused with and partially retracted in the prothorax (Courtney et al. 2000; Wipfler et al. 2013). The last abdominal segment, A8, is more appropriately named "anal division" as it is formed by the fusion of at least two abdominal segments A8 and A9 (Figure 1A'').

The largest sense organs of *Drosophila* larvae are arranged in pairs on the right and left side of the head (Figure 1A, inset left bottom). The DO and the TO are prominently located on the tip of the head lobes (Chu und Axtell 1971; Chu-Wang und Axtell 1972a; Singh und Singh 1984; Heimbeck et al. 1999; Oppliger et al. 2000; Python und Stocker 2002; Fishilevich et al. 2005; Kreher et al. 2005; Rist und Thum 2017). The VO and the LO are smaller and their ultrastructure has rarely been studied (Hertweck 1931; Kankel 1980). The VO is situated ventral to the DO/TO complex on the front of the larval head hidden behind rows of cuticle cirri (Figure 1A', Figure 8B). The LO is inconspicuously located below the larval mouth opening (Figure 1A', Figure 9B). In this work, we describe the morphology of the DO, VO, and LO each in a specific result section and present a conclusive nomenclature of their sensilla (Figure 2-9, Table 1). The detailed morphology of the TO was described in our previous work (Rist und Thum 2017). The anatomical data is therefore not shown again. However, its morphology is part of Table 1 to complement the description of the external head sensory organs.

Sensory organs located on the thoracic and abdominal segments are of simpler organization mostly consisting of only one sensillum (Figure 1B). Different names have been given to these sensilla (Table

2). In the present work, we identified three basic types of thoracic and abdominal sensilla and refer to them as papilla (p), hair (h) and knob (k) sensilla (Figure 1B, 10, 11, 13, Table 2). This nomenclature corresponds to the one of Dambly-Chaudière and Ghysen (1986), which is most consistent with our findings. Please note that we have translated their term "kölbchen sensilla" into English as "knob sensilla". The term knob or knob-in-pit sensillum was already used in previous studies (Singh und Singh 1984; Rist und Thum 2017; Singh 1997). It allows us to use the same abbreviation (e.g. vk for ventral knob sensillum), which also allows for comparison with these studies. We are aware that the term papilla sensilla is questionable, as the outer and inner morphology resembles the one of the spot sensilla we found in the TO in our previous work (Rist und Thum 2017). The term papilla sensilla is based on findings in light microscope data and does not describe the outer morphology appropriately. Nevertheless, renaming these sensilla would be inconvenient for the comprehension and comparability with already published data and would make it necessary to use different abbreviations.

Papilla, hair and knob sensilla are in some studies called campaniform, trichoid, and basiconic sensilla, respectively (Hartenstein 1988; Campos-Ortega und Hartenstein 1997; Green und Hartenstein 1997). Of course, these terms also have their validity and are therefore listed in Table 1. However, since in our view these terms were structurally more difficult to assign and could lead to confusion from a functional point of view, we prefer the former. Trichoid sensilla in the adult olfactory system of *Drosophila* express odorant receptor genes and thus exert a chemosensory function (Couto et al. 2005; Miller und Carlson 2010; van Goes Naters und Carlson 2007). In contrast, any potential larval trichoid sensilla most-likely have only a mechanosensory function due to their ultrastructure.

In general, most external sensilla are arranged along the vertical (dorso-ventral) axis close to the middle of each segment (Figure 1B). In accordance with previous studies (Lohs-Schardin et al. 1979; Dambly-Chaudière und Ghysen 1986; Green und Hartenstein 1997), we found a stereotypic and fixed pattern of these sensilla. This structural consistency allowed us to generate a spatial map defining each sensillum and sense organ on the larval body by their precise position (Figure 1B). Furthermore, we were able to find the associated sensory and accessory (support) cells (Figure 1C). The spatial pattern and abundance of types of sensilla differ between segments. We noticed varying arrangements for T1, T2-T3, and A1-A7, with a consistent sequence of sensilla in each configuration. The head and the last abdominal segments represent unique cases with specialized sense organs like the terminal sensory cones (t) (Singh und Singh 1984; Dambly-Chaudière und Ghysen 1986).

Papilla sensilla are most abundant in terms of number. We counted six papilla sensilla on the head, ten papilla sensilla on T1, seven on T2-T3, and nine on A1-A7 (Figure 1B and Figure 10). Additionally, we find one papilla sensillum in the terminal sensory cone t_1 of segment A8/A9. Please note that the numbers are given per hemisegment, which is true for all sensilla but the unpaired ventral papilla sensillum (vas). We found three hair sensilla on T1-T3 and four hair sensilla on A1-A7, including the two hair sensilla h_3 and h_4 of the double hair organ (Figure 1B, Figure 11-12). Four hair sensilla are organized in the terminal sensory cones t_1, t_2, t_4 and t_6 in segment A8/A9. The KO is exclusively found on thoracic segments and is situated on the ventral side of each hemisegment of T1 -T3 (Figure 1B and Figure 14). Knob sensilla are found on the thoracic segments but also in the TO of the head and in the terminal sensory cones, although the number of neurons innervating these knob sensilla differs from one to three (Figure 1C, 13, 16). Two knob sensilla are restricted to the TO (Figure 16G) and T1 - T3 (Figure 1B and Figure 13). In A8/A9 we find five knob sensilla in the terminal sensory cones t_1,

t_2, t_3, t_5 and t_7. In addition, we find the spiracle sense organ on the last segment, which consists of four papilla-like sensilla located at the posterior spiracle. This sensilla configuration is based on the single ssTEM and various SEM scans we compared with published data (Lohs-Schardin et al. 1979; Dambly-Chaudière und Ghysen 1986; Green und Hartenstein 1997).

In the following, sense organs and sensilla of the larval head, thoracic and abdominal segments are classified based on their external and internal morphology. Also, developmental aspects are addressed by comparison of first (L1) and third instar (L3) larvae.

Description of individual external sensory organs of the *Drosophila* larva

DORSAL ORGAN

Despite previous studies on the ultrastructure of the DO (Chu und Axtell 1971; Singh und Singh 1984), many aspects of its structural organization, like the peripheral sensilla and the corresponding accessory cells (ACs), remained unclear. The 3D EM volumes recorded in the present work allow to complement and clarify the knowledge on the anatomy of the DO (Figure 2-7, Table 1). Figures 2-7 provide a comprehensive description of the organization of the entire organ. Therefore, by means of targeted FIB-SEM and ssTEM, we obtained continuous image stacks of the DO covering the distance from its outer sensory parts to the region of the DO ganglion (DOG), where the cell bodies of the sensory neurons are located. It enabled us to trace dendrites from their tips at the cuticle surface to the neuron's cell body in the DOG and to generate a 3D reconstruction visualizing the spatial organization of the neuronal components of the DO (Figure 2A, C). Furthermore, accessory support cells were identified and described in detail (Figure 7). Most sensilla display a repertoire of these cells in a highly stereotyped fashion: a thecogen, a trichogen and a tormogen cell. Due to their role in the formation of the sensillum, they have also been termed sheath, shaft and socket cell, respectively (Prelic et al. 2021).

The DO is the primary olfactory organ of the larva. Its central structure is the dome (Figure 2B-E), which comprises seven olfactory sensilla with three dendrites each (Figure 3B-F), as reported in the literature (Chu und Axtell 1971; Singh und Singh 1984). Olfactory dendrites branch multifold in the dome region of the DO and connect to pore tubules spanning the outer cuticle, each leading to one of the tiny pores perforating the dome (Figure 2B, D, E). Apart from these tiny pores, the dome is interspersed with seven larger pores arranged in a circle (Figure 2B, D). In contrast to L3, these pores are missing in L1 larvae (Figure 2E), which suggests that these are molting pores formed during ecdysis when olfactory sensory neurons pass through the developing cuticle of the new DO. The seven olfactory triplets are housed in a common outer sensillum lymph space, which is built by the ACs (Figure 3B, C, E and Figure 7). In the outer lymph space, the triplets are enclosed by a dendritic sheath (Figure 3G), which is most likely segregated by the thecogen cell (Figure 7). Further distal, the three olfactory dendrites are bathed in a small inner sensillum lymph cavity enclosed by the thecogen cell (Figure 3D, F), also called the perineuronal lumen (Prelic et al. 2021). Inside the cavity lays the ciliary constriction (cc), which marks the transition from the outer dendritic segment (ods) to the inner dendritic segment (ids) (Figure 3G).

All cell bodies of DO sensory neurons lie in the dorsal organ ganglion (DOG), in which the soma of olfactory receptor neurons (ORNs) are located more to the center compared to those of the peripheral sensilla (Figure 2A, C). The cell bodies of neurons innervating individual peripheral sensilla lie adjacent (Figure 2A, C). Cell bodies of olfactory neurons appear elliptically shaped and are relatively large compared to peripheral neurons' cell bodies, which have a roundish appearance and

are smaller in diameter (Figure 2F, G). Also located within the DOG are additional cell bodies of the sensory cells of the papillum sensillum of the dorsolateral group of the TO (Pdo), seven additional non-sensory cells of unknown function but most likely glial cells and one sensory cell of the papilla sensillum (p6) in close proximity to the DO. Their cell bodies lie in the proximal end of the DOG from where they wrap around the whole ganglion.

The six peripheral sensilla lie in the rim between the dome and the surrounding cuticle ridge. They are not visible by external investigation (Figure 2B and Figure 3B, C). The outer cuticle part of all six peripheral sensilla appears similar in its structure. Its organization is very simple, consisting of a small cuticle bulge with a tiny pore in its center (Figure 3C). The pore is first surrounded by a short cuticle channel that leads to the dendrites (Figure 3C). Remarkably, the pores are absent in L1 larvae (Figure 3B) and are therefore most likely molting pores. Internally, however, peripheral sensilla have different structural properties (Figure 4 and Figure 5).

The spatial arrangement of the peripheral sensilla was consistent in all analyzed samples. This stereotypical pattern allowed us to number the peripheral sensilla DO_{p1} to DO_{p6} (dorsal organ peripheral sensilla 1 to 6). DO_{p1} is the posterior most sensillum. The six DO_p were numbered from 1 to 6 in a clockwise direction in the left and anti-clockwise direction in the right hemisphere when seen from above (see supplement Figure S2).

Within these six sensilla, we find three structurally similar types (type 1: DO_{p1}; type 2: DO_{p2} and DO_{p4}; type 3: DO_{p3}, DO_{p5}, and DO_{p6}; see Table 1). DO_{p1} is characterized by a single dendrite with a tubular body that terminates at the base of the epicuticle (Figure 4B, C). DO_{p2} and DO_{p4} can be identified by the presence of two dendrites; one (DO_{p2A} and DO_{p4A}) ends with a tubular body, the other one (DO_{p2B} and DO_{p4B}) not (Figure 4D-G). Both dendrites are enclosed by a common dendritic sheath. Similar to the olfactory neurons, $DO_{p1/2/4}$ dendrites are bathed in a small inner sensillum lymph space which is enclosed by the thecogen cell (Figure 4C, E, G). DO_{p3}, DO_{p5} and DO_{p6} share a similar structural organization and house two dendrites each (Figure 5F, G). DO_{p3A}, DO_{p5A} and DO_{p6A} end below the epicuticle and are enclosed by a dendritic sheath (Figure 5B, C). DO_{p3B}, DO_{p5B} and DO_{p6B} end inside the inner sensillum lymph space.

The dendrites of DO_{p3}, DO_{p5} and DO_{p6} form the ciliary constriction inside an inner sensillum lymph cavity, like other DO sensilla. $DO_{p3/5/6\text{-}A}$ have a small dendritic outer and a larger dendritic inner segment like canonical receptor neurons. In contrast, $DO_{p3/5/6\text{-}B}$ are lamellated and form membrane staples, called dendritic bulbs (db), inside the lumen (Figure 5D-G). In L1 larvae, their dendrite terminates clearly inside the lumen; in L3 larvae, it might extend further into the dendritic sheath. Besides the dendritic bulb, the dendritic inner segment is heavily swollen after the ciliary constriction, forming another bulb-like structure (Figure 5E-G). This fits with confocal image data, where the dendritic bulb seems to be divided (Ni et al. 2016). In the DOG, the cell bodies of both neurons lie adjacent (Figure 2A, C).

In addition to the peripheral sensilla $DO_{p1\text{-}6}$, we find one papilla sensillum, p_6, in close proximity to the DO, whose sensory cell body (des_{1B}) lies in the DOG. The structure of papilla sensilla will be presented in a separate results section (see Figure 10).

It is difficult to compare our findings to Singh and Singh (1984) because their description of peripheral sensilla is vague. In *Musca*, Chu-Wang and Axtell (1971) classified the peripheral sensilla into four types: contact chemoreceptor, unclassified receptor, lateral pore receptor and scolopidium-like receptor. Based on the numbers of dendrites and other structural properties, DO_{p4} and DO_{p2}

might correspond to the unclassified receptor and DO_{p5} and DO_{p3} might correspond to the contact chemosensory receptor. DO_{p1} most likely corresponds to the scolopidium-like receptor, even though the classification is misleading, as scolopales are associated with chordotonal organs, which have no connection to the surface. From today's perspective, it would rather be classified as a campaniform or papilla sensillum, and misclassification might be due to the interpretation of dendritic sheaths as scolopales in campaniform sensilla.

The seven olfactory sensilla composing the dome of the DO share a similar structural organization (Figure 3B-G). Therefore, discrimination between them, like done for the peripheral sensilla, was not feasible. At the base of the dome, olfactory dendrites form seven tightly packed clusters of three dendrites (Figure 3B, C). These olfactory triplets lie in a circle immersed in common sensillum lymph space, which is filled with a substance of heterogeneous electron density (Figure 3B, C). The peripheral sensilla are arranged as a circle around the olfactory triplets. They lie outside of the sensillum lymph space (Figure 3B, C, E). Dendrites of all DO sensilla are enclosed by ACs further proximal to the dome base (Figure 7). The olfactory sheath cells form the common olfactory receptor lymph space. Further proximal, the olfactory triplets are bathed in electron-dense inner sensillum lymph inside their individual lymph cavity (Figure 3D and F, Figure 7). In comparison to dendrites of the peripheral sensilla, olfactory dendrites appear quite large in diameter, whereas DO_{p3}, DO_{p5} and DO_{p6} appear very tiny, especially in L3 larvae (Figure 3C, E).

The dendrites of DO sensilla are separated into an inner and an outer dendritic segment by a ciliary constriction inside the inner sensillum lymph cavity (Figure 3G; 4C, E, G; 5E-G). Dendritic inner segments of olfactory and peripheral sensilla are considerably larger in diameter than the outer segments, which is the typical structure of insect sensilla dendrites (Keil 1997). A dendritic sheath surrounds the dendritic outer segments (e.g., Figure 3G; 4B, D, E; 5B, C) and disappears inside the lumen (Figure 3G). Dendrites of one sensillum seem to stay together after leaving their common lymph space and their cell bodies lie adjacent inside the DOG (Figure 2A, C).

In total, we find 43 cell bodies in the DOG, 36 of them being of sensory and seven being of non-sensory origin. The sensory cells in the DOG include the cell bodies of the 21 olfactory neurons, the 11 peripheral neurons, the neuron of the peripheral papilla sensillum and the three neurons of the papillum P_{do} of the dorso-lateral group of the TO (Rist und Thum 2017). The seven non-sensory cells are of unknown origin, but most likely peripheral glial cells (see discussion).

Within the DO, we also find the (accessory) cells that build the structure of the organ. We find 60 cells in total, 28 (7x4) being associated with the olfactory sensilla, 24 (6x4) being associated with the six peripheral sensilla and one being associated with the papilla sensillum p_6. The seven remaining cells are of unknown origin but might also be peripheral glial cells. The remaining ACs of p_6 and P_{do} lay outside the DO.

CHORDOTONAL ORGAN IN CLOSE PROXIMITY TO DORSAL ORGAN

In close proximity to the DO, we find a single-innervated (monodynal) chordotonal organ (ChO) (Figure 6A, B). It lays diagonally to the DO dome in between the non-sensory cells that build up the DO (Figure 6C, D), but it is not part of the DOG. The bipolar sensory cell ends with a ciliary structure of type 1 (Yack 2004) (Figure 6E). The cilium is growing out of the dendritic inner segment and is surrounded by the prominent scolopale, which is made up of the scolopale rods (Figure 6D, E). The rods are segregated by the scolopale cell. The end of the cilium is inserted into a cap, which is ensheathed by the cap cell (Figure 6 D). The cilium is bathed in sensillum lymph within the scolopale

(Figure 6 E) and exhibits a ciliary dilation (Figure 6D). The inner dendritic segment contains a very noticeable striated ciliary rootlet (Figure 6F), which originates from the basal body towards the cell body. We find these DO-associated ChO (doChO) not only in L1 but also in L3 larvae (Figure 6G, white arrow).

VENTRAL ORGAN

The ventral organ is located ventral to the terminal organ and lateral to the mouth hooks. The sensilla of the VO are located in a cuticle invagination, hidden by a row of cirri (Figure 8B). We identified four sensilla in the VO (Figure 8A-I, Table 1). Three of them (VO_1, VO_3 and VO_4) are innervated by a single neuron and one (VO_2) by two neurons (Figure 8F-I). This number is in accordance with previous findings in other cyclorrhaphan larvae (Honda und Ishikawa 1987) but contradicts a study on *Drosophila* larvae reporting that five sensilla belong to the VO (Singh und Singh 1984).

We name these sensilla VO_1- VO_4. Starting from the medial most sensillum VO_1, we number the four sensilla in a clockwise direction in the left and an anti-clockwise direction in the right hemisphere when seen from the front. VO_1 forms a shallow dome centering a tiny pore (Figure 8B). VO_1 is innervated by one dendrite that terminates with a tubular body at the base of the pore and is encased by a dendritic sheath (Figure 8C, F, G). The microtubules can be clearly distinguished and are evenly distributed in the tubular body area (Figure 8C''). The VO_1 sensillum was also termed plate sensillum in earlier literature (Honda und Ishikawa 1987). VO_2, VO_3 and VO_4 lie in pits (Figure 8). In L3 larvae, we could observe terminal pores, which are absent in L1 larvae and thus are likely molting pores. VO_3 and VO_4, like VO_1, resemble papilla sensilla. All are innervated by only one dendrite, which composes a tubular body at its tip at the base of the pore openings or the epicuticle, respectively (8 A, C, F, G). The tubular body of VO_3 consists of more densely packed microtubules that are not distinguishable from each other (Figure 8C'). VO_4 displays a unique type of tubular body, which can only be found in this sensillum. It is rather large compared to other tubular bodies, and the dendrite intermingles with electron-dense material of unknown origin in this area (Figure 8C, D) (for potential functional implications, please refer to the related section in the discussion). Unlike the other three sensilla, VO_2 is innervated by two dendrites (Figure 8H, I). Distinguishing it from the dendrites innervating the other sensilla of the VO, the dendrites of VO_2 are distally surrounded by a cuticle tube (Figure 8A, C), lack a tubular body and branch multifold distally of the ciliary constriction (Figure 8E). The terminal pore is also present in L1 larvae. Each of the VO sensilla possesses its individual set of three ACs (Figure 8 F-I), but the thecogen cell and the trichogen cell of VO_2 appear substantially more electron-lucent (Figure 8H, asterisks), with mitochondria of altered structure (Figure 8H, white arrowhead) compared with ordinary ones (Figure 8H, black arrowhead).

LABIAL ORGAN

Located on the ventral side of the ventral lip (labium) lays the labial organ (LO – also called lbo) (Figure 9A, B). In the present study, we find two sensilla associated with the LO in accordance with Kankel et al. (1980) (Figure 9C, I). In contrast, Singh and Singh (1980) describe three sensilla based on examination of internal ultrastructure. We name the two identified sensilla LO_1 and LO_2 (Figure 9C). LO_1 forms a cavity with a pore in the center and sits on a small, shallow socket (Figure 9C). The pore is absent in L1 larvae and thus likely a molting pore. LO_1 is innervated by one neuron that composes a tubular body on the tip of its dendrite, which terminates below the pore opening. The dendrite is surrounded by a dendritic sheath (Figure 9E, F). LO_2 forms a knob-like cuticle shaft protruding from the cuticle. The knob's cuticle has a rough texture and appears more electron-lucent

than the cuticle of the surrounding body wall (Figure 9C). Internally, the knob is filled with an electron-dense material (Figure 9E). Like LO_1, LO_2 is innervated by one dendrite composing a tubular body, which terminates at the base of the knob where a molting pore is present in L3 larvae and absent in L1 larvae (Figure 9D-F). The two labial organ sensilla both have their own set of ACs: a thecogen cell, which forms the dendritic sheath; a trichogen cell, which forms the shape of the sensillum; and a tormogen cell, which forms the sensillar socket. We find two more cells in the LO, most likely non-apoptotic glial cells originating from the sensory organ precursor cell (SOP) or its secondary precursor cell (pIIb), respectively (Fichelson und Gho 2003).

Sensilla of thoracic and abdominal segments

PAPILLA SENSILLA

The papilla sensillum is most similar to the canonic type of the campaniform sensillum. Papilla sensilla form a shallow depression in the cuticle (Figure 10A, B) with a pore in its center in L3 larvae (Figure 10B, D). In L1 larvae, the pore is absent and therefore a molting pore (Figure 10C, E). Papilla sensilla are innervated by one dendrite which terminates with a tubular body below the pore or the epicuticle, respectively (Figure 10C-E). The tubular bodies show no organized distribution of microtubules which are difficult to distinguish as they occur in densely packed clusters (Figure 10E). The tubular body of the p6 sensillum in the abdominal segments is of a similar shape, although another sensory neuron without a tubular body exists in a shared sensillum space (Figure 10G). The dendrites of abdominal sensilla p_5, the so-called slit papilla, and the p_y papilla of the first thoracic segment don't show the typical dendritic swelling at the tip and the tubular body appears to be more delicate (Figure 10G', G''). In contrast, the tip of the thoracic p_x neuron is thickened and the tubular body is quite noticeable, as the whole inner area is packed with electron-dense material (Figure 10G'''). For all types, the dendrite tip is anchored in the endocuticle by a socket septum (Figure 10C-E). The dendrites are enclosed by a dendritic sheath, which is most likely segregated by the thecogen cell (Figure 10C-E). The thecogen cell also forms an inner sensillum lymph cavity at the transition from the outer to the inner dendritic segment at the level of the ciliary constriction (Figure 10C, H, I). Furthermore, the sensillum is enveloped by the thecogen cell and the tormogen cell (Figure 10H, I). In some exceptional cases, we find a short hair-like structure protruding from papilla sensilla or positions where we would expect papilla sensilla (Figure 10F).

HAIR SENSILLA

A hair sensillum (Figure 11A) is most similar to the canonic type of the trichoid sensillum. Hair sensilla comprise a round, hair-shaped shaft that sits in the center of a shallow cuticle depression (Figure 11B). In accordance with previous literature (Kankel 1980), we find that the shaft of hair sensilla varies greatly in size. It might be very short, reduced to a stump, or very long up to more than 15 µm (Figure 11B). The form of the hair shaft might vary, too. We observed bifurcated shafts forming two branches (Figure 11B'). Further, we observed hair sensilla that come in a pair ('double hair', Figure 12). The double hair h_3/h_4 was exclusively found on abdominal segments. Because of the differences in external morphology of the hair shaft, Kankel et al. (1980) classified hair sensilla into three different types, called type C, D and E (Table 2). However, we here find that the internal ultrastructure of hair sensilla (Figure 11C-I) is in general similar irrespective of the length and the shape of the shaft. The interior of the hair shaft is electron-lucent, surrounded by an electron-dense sheath (Figure 11C, D). A pore, presumably a molting pore, can be found at the base of the shaft (Figure 11D) in L3 larvae. All hair sensilla are innervated by a single dendrite terminating at the base

of the shaft composing a tubular body (Figure 11E, F). The tubular body of the hair sensilla is even more thickened than the canonical tubular body of papilla sensilla, and the microtubules are clearly visible and distinguishable from each other. A socket septum is clearly visible (Figure 11E, F). Apart from the difference in outer appearance and structure of the tubular body, the hair sensilla are quite similar to the papilla sensilla, with a typical set of ACs (Figure 11G - I) and a small inner sensillum lymph cavity at the transition from the outer to the inner dendritic segment at the level of the ciliary constriction (Figure 11E, H, I).

DOUBLE HAIR ORGAN

As mentioned previously, the abdominal hair sensilla h_3 and h_4 represent a special case of compound hair sensilla. It consists of two hairs of different sizes, which are adjacent to each other, sitting in one cuticle depression (Figure 12A, B). Usually, the h_4 sensillum structure is of the same type as a canonical hair sensillum, containing one sensory cell with a tubular body at the base of the hair (Figure 12D). In contrast, the outer hair of h_3 is comparatively short and therefore called a bristle. The key aspects are similar to the abdominal papilla p_6, with two sensory cells (Figure 12 E, F), one containing a tubular body (which rather exhibits the structural properties of papilla than hair sensilla) (Figure 12C, D). Both h_3 and h_4 possess their own set of ACs and are therefore individual sensilla (Figure 12H, I), although in one exceptional case, they shared one lymph space (Figure 12G). At the level of the ciliary constriction, the thecogen cell forms an inner sensillum lymph cavity (Figure 12E, F).

KNOB SENSILLA

The knob sensillum is most similar to the canonic type of the basiconic sensillum. Knob sensilla are present on thoracic segments (Figure 13A) and on the sensory cones of the last abdominal segment (Figure 16A), but similar structures can also be found in the terminal organ (Figure 16G) (Rist und Thum 2017). Knob sensilla have been described under various names such as koelbchen, knob-in-pits, hair-type B, black sensory organs, black dots, sensory papillae or dorsal/ventral pits (Hertweck 1931; Lewis 1978; Lohs-Schardin et al. 1979; Kankel 1980; Singh und Singh 1984; Campos-Ortega und Hartenstein 1985; Sato und Denell 1985; Dambly-Chaudière und Ghysen 1986; Hartenstein 1988; Campos-Ortega und Hartenstein 1997) (Table 2).

The knob sensilla of the thoracic segments display a common external morphology, a knob-shaped cuticle shaft sunken into a round cuticle cavity (Figure 13B). The cuticle shaft slightly protrudes from the cavity. Investigation of internal ultrastructure by targeted FIB-SEM and ssTEM reveals that three dendrites are associated with one thoracic knob sensillum (Figure 13C-I). One dendrite innervates the shaft, proceeding to its tip (Figure 13C). The other two dendrites end at the base of the knob, one with a tubular body (Figure 13C-E). All dendrites are surrounded individually by one dendritic sheath (Figure 13C-E), which arises from the common thecogen cell. Each sheath is connected to a pore at the base of the knob in L3 larvae (Figure 13D). This pore is not present in L1 larvae (Figure 13 C, E) and is therefore most likely a molting pore. The dendritic sheath of the three dendrites disappears at the epidermal layer. Here, dendrites are surrounded by three common sheath cells (Figure 13H, I). In T1, we find one dorsal knob sensillum (dk) and one ventral knob sensillum (vk), whereas in T2-T3, we find one lateral knob sensillum (lk) and one ventral knob sensillum (Figure 1B and Figure 13A). All thoracic knob sensilla were examined and no difference in structural organization was recognized. In contrast, the knob sensilla of the sensory cones are inconsistent and house either two (Figure 16D, E) or three (Figure 16F) neurons, whereas the knob sensilla of the TO only contain one

sensory cell (Figure 16G) (Rist und Thum 2017), which dendrite protrudes into the shaft. Knob sensilla of the last abdominal segment are discussed in a separate results section, as they are organized in specialized terminal sense organs.

KEILIN'S ORGAN

The KO is exclusively located on the ventral side of the thoracic segments T1-T3 (Figure 14A). The KO is relatively easy to identify and was described for larvae of several dipteran species (Keilin 1915; Lakes und Pollack 1990; Lakes-Harlan et al. 1991). The KO of *Drosophila* larvae has so far been described as consisting of three hairs (Kankel 1980). In L1 larvae, we find that two papilla-like sensilla are associated with the organ in addition to three hair sensilla (Figure 14 A, E, G). One of the papilla-like sensilla is degenerating during the L1 stage (Figure 14E-F). Signs of degeneration are the comparatively small diameter of the dendrite (Figure 14E) and poor axonal development, like the absence of growth cones and axon branching (not shown). This finding is congruent with a study of the KO of the larvae of *Phormia* (Lakes-Harlan et al. 1991) and provides an explanation for studies that find five sensory neurons innervating the KO of *Drosophila* larvae (Dambly-Chaudière und Ghysen 1986; Campos-Ortega und Hartenstein 1997). In L3 larvae, the (surviving) papilla sensillum is externally recognizable by a tiny pore in the cuticle (Figure 14B). Also, a pore is found on the base of each of the hairs (Figure 14D). Because these pores are not found in L1 larvae, they are most likely molting pores. Investigation of the internal ultrastructure reveals that each of the three hair sensilla and the two papilla sensilla are associated with a single dendrite. All dendrites terminate with a tubular body below the cuticle; this organization represents the standard types of hair or papilla sensilla (Figure 14E, F). Also, all KO sensilla possess their own set of enveloping ACs (Figure 14H, I).

Sensilla of the anal division

TERMINAL SENSORY CONES

The terminal sense organs or sensory cones are located at the fused terminal segments (Figure 1A, Figure 15A, Figure 16A). According to the literature (Whittle et al. 1986; Denell und Frederick 1983; Dambly-Chaudière und Ghysen 1986; Jürgens 1987), we could identify seven distinct sensory cones t_1 – t_7. They either house a knob sensillum (t_3, t_5, t_7), a hair sensillum (t_4, t_6), both (t_2) or both plus an additional papilla sensillum at the base of the cone (t_1) (Figure S3). These results are consistent with previous findings in L1 larvae (Dambly-Chaudière und Ghysen 1986; Jürgens 1987), although the number of corresponding neurons is slightly different. We found that knob sensilla of t_1, t_5 and t_7 are only innervated by two sensory neurons (Figure 16E) in contrast to three sensory neurons that were reported in the embryo (Dambly-Chaudière und Ghysen 1986) and that we find in t_2 and t_3 (Figure 16C). These knob sensilla are still innervated by one neuron protruding into the shaft and one neuron containing a tubular body that sits at the base of the shaft. A third neuron without a tubular body is absent (Figure 16E). The hair sensilla associated with the sensory cones are innervated by one sensory cell with a tubular body on its tip (Figure 15B) and exhibit similar features as the canonic hair sensilla of the body wall. The only papilla sensillum associated with the sensory cones sits at the base of the t_1 and shares the same structure as the canonic papilla sensilla. The t_1 lays in close proximity to the anal plate towards the caudal end. T_2 is situated dorso-caudal of t_1, halfway in between the anal plate and the posterior spiracle. t_3 lays anterodorsally of t_2 and the cone of t_4 lays anterodorsally of t_3. The cone of t_5 is located dorsal of t_4, whereas t_6 is located closer to the dorsal midline than t_5. The cone of t_7 is located at the dorsal midline and at the base of the posterior spiracle. All knob sensilla of the terminal sensory cones show a similar external structure as thoracic knob

sensilla, but their shafts protrude far out of the cavity in L1 larvae (Figure 16B, C; Figure S3). In L3 larvae, the sensory cones further change in appearance, and the knob and hair sensilla are sunken into the full-grown cone and surrounded by broad-based apposing leaflets (Kuhn et al. 1992). All sensilla associated with the terminal sensory cones display a typical sensilla configuration: their dendrites are bathed in the inner sensillum lymph and ensheathed by a typical set of support cells (Figure 15 C, D and Figure 16F, H, I). Besides the prominent sensory cones, there are some less noticeable external sensilla.

SPIRACLE SENSE ORGAN

The spiracle sense organ (sp) consists of four sensilla (sp_{A-D}) which are located in close proximity to the spiracular openings at the base of the spiracular hairs (Figure 17A-D). They are all single-innervated, contain a tubular body (Figure 17D) and display a canonic set of support cells (Figure 17 E, F). The spiracular glands lay in close proximity to these sensilla (Figure 17E, F).

VENTRAL ANAL PAPILLA SENSILLUM

One papilla sensillum can be found close to the anal plates. It is located at the anal opening and called ventral anal papilla sensillum (vas) in the literature (Campos-Ortega und Hartenstein 1997). In contrast to Hartenstein's findings, we find it to be only single-innervated. Notably, one unpaired anal cone or anal tuft (Lohs-Schardin et al. 1979; Denell und Frederick 1983) is located in close proximity and was mistaken as a sensory cone before. We could not find any sensory cell associated with this structure, although vas lies in close proximity (Figure 1B).

Overall, we obtained a complete picture of all larval external sensory structures and their associated sensory neurons. In the following, we discuss their putative sensory mechanism and function according to their internal morphology and ultrastructure and classify the different sensilla and their associated neurons.

DISCUSSION

We present a comprehensive anatomical analysis of external sensory organs of the head, thoracic and abdominal segments of the *Drosophila* larva. The application of optimized FIB-SEM and ssTEM allowed us to image and reconstruct small sensilla as well as large and complex sensory organs. Our experimental FIB-SEM approach can easily be adapted to study the morphology of external sensilla and other external structures of further insect species. This methodology is a prerequisite to investigate the different characteristics of insect peripheral nervous systems in a comparative way. With respect to *Drosophila* larvae, our work provides fundamental anatomical insights necessary to further decipher the relation between the structure and function of sensory organs. Certainly, a future key step would be to establish transgenic fly lines that label the sensory neurons of the sensilla, allowing the study of their functionality through molecular, behavioral and physiological experiments. This might be possible through a variety of genetic driver lines from different Gal4, LexA, and Q system collections (Lewis 1978; Brand und Perrimon 1993; Lai und Lee 2006; Pfeiffer et al. 2010; Li et al. 2014; Gohl et al. 2011; Tirian und Dickson 2017). In addition, there are even more specific lines based on multiple overlapping promoter expression patterns such as the split-Gal4 system (Luan et al. 2006). Unfortunately, these lines have mostly been studied only with respect to their expression in the central nervous system, and anatomical studies of the peripheral nervous system are limited. It will be equally important to connect the described peripheral sensory system of the larva with the already existing brain connectome in order to better understand the processing

of external environmental information and its relevance for behavior (Hückesfeld et al. 2021; Miroschnikow et al. 2018; Eichler et al. 2017; Eschbach et al. 2020; Ohyama et al. 2015). Such linkage would be important, for example, to analyze whether mechanosensory information from different body segments converges in a particular brain region and forms a stable, spatially conserved map of inputs - similar to the olfactory system (Ramaekers et al. 2005; Berck et al. 2016). Similarly, it would allow us to understand for the first time how taste information from different external sensory organs is interconnected with the internal pharyngeal and enteric nervous systems.

The standard configuration of the larval body wall covers a total of 541 sensory cells associated with the external sensilla. 363 are probably mechanosensory according to their internal structure, as they possess a tubular body. The 363 mechanosensory cells can further be grouped into 201 neurons belonging to papilla sensilla, 100 to hair sensilla and 22 to knob sensilla. The remaining 40 mechanosensory cells can be found in the major head organs and in the spiracle sense organ. We find 42 olfactory and 12 thermosensory neurons in the DOs and 50 gustatory neurons of which 46 cells are distributed in the TOs and 4 in the VOs. We find additional 26 sensory neurons in knob sensilla that are probably important for oxygen and carbon dioxide sensing. Their dendrites protrude into the sensillum shaft, where the dendritic sheath is perforated and, therefore, susceptible to chemical compounds that are able to diffuse into the cuticle. We also find 48 sensory cells whose ultrastructure was insufficient to make well-grounded predictions about their sensory mechanism, as they are lacking noticeable structural components. These cells are distributed evenly throughout the larval body. We find two in each of the DOs, one in each thoracic knob sensillum, one each in the abdominal papilla sensilla p_6, one in the abdominal hair sensilla h_3 and one each in the knob sensilla of the terminal sensory cones t_2 and t_3. Apart from these sensory cells, there are more to be found in the larval body, like in chordotonal organs, pharyngeal organs or multidendritic neurons. These were not regarded in this study but will be the subject of future studies.

Organization of larval sensilla types

NOMENCLATURE, VARIABILITY AND ULTRASTRUCTURE

As mentioned before, various names were given to the sensilla, not only of immature insects but also larval *Drosophila*. Here, we aimed to list all names given to them (Table 1 and 2) and to establish a standard nomenclature for *Drosophila* larval sensilla, using our detailed and comparative approach as a basis for the classification of all external sensilla. We identified three major types of sensilla which are most abundant on the larval body wall: papilla sensilla, hair sensilla and knob sensilla. They occur either as solitary sensilla or are integrated into sensory organs or compound sensilla like the terminal organ, the keilin's organ or the terminal sensory cones. Also, they exhibit slight differences in terms of associated sensory cells or external appearance. Besides these most abundant types, we found specialized (olfactory and gustatory) sensilla, mainly in the organs of the head region.

Taking advantage of the whole larval volume, we were able to identify and name all neurons associated with the external sense and chordotonal organs (Figure 1C). Again, we used the nomenclature of Dambly-Chaudière and Ghysen (external sense organs) and Campos-Ortega and Hartenstein (chordotonal organs) but made slight modifications to incorporate deviating cell numbers and to create a consistent nomenclature that can be used in databases.

These changes are: (i) for all external sensilla, the associated neurons are named in the following pattern: position within the segment (dorsal (d), lateral (l), ventral 1 (v), ventral 2 (v'), ventral 3 (v'')), type of sensillum (external sensilla/sense organs (es) or chordotonal organs (Ch)), number of

associated neurons (1, 2, 3,…) and order of appearance from ventral to dorsal (A, B, C, …); (ii) for the fused head and abdominal segments, we also used this pattern for simplification and clarity, even though we thereby ignore the segmental borders; (iii) to avoid confusion, we did not assign names that were used for other neurons again, for example, the neurons of abdominal hair sensillum h_3 were named des_A before, as Dambly-Chaudière and Ghysen (1986) only could identify one neuron in their camera lucida drawings in the embryo. On the contrary, we did always see two neurons innervating h_3, and therefore called these des_{2A}. The remaining dorsal external sense neurons did not change in naming, even though des_{1A} is not assigned. A full list of the external sense neurons is given in Table 2. In the following, we discuss different criteria used to assign putative functions to the identified sensilla and sensory cells.

TUBULAR BODIES

Within the larval sensilla, we find a variation in the shape and size of tubular bodies, a well-known structure regarded to mediate mechanical sensation in insect sensilla sensory neurons (Thurm 1964; Keil 1997). These variations likely correlate with different mechanisms of mechanotransduction. For example, the tubular body of the hair sensilla is shaped in a way to transduce directional force applied to the hair (see Figure S4). When the hair is deflected, pressure is either applied or released from the dendrite tip via the cuticular structures (like a lever). In papilla sensilla, the force is applied unidirectional, either through deformation of the cuticle through external touch or movement of the body wall during motion. Abdominal p_5 papilla are contained in vertical slits (slit papilla), and the tubular body sits beneath an elongated, cuticular mound in the center of the slit (Figure 10G', G''). Putatively, the tubular body is deformed by compression of the slit during movement. In contrast to the other tubular bodies (and especially to the delicate tubular bodies of p_5 and p_y sensilla), the tubular body of p_x at the first thoracic segment appears to be very dense (Figure 10G'''). It can be inferred that a compact tubular structure is also more rigid, leading to an increased sensitivity of the mechanotransduction apparatus, as it acts as an abutment for the spring-like proteins that work as mechanotransducers. However, additional physiological data on these sensory neurons is required to substantiate this hypothesis linking structure and function.

DEVELOPMENTAL ASPECTS

Morphological studies on the ultrastructure of the sensory neurons in *Drosophila* were either executed on *Drosophila* embryos (Campos-Ortega und Hartenstein 1997; Dambly-Chaudière und Ghysen 1986), first (Hartenstein 1988), second (Singh und Singh 1984) or third instar larvae (Dambly-Chaudière und Ghysen 1986). Over the years, these works led to contradictory assumptions about the number and location of the larval sense organs and their corresponding sensory cells. In addition, various functions were to some extent assigned to the sensilla. Our analysis, using L1 and L3 larvae, allowed for clarification of several ambiguities. Primarily, we could address the difference between functional pores and molting pores. Pores that were found in L3 larvae but absent in L1 larvae were considered to be traces of molting and therefore not necessary for the sensory function of these sensilla. In most cases, this was true for mechanosensitive sensilla that are widely distributed on the larval body wall. Given their pore-like appearance in L3, especially papilla sensilla were suspected to serve chemosensory function in the past. Additionally, the sensilla of the KO were assumed to serve different sensory functions before (Hafez 1950; Benz 1956) and some of the peripheral sensilla of the DO were termed lateral pore receptors (Singh und Singh 1984; Chu und Axtell 1971) or classified as contact chemoreceptors (Chu und Axtell 1971). If pores are absent in sensilla of L1 larvae, they probably do not serve chemosensory function, although we cannot rule out

this function completely given the lack of physiological experiments. On the other hand, pores that were found in both instars were considered to be functional pores and therefore most likely associated with external gustatory sensilla. Pore-containing sensilla are limited and restricted to the VO_2 of the ventral organ (Figure 8C, E) and the pit and papilla sensilla of the terminal organ (data not shown; see results of (Rist und Thum 2017)).

Secondly, we could address the open questions regarding the number of sensilla and sensory neurons. For example, Singh and Singh (1984) reported five sensilla in the VO, but our results show only four sensilla in L1 as well as in L3 larvae. Furthermore, they reported five dendrites in VO_2. Because we obtained volumes of the VO including the sensory cell bodies, we could show that VO_2 is innervated by two sensory cells with one proximal dendrite each, which branch multifold when entering the pore channel. In the abdominal double hair, the h_3 sensillum houses two sensory cells instead of one reported before (Campos-Ortega und Hartenstein 1997; Dambly-Chaudière und Ghysen 1986). The keilin's organ was reported to house either four (Lakes-Harlan et al. 1991) or five (Campos-Ortega und Hartenstein 1985; Campos-Ortega und Hartenstein 1997; Dambly-Chaudière und Ghysen 1986; Lakes-Harlan et al. 1991) sensilla previously. With our work, we could explain these differences: one papilla sensillum is still abundant in L1 larvae, but already shows signs of degeneration and is completely missing in L3 larvae (Figure 14F). This is the only example of age-specific degeneration of sensilla between larval moltings that we could identify.

Hypothetical functions of larval head, thoracic, and abdominal sensilla

DORSAL ORGAN

In *Drosophila*, the six peripheral sensilla of the DO were hypothesized to serve different modalities: contact chemosensation (gustation), mechanosensation, thermosensation and hygrosensation (Chu und Axtell 1971; Python und Stocker 2002; Kwon et al. 2011; Klein et al. 2015; Ni et al. 2016; Hernandez-Nunez et al. 2021). Evidence derives from observed ultrastructure indicating certain functions (Chu und Axtell 1971), and more recently from anatomical, physiological and behavioral experiments (Kwon et al. 2011; Klein et al. 2015; Ni et al. 2016; Hernandez-Nunez et al. 2021). We conclude that DO_{p3}, DO_{p5} and DO_{p6} are candidates for thermosensory function, which was confirmed recently (Hernandez-Nunez et al. 2021). Typically, insect thermosensory sensilla are associated with neurons that terminate below the other neurons of the sensillum and form extensive lamellation (Steinbrecht 1984). DO_{p3}, DO_{p5} and DO_{p6} each house two neurons. One neuron ends right below the cuticle surface of the sensillum (Figure 5A, B) and the other becomes visible within the inner sensillum lymph cavity and forms a lamellated dendritic bulb (Figure 5E, F). This remarkable structure might be similar to the 'dendritic bulb' described by recent studies using fluorescence microscopy of transgenic fly lines (Klein et al. 2015; Ni et al. 2016; Hernandez-Nunez et al. 2021). It was shown that the DO neurons associated with these structures trigger cool avoidance behavior in larvae (Klein et al. 2015). Presumably, this response is mediated by Ir21a (Ni et al. 2016). In addition, two of these sensilla play a role in warmth sensing via Ir68a. This receptor is expressed in the neurons without a dendritic bulb. Both neurons were shown to act together as synchronous and opponent thermosensors (Hernandez-Nunez et al. 2021). Contact chemosensory function was assumed for at least two peripheral DO sensilla based on structural characteristics in *Musca* larvae (Chu und Axtell 1971). Further evidence for gustatory function of the DO came from the report of Gr2a and Gr28a gene expression in DO neurons of *Drosophila* larvae (Colomb et al. 2007; Kwon et al. 2011). DO_{p2} and DO_{p4} each house two neurons, of which one is likely to be mechanosensory. This function is indicated by the presence of a tubular body located in the tip of the neurons' dendrite

(Figure 4D, F). However, their sensilla structure differs from the gustatory sensilla found in the TO (Rist und Thum 2017). There, dendrites of one gustatory sensillum are surrounded by a common dendritic sheath, which forms the lymph-filled lumen of the sensillum. DO_{p2} and DO_{p4} are of simpler organization, lacking an obvious sensillum lumen as each dendrite is enclosed by an individual dendritic sheath. A cuticle tube, present in all gustatory TO sensilla, is absent, too. Furthermore, a terminal pore is missing in L1 larvae, which argues against a role in contact chemosensation. In adult *Drosophila*, Gr2a and Gr28a have been reported to be expressed not only in gustatory but also in other sensilla of another, yet unknown function (Thorne und Amrein 2008). In addition, Gr28a was also reported to be expressed in the larval gut (Park und Kwon 2011). Consequently, we are questioning the chemosensory roles of DOp2 and DOp4. The structural arrangement of DOp1 and papilla sensillum p6 suggests mechanosensation, as evidenced by the presence of a single neuron forming a tubular body at its dendritic tip (Figure 4B). Thus, our primary inference is that p6, DOp1, DOp2, and DOp4 predominantly serve mechanosensory functions, while DOp2B and DOp4B may potentially be associated with a distinct sensory mechanism.

The DO has been reported to consist of 14 sheath cells, 14 shaft cells and 13 socket cells (Grillenzoni et al. 2007). Therefore, it has been concluded that the DO derives from 14 sensory organ precursor cells (SOP) and consists of 14 sensilla. With our data, we could confirm and even extend these assumptions. We hypothesize that the DO consists of 14 sensilla, too, although the 14th sensilla is not the P_{do} but the papilla sensillum p_6. Some of its ACs lie outside the DO, which is possibly the reason for the missing 14th socket cell. P_{do} on the other hand, has its sensory cell bodies in the DOG, but all the ACs lie outside the DO.

Furthermore, we could find a total of 60 cells within the DO and a total of 43 cells in the DOG. In one exceptional case, we observed an eighth olfactory triplet in the DO, leading to an altered cell count of three more sensory cells in the DOG and four more potential ACs inside the DO. Therefore, we hypothesize that the olfactory DO sensilla, if not all (DO sensilla), possess four ACs derived from the SOPs. If the fourth one is a second tormogen cell, like in some adult olfactory sensilla (Shanbhag et al. 2000; Nava Gonzales et al. 2021), or a non-apoptotic glial cell, can't be finally resolved with our data. In addition to the hypothesized 53 ACs (4 x 7 olfactory ACs, 4 x 6 peripheral ACs, 1 x p6 glial cell) and 36 sensory cells (21 olfactory, 11 peripheral, 1 p_6 and 3 P_{do} neurons), we find seven cells of unknown origin in the DO and in the DOG respectively. They either also derive from SOPs or, more likely, are peripheral glial cells generated in the CNS that migrate towards their final destination (Hilchen et al. 2008).

VENTRAL ORGAN

We conclude that the VO is mainly a mechanosensory organ and its only gustatory sensillum might be VO_2. Contrary, a mainly gustatory function of the VO was assumed previously based on the presence of sensillum-terminal pores and the expression of gustatory receptor (Grs) genes in neurons of the VO (Chu-Wang und Axtell 1972b; Singh und Singh 1984; Python und Stocker 2002; Colomb et al. 2007). In fact, the terminal pores of most VO sensilla might be traces of molting, as they were absent in L1 larvae of onion and seed-corn flies (Honda und Ishikawa 1987), which have not undergone molting in this stage. Our results validate these findings, as there were no visible terminal pores (Figure 8C). VO sensilla VO_1, VO_3, and VO_4 display structural characteristics typical for mechanosensation (Keil 1997): innervation by a single dendrite terminating with a tubular body (Figure 4C). Their different size and microtubule organization likely correlate with the processing of different stimulus intensities applied to the mechanotransduction apparatus (Bechstedt et al.

2010).VO_2, in contrast, displays a morphology similar to the gustatory pit sensilla T_3 and T_4 of the TO (Rist und Thum 2017). Therefore, VO_2 might be the single sensillum of the VO serving contact chemosensation.

LABIAL ORGAN

We conclude that the main function of the LO lies in the detection of mechanical stimuli, too. The two single neurons of the LO sensilla each compose a tubular body at their endings (Figure 9E, F), indicating mechanosensory function. On the other hand, we cannot exclude additional sensory functions, especially for the LO_2, which shows a noticeable outer appearance. It is possible that the club-shaped structure acts in hygrosensation by exerting pressure on the tubular body depending on humidity levels, acting as a hygromechanical transducer (Tichy und Kallina 2010).

PAPILLA SENSILLA

Papilla sensilla are the most abundant type of sensory structure throughout the larval sensory system (Figure 1B and Figure 10A). They occur in each segment, including the anal division and the head capsule. We conclude that their main function is the detection of mechanical stimuli, given the fact that they all possess a tubular body at the tip of their dendrites (Figure 10C-G). Most of the papilla sensilla probably detect mainly deformation of the cuticle by motion or external pressure applied, although the direction of force detection might differ in some papilla, like the abdominal slit papilla p_5. The same is true for the abdominal papilla sensilla p_6, but they house two sensory cells, $v'es_{2A}$, one of them lacking a tubular body and therefore possibly serving a different sensory function.

HAIR SENSILLA

Hair sensilla are abundant on the thoracic and abdominal segments. Like papilla sensilla, their sensory neurons all end with a tubular body at the dendrite tip, indicating mechanosensation (Figure 10C, E, F). As discussed above, hair sensilla most likely transduce directional force applied to the distal end of the hair. In addition to mechanosensory function, another unknown function can be assumed for the abdominal hair sensilla h_3. It houses two sensory cells, des_{2A}, one of them with and one without a tubular body. The sensory function of these neurons is difficult to assume only by ultrastructural analysis, as they lack obvious structures like pores (gustatory), tubular bodies (mechanosensory) or dendritic bulbs or lamellated outer dendritic segments (hygro- and thermosensory).

KNOB SENSILLA

Hygro- and thermosensory function was assumed for knob sensilla (Hartenstein 1988), based on structural similarities with hygro-and thermosensory insect sensilla (Altner und Prillinger; Altner et al. 1981; Steinbrecht 1984). Thereafter, knob-shaped sensilla sunken in a cuticle cavity associated with three dendrites typically hint towards a hygro- and or thermosensory function. One of the three neurons typically associated with hygro- and thermosensory sensilla displays peculiar structural characteristics as it might be branched or highly lamellated in its tip that ends beneath the knob (Altner und Prillinger; Altner et al. 1981; Steinbrecht 1984). Instead of lamellation, we find that one neuron of the thoracic knob sensilla contains a tubular body (Figure 13D, E). Knob sensilla organized in sensory cones also display one sensory cell containing a tubular body, irrespective if they are innervated by two or three neurons in total (Figure 16D, E). This result indicates a mechanosensory and not a hygro- and thermosensory function for these neurons. In the absence of physiological data, however, the sensory function of the knob sensilla remains unclear. A sensory function of the other

two knob sensilla neurons in contact chemosensation is not inconceivable. The knob sensilla of the TO are similar in external morphology and are candidates of contact chemosensation due to the indicated expression of certain Grs in their sensory neurons (Rist und Thum 2017). In sensory neurons of thoracic segments, too, expression of Grs (Gr2a) was assumed based on GAL4 driver line analysis (Colomb et al. 2007). To which sensillum type these sensory neurons belong can now be determined based on the presently established morphological classification.

Additionally, knob sensilla of the larval thoracic segments were associated with two atypical soluble guanylyl cyclases (asGC), Gyc-89Da and Gyc-89Db, which were shown to sense oxygen and are important for response to hypoxia and in larval ecdysis (Vermehren-Schmaedick et al. 2010; Morton et al. 2008). Two neurons were found on each thoracic hemisegment which express both subunits, which fits with the number of thoracic knob sensilla. In addition, each subunit was found to be expressed in two different neurons innervating the TO (per side), which also fits the number of knob sensilla in the TO (Rist und Thum 2017). Furthermore, both subunits were co-expressed in neurons innervating the terminal sensory cones. It was stated that this is true for all cones (Morton et al. 2008). However, the assigned position seems to be slightly off. We hypothesize that these asGC were actually found in cones containing a knob sensillum (t_1, t_2, t_3, t_5, t_7). The sixth one, which also appears to be of a different color in the confocal data, is most likely a tracheal dendrite (td) neuron, which we found to occur in this region (not shown). This interpretation is supported by findings that these asGC subunits were also individually expressed in two td neurons in A1 and A2 (per hemisegment) (Morton et al. 2008). Because the knob sensilla of the TO are only innervated by one neuron, which protrudes into the knob structure, we conclude that these neurons, in general (for all knob sensilla), are the ones expressing the asGC. Also, within the knob, the dendrites are swollen and not encased by a dendritic sheath, which makes them the most likely candidates for sensing external cues like oxygen (Figure 13C, Figure 16C, G). Therefore, we conclude that knob sensilla mainly serve chemosensory function (oxygen perception) and mechanosensory function (the latter is not true for TO-associated knob sensilla). K_2 in the TO was also associated with CO2 perception, as its single neuron expresses Gr21a and Gr63a (Rist und Thum 2017), which were shown to mediate CO2 responses (Kwon et al. 2007, 2011; Jones et al. 2007; Faucher et al. 2006). In contrast to other larval knob sensilla, the dendrite of K_2 is lamellated at its tip, which could also indicate a hygrosensory mechanism (Altner und Prillinger; Rist und Thum 2017). The function of the third neuron innervating the thoracic and some of the knob sensilla of the anal division is not known and will have to be determined in the future.

KEILIN'S ORGAN

The KO of *Drosophila* larvae was assumed to serve hygro- and thermosensory functions (Hafez 1950; Benz 1956). However, electrophysiological recordings of the KO of Phormia larvae indicate mechanosensory function, probably associated with the crawling behavior of the larvae (Lakes-Harlan et al. 1991). This finding is in line with the anatomical characteristics of the KO. The organ consists of 3 hair-like and one respectively two papilla-like sensilla. Each sensory dendrite terminates with a tubular body, which strongly indicates mechanosensory function. The arrangement of the sensory hair sensilla indicates that they are deflected by forces from different directions and, therefore, could be important for orientation. The exploratory behavior of the larva includes straight crawls interspersed with head casts and turns, that the larva executes to redirect the crawling directory. Turns are carried out by backward contractions of the most anterior segments as far as segment four (Berni et al. 2012). Therefore, the strongest directional change

appears in the thoracic segments, where the KO could sense these changes in direction. In addition, it would also be imaginable that they are involved in the perception of upward and downward movements during orientation behaviors like rearing (Green et al. 1983).

TERMINAL SENSORY CONES

The terminal sensory cones of the last abdominal segments are specialized sense organs, which house mainly hair and knob sensilla. Their prominent cone-like structures stick out of the food when the larvae are feeding, putting them in an ideal location to sense changes in oxygen concentrations in their surrounding environment (Vermehren-Schmaedick et al. 2010). Dwelling into the media enables the larvae to hide from predators and strong daylight to prevent desiccation (Kim et al. 2017). But completely submerging into the medium is dangerous as well, as it leads to hypoxia and death, eventually. Therefore, it is essential to dig exactly deep enough to be sheltered but not completely covered. The cone-associated mechanosensory hair sensilla might be activated when the cones are immersing into the medium, and therefore act as a warning signal for the larva.

SPIRACLE SENSE ORGAN

The sense organ of the posterior spiracle consists of four sensilla that sit around the spiracular opening (Figure 17A). They contain one sensory neuron each, with a tubular body at their dendrites' tip (Figure 17D), which indicates mechanosensory function. The tubular body is surrounded by a dendritic sheath that is connected to electron-dense cuticular material and the spiracular hairs, which sit on top of the spiracle. The hairs protrude at a 90-degree angle from the spiracle (Figure 17 C, D) and are probably deflected when the larva submerges into the substrate. Therefore, the spiracle sense organ could be important for the positioning of the spiracle in the right oxygen-rich environment.

OUTLOOK

In this work, we further extend the understanding of the larval sensory system. We complete the spatial map of all external sensory structures and internal chordotonal organs. We used ultrastructural details to make well-grounded predictions about the putative sensory functions of these sensory organs. These results will serve as a basis for further molecular and functional studies. To complete the understanding of the different modalities of larval sensation, it will be necessary in the future to also address the somatosensory, pharyngeal, and enteric sensory systems with all their sensilla, cells, and ultrastructure. This can now be done in subsequent studies of the EM volume of the entire body of the larva. A complete description of all external and internal sensory inputs of the *Drosophila* larva is now within reach.

MATERIAL AND METHODS

FLY HUSBANDRY

Drosophila wild-type Canton S flies were kept on standard corn meal medium at room temperature, as previously described (Selcho et al. 2009; Rohwedder et al. 2012; Apostolopoulou et al. 2014). For all experiments, third instar larvae prior to the wandering stage were used.

SCANNING ELECTRON MICROSCOPY (SEM)

L3 larvae were rinsed with tap water to remove food residuals. Then, specimens were incubated in tap water at 90° C for two minutes. Subsequently, larvae were fixed in 2.5 % glutaraldehyde in 0.1 M

HEPES buffer for three hours. The fixative was exchanged each hour. Primary fixation was followed by three washing steps in 0.1 M HEPES buffer, each for ten minutes. Then, samples were incubated in 1 % osmium tetroxide buffered in 0.1 M HEPES for two hours, followed by three washing steps in 0.1 M HEPES for ten minutes each. All steps were performed at pH 7 and 4° C. Next, samples were gradually dehydrated in an increasing ethanol series: 30 %, 50 %, 70 % two times for ten minutes and then 70 % overnight (all at 4° C). The next day, dehydration was continued with 80 %, 90 %, three times 96 % for ten minutes, and 100 % four times for ten minutes (at room temperature). Dehydrated samples were transferred to a critical point drier (Bal-Tec CPD 030, Liechtenstein) and critical point dried over liquid CO2. Afterward, samples were glued to aluminum SEM-stubs using adhesive conductive carbon pads (Plano GmbH, Germany) or Conduct-C (Conductive Carbon Cement, Plano GmbH) and subsequently coated with ca. 12 nm platinum in a sputter coater (Quorum Q 150R ES Sputter-Coater, UK). SEM micrographs were acquired on a FESEM Auriga Crossbeam workstation (Zeiss, Germany) using the SmartSEM software package (Zeiss, Germany).

FOCUSED ION BEAM-SEM (FIB-SEM)

Larvae were rinsed in phosphate-buffered saline (PBS) to remove food residuals. For the study of head organs, the anterior half of the larva was incubated in 2 % formaldehyde fixative (Sigma-Aldrich, Germany) with 2.5 % glutardialdehyde in 0.1 M Na-cacodylate buffer, pH 7.4 for 30-60 min. Then, the head region was cut off and incubated in fresh fixative for another 90 min. For the investigation of thoracic and abdominal segments, the larva was cut into pieces not larger than four segments. Fixation was carried out similarly to larval heads. Wash- and post-fixation steps were similar to SEM preparation. En-bloc staining was carried out with 1 % uranyl acetate and 1 % phosphotungstic acid in 70 % EtOH in the dark overnight before continuing the alcohol dehydration the next day. Samples were transferred to propylene oxide before embedding in Spurr (Plano, GmbH, Germany) using ascending Spurr concentrations diluted in propylene oxide for optimal tissue infiltration (Rist und Thum 2017). The resin was drained of the samples by gravity during polymerization. Polymerization was carried out at 65° C for 72 hours. Samples were mounted on aluminum SEM stubs using adhesive conductive carbon pads (Plano GmbH, Germany). Samples were sputter-coated with ~100 nm platinum.

FIB-SEM serial sectioning was carried out using a FESEM Auriga Cross-beam workstation (Zeiss, Germany). Images were acquired using a secondary electron detector or a backscattered electron detector. The three-dimensional FIB-Stack of the DO was acquired using the FIB-SEM operating software package ATLAS 3D Nanotomography (Fibics Inc., Canada).

In FIB-SEM, layers of the sample are mechanically removed by the ion beam of the FIB. This procedure works only for relatively small volumes. Therefore, samples that are embedded conventionally in a block of resin require cutting off excess resin to expose the tissue of interest to FIB-SEM slicing and imaging. Often, this is very difficult because structures like insect sensilla and sense organs might be too small to be visible through the block surface. Also, the sample lacks contrast as it is dark from the en-bloc-staining with osmium. In this work, we let the samples harden in only minimal amounts of resin instead of embedding the samples in a block of resin (Schieber et al. 2017). The results of this approach were 'sculptures' of the samples covered only with a very thin layer of resin that left the surface topology of the larva intact. Immediately, these sculptures could be mounted on EM stubs, avoiding further, time-consuming preparation steps. On the minimal embedded sculptures, larger sense organs but also the smallest body wall sensilla could be clearly identified and therefore be precisely targeted by FIB-SEM for serial slicing and imaging.

WHOLE LARVAL VOLUME

Sensilla and neuron reconstruction was done on a STEM (scanning transmission electron microscopy) volume of a whole first instar larva; information on the technical details of its generation is mentioned in Schoofs et al. 2023.

IMAGE PROCESSING

Out of the whole larval volume, we extracted smaller volumes of the sensory organs. The obtained image stacks were imported to Amira (Thermo Fischer Scientific, v2019). Because the whole larval volume was already aligned, the stacks were only slightly realigned by manual correction. FIB-SEM stacks were aligned in FIJI (Schindelin et al. 2012) using the TrakEM2 plugin (Cardona et al. 2012). In Amira, structures of interest were segmented and transformed into 3D objects. Next, the segmentations were imported to Blender (Blender Institute, Amsterdam), where the 3D reconstructions were manually finished using the preliminary segmentation as a template.

FIB-SEM/SEM IMAGE PROCESSING

Micrographs were processed in FIJI/ImageJ (NIH, USA) for slight contrast and brightness adjustments.

ACKNOWLEDGEMENTS

This work was supported by the Deutsche Forschungsgemeinschaft (Grant No. 441181781, 426722269, 432195391), by EU funds from the ESF Plus Program (Grant No. 100649752) and by the Open Access Publishing Fund of Leipzig University supported by the German Research Foundation within the program Open Access Publication Funding.

We thank Dennis Pauls, Mareike Selcho, Tilman Triphan, Wolf Hütteroth, Denise Weber, Bert Klagges and Reini Stocker for discussions and comments.

COMPETING INTERESTS

The authors declare no competing interests.

DATA AVAILABILITY STATEMENT

The data that support the findings of this study are available from the corresponding author upon reasonable request.

REFERENCES

Altner, H.; Routil, C.; Loftus, R. (1981): The structure of bimodal chemo-, thermo-, and hygroreceptive sensilla on the antenna of Locusta migratoria. In *Cell and tissue research* 215 (2), pp. 289–308. DOI: 10.1007/BF00239116.

Altner, Helmut; Prillinger, Linde: Ultrastructure of Invertebrate Chemo-, Thermo-, and Hygroreceptors and Its Functional Significance 67, pp. 69–139. DOI: 10.1016/S0074-7696(08)62427-4.

Alves, Georges; Sallé, Jérémy; Chaudy, Sylvie; Dupas, Stéphane; Manière, Gérard (2014): High-NaCl perception in Drosophila melanogaster. In *J. Neurosci.* 34 (33), pp. 10884–10891. DOI: 10.1523/JNEUROSCI.4795-13.2014.

Apostolopoulou, Anthi A.; Köhn, Saskia; Stehle, Bernhard; Lutz, Michael; Wüst, Alexander; Mazija, Lorena et al. (2016): Caffeine Taste Signaling in Drosophila Larvae. In *Frontiers in cellular neuroscience* 10, p. 193. DOI: 10.3389/fncel.2016.00193.

Apostolopoulou, Anthi A.; Mazija, Lorena; Wüst, Alexander; Thum, Andreas S. (2014): The neuronal and molecular basis of quinine-dependent bitter taste signaling in Drosophila larvae. In *Frontiers in behavioral neuroscience* 8, p. 6. DOI: 10.3389/fnbeh.2014.00006.

Apostolopoulou, Anthi A.; Rist, Anna; Thum, Andreas S. (2015): Taste processing in Drosophila larvae. In *Frontiers in integrative neuroscience* 9, p. 50. DOI: 10.3389/fnint.2015.00050.

Bechstedt, S.; Albert, J. T.; Kreil, D. P.; Müller-Reichert, T.; Göpfert, M. C.; Howard, J. (2010): A doublecortin containing microtubule-associated protein is implicated in mechanotransduction in Drosophila sensory cilia. In *Nature communications* 1 (1), p. 11. DOI: 10.1038/ncomms1007.

Benz, G. (1956): Der Trockenheitssinn bei Larven vonDrosophila Melanogaster. In *Experientia* 12 (8), pp. 297–298. DOI: 10.1007/BF02159618.

Berck, Matthew E.; Khandelwal, Avinash; Claus, Lindsey; Hernandez-Nunez, Luis; Si, Guangwei; Tabone, Christopher J. et al. (2016): The wiring diagram of a glomerular olfactory system. DOI: 10.1101/037721.

Berni, Jimena; Pulver, Stefan R.; Griffith, Leslie C.; Bate, Michael (2012): Autonomous circuitry for substrate exploration in freely moving Drosophila larvae. In *Current biology : CB* 22 (20), pp. 1861–1870. DOI: 10.1016/j.cub.2012.07.048.

Brand, A. H.; Perrimon, N. (1993): Targeted gene expression as a means of altering cell fates and generating dominant phenotypes. In *Development* 118 (2), pp. 401–415. DOI: 10.1242/dev.118.2.401.

Bumbarger, Daniel J.; Riebesell, Metta; Rödelsperger, Christian; Sommer, Ralf J. (2013): System-wide rewiring underlies behavioral differences in predatory and bacterial-feeding nematodes. In *Cell* 152 (1-2), pp. 109–119. DOI: 10.1016/j.cell.2012.12.013.

Burgos, Anita; Honjo, Ken; Ohyama, Tomoko; Qian, Cheng Sam; Shin, Grace Ji-Eun; Gohl, Daryl M. et al. (2018): Nociceptive interneurons control modular motor pathways to promote escape behavior in Drosophila. In *eLife* 7. DOI: 10.7554/eLife.26016.

Campos-Ortega, J. A.; Hartenstein, Volker (1997): The embryonic development of Drosophila melanogaster. 2nd ed. Berlin, London: Springer. ISBN: 3540570799

Campos-Ortega, José A.; Hartenstein, Volker (1985): The Embryonic Development of Drosophila melanogaster. DOI: 10.1007/978-3-662-02454-6.

Cardona, Albert; Saalfeld, Stephan; Schindelin, Johannes; Arganda-Carreras, Ignacio; Preibisch, Stephan; Longair, Mark et al. (2012): TrakEM2 software for neural circuit reconstruction. In *PloS one* 7 (6), e38011. DOI: 10.1371/journal.pone.0038011.

Carreira-Rosario, Arnaldo; Zarin, Aref Arzan; Clark, Matthew Q.; Manning, Laurina; Fetter, Richard D.; Cardona, Albert; Doe, Chris Q. (2018): MDN brain descending neurons coordinately activate backward and inhibit forward locomotion. In *eLife* 7. DOI: 10.7554/eLife.38554.

Choi, Jaekyun; van Giesen, Lena; Choi, Min Sung; Kang, KyeongJin; Sprecher, Simon G.; Kwon, Jae Young (2016): A Pair of Pharyngeal Gustatory Receptor Neurons Regulates Caffeine-Dependent Ingestion in Drosophila Larvae. In *Frontiers in cellular neuroscience* 10, p. 181. DOI: 10.3389/fncel.2016.00181.

Chu, I. W.; Axtell, R. C. (1971): Fine structure of the dorsal organ of the house fly larva, Musca domestica L. In *Zeitschrift fur Zellforschung und mikroskopische Anatomie (Vienna, Austria : 1948)* 117 (1), pp. 17–34. DOI: 10.1007/BF00331098.

Chu-Wang, I. W.; Axtell, R. C. (1972a): Fine structure of the terminal organ of the house fly larva, Musca domestica L. In *Zeitschrift fur Zellforschung und mikroskopische Anatomie (Vienna, Austria : 1948)* 127 (3), pp. 287–305. DOI: 10.1007/BF00306874.

Chu-Wang, I. W.; Axtell, R. C. (1972b): Fine structure of the ventral organ of the house fly larva, Musca domestica L. In *Zeitschrift fur Zellforschung und mikroskopische Anatomie (Vienna, Austria : 1948)* 130 (4), pp. 489–495. DOI: 10.1007/BF00307003.

Colomb, Julien; Grillenzoni, Nicola; Ramaekers, Ariane; Stocker, Reinhard F. (2007): Architecture of the primary taste center of Drosophila melanogaster larvae. In *The Journal of comparative neurology* 502 (5), pp. 834–847. DOI: 10.1002/cne.21312.

Cook, Steven J.; Jarrell, Travis A.; Brittin, Christopher A.; Wang, Yi; Bloniarz, Adam E.; Yakovlev, Maksim A. et al. (2019): Whole-animal connectomes of both Caenorhabditis elegans sexes. In *Nature* 571 (7763), pp. 63–71. DOI: 10.1038/s41586-019-1352-7.

Courtney, Gregory W.; Sinclair, Bradley J.; Meier, Rudolf (2000): Morphology and terminology of Diptera larvae. With assistance of Lazló Papp, Béla Darvas. Budapest: Science Herald (Contributions to a manual of palaearctic diptera, Vol. 1).

Couto, Africa; Alenius, Mattias; Dickson, Barry J. (2005): Molecular, anatomical, and functional organization of the Drosophila olfactory system. In *Current biology : CB* 15 (17), pp. 1535–1547. DOI: 10.1016/j.cub.2005.07.034.

Croset, Vincent; Schleyer, Michael; Arguello, J. Roman; Gerber, Bertram; Benton, Richard (2016): A molecular and neuronal basis for amino acid sensing in the Drosophila larva. In *Scientific reports* 6, p. 34871. DOI: 10.1038/srep34871.

Dambly-Chaudière, Christine; Ghysen, Alain (1986): The sense organs in theDrosophila larva and their relation to the embryonic pattern of sensory neurons. In *Roux's archives of developmental biology : the official organ of the EDBO* 195 (4), pp. 222–228. DOI: 10.1007/BF02438954.

Denell, R. E.; Frederick, R. D. (1983): Homoeosis in Drosophila: a description of the Polycomb lethal syndrome. In *Developmental Biology* 97 (1), pp. 34–47. DOI: 10.1016/0012-1606(83)90061-1.

Denk, Winfried; Horstmann, Heinz (2004): Serial block-face scanning electron microscopy to reconstruct three-dimensional tissue nanostructure. In *PLoS Biology* 2 (11), e329. DOI: 10.1371/journal.pbio.0020329.

Eichler, Katharina; Li, Feng; Litwin-kumar, Ashok; Park, Youngser; Andrade, Ingrid; Schneider-Mizell, Casey M. et al. (2017): The complete connectome of a learning and memory centre in an insect brain. In *Nature* 548 (7666), pp. 175–182. DOI: 10.1038/nature23455.

Eschbach, Claire; Fushiki, Akira; Winding, Michael; Schneider-Mizell, Casey M.; Shao, Mei; Arruda, Rebecca et al. (2020): Recurrent architecture for adaptive regulation of learning in the insect brain. In *Nature neuroscience* 23 (4), pp. 544–555. DOI: 10.1038/s41593-020-0607-9.

Faucher, Cécile; Forstreuter, Manfred; Hilker, Monika; Bruyne, Marien de (2006): Behavioral responses of Drosophila to biogenic levels of carbon dioxide depend on life-stage, sex and olfactory context. In *The Journal of experimental biology* 209 (Pt 14), pp. 2739–2748. DOI: 10.1242/jeb.02297.

Fichelson, Pierre; Gho, Michel (2003): The glial cell undergoes apoptosis in the microchaete lineage of Drosophila. In *Development* 130 (1), pp. 123–133. DOI: 10.1242/dev.00198.

Fishilevich, Elane; Domingos, Ana I.; Asahina, Kenta; Naef, Félix; Vosshall, Leslie B.; Louis, Matthieu (2005): Chemotaxis behavior mediated by single larval olfactory neurons in Drosophila. In *Current biology : CB* 15 (23), pp. 2086–2096. DOI: 10.1016/j.cub.2005.11.016.

Gerber, Bertram; Stocker, Reinhard F. (2007): The Drosophila larva as a model for studying chemosensation and chemosensory learning: a review. In *Chemical senses* 32 (1), pp. 65–89. DOI: 10.1093/chemse/bjl030.

Gohl, Daryl M.; Silies, Marion A.; Gao, Xiaojing J.; Bhalerao, Sheetal; Luongo, Francisco J.; Lin, Chun-Chieh et al. (2011): A versatile in vivo system for directed dissection of gene expression patterns. In *Nature methods* 8 (3), pp. 231–237. DOI: 10.1038/nmeth.1561.

Gomez-Marin, Alex; Louis, Matthieu (2012): Active sensation during orientation behavior in the Drosophila larva: more sense than luck. In *Current opinion in neurobiology* 22 (2), pp. 208–215. DOI: 10.1016/j.conb.2011.11.008.

Green, C. H.; Burnet, B.; Connolly, K. J. (1983): Organization and patterns of inter- and intraspecific variation in the behaviour of Drosophila larvae. In *Animal Behaviour* 31 (1), pp. 282–291. DOI: 10.1016/s0003-3472(83)80198-5.

Green, P.; Hartenstein, V. (1997): Structure and spatial pattern of the sensilla of the body segments of insect larvae. In *Microscopy research and technique* 39 (6), pp. 470–478. DOI: 10.1002/(SICI)1097-0029(19971215)39:6<470::AID-JEMT2>3.0.CO;2-I.

Grillenzoni, Nicola; Vaux, Véronique de; Meuwly, Jocelyne; Vuichard, Séverine; Jarman, Andrew; Holohan, Eimear et al. (2007): Role of proneural genes in the formation of the larval olfactory organ of Drosophila. In *Dev Genes Evol* 217 (3), pp. 209–219. DOI: 10.1007/s00427-007-0135-6.

Hafez, M. (1950): On the behaviour and sensory physiology of the house-fly larva, Musca domestica L. I. Feeding stage. In *Parasitology* 40 (3-4), pp. 215–236. DOI: 10.1017/s0031182000018072.

Hartenstein, Volker (1988): Development of Drosophila larval sensory organs: spatiotemporal pattern of sensory neurones, peripheral axonal pathways and sensilla differentiation. In *Development* 102 (4), pp. 869–886. DOI: 10.1242/dev.102.4.869.

Heimbeck, G.; Bugnon, V.; Gendre, N.; Häberlin, C.; Stocker, R. F. (1999): Smell and taste perception in Drosophila melanogaster larva: toxin expression studies in chemosensory neurons. In *J. Neurosci.* 19 (15), pp. 6599–6609. DOI: 10.1523/JNEUROSCI.19-15-06599.1999.

Helmstaedter, Moritz; Briggman, Kevin L.; Denk, Winfried (2011): High-accuracy neurite reconstruction for high-throughput neuroanatomy. In *Nature neuroscience* 14 (8), pp. 1081–1088. DOI: 10.1038/nn.2868.

Helmstaedter, Moritz; Briggman, Kevin L.; Turaga, Srinivas C.; Jain, Viren; Seung, H. Sebastian; Denk, Winfried (2013): Connectomic reconstruction of the inner plexiform layer in the mouse retina. In *Nature* 500 (7461), pp. 168–174. DOI: 10.1038/nature12346.

Hernandez-Nunez, Luis; Chen, Alicia; Budelli, Gonzalo; Berck, Matthew E.; Richter, Vincent; Rist, Anna et al. (2021): Synchronous and opponent thermosensors use flexible cross-inhibition to orchestrate thermal homeostasis. In *Science advances* 7 (35). DOI: 10.1126/sciadv.abg6707.

Hertweck, H. (1931): Anatomie und Variabilität des Nervensystems und der Sinnesorgane von Drosophila melanogaster (Meigen).

Hilchen, Christian M. von; Beckervordersandforth, Ruth M.; Rickert, Christof; Technau, Gerhard M.; Altenhein, Benjamin (2008): Identity, origin, and migration of peripheral glial cells in the Drosophila embryo. In *Mechanisms of development* 125 (3-4), pp. 337–352. DOI: 10.1016/j.mod.2007.10.010.

Honda, Ikuro; Ishikawa, Yukio (1987): Ultrastructures of the Larval Cephalic Sensory Organs of the Onion and Seed-Corn Flies, Hylemya antiqua MEIGEN and H. platura MEIGEN : Diptera : Anthomyiidae. In *Appl. entomol. Zool* 22 (3), pp. 325–334. DOI: 10.1303/aez.22.325.

Hong, Ray L.; Riebesell, Metta; Bumbarger, Daniel J.; Cook, Steven J.; Carstensen, Heather R.; Sarpolaki, Tahmineh et al. (2019): Evolution of neuronal anatomy and circuitry in two highly divergent nematode species. In *eLife* 8. DOI: 10.7554/eLife.47155.

Hückesfeld, Sebastian; Schlegel, Philipp; Miroschnikow, Anton; Schoofs, Andreas; Zinke, Ingo; Haubrich, André N. et al. (2021): Unveiling the sensory and interneuronal pathways of the neuroendocrine connectome in Drosophila. In *eLife* 10. DOI: 10.7554/eLife.65745.

Humberg, Tim-Henning; Bruegger, Pascal; Afonso, Bruno; Zlatic, Marta; Truman, James W.; Gershow, Marc et al. (2018): Dedicated photoreceptor pathways in Drosophila larvae mediate navigation by processing either spatial or temporal cues. In *Nature communications* 9 (1), p. 1260. DOI: 10.1038/s41467-018-03520-5.

Jones, Walton D.; Cayirlioglu, Pelin; Kadow, Ilona Grunwald; Vosshall, Leslie B. (2007): Two chemosensory receptors together mediate carbon dioxide detection in Drosophila. In *Nature* 445 (7123), pp. 86–90. DOI: 10.1038/nature05466.

Joseph, Ryan M.; Carlson, John R. (2015): Drosophila Chemoreceptors: A Molecular Interface Between the Chemical World and the Brain. In *Trends in genetics : TIG* 31 (12), pp. 683–695. DOI: 10.1016/j.tig.2015.09.005.

Jovanic, Tihana; Schneider-Mizell, Casey Martin; Shao, Mei; Masson, Jean-Baptiste; Denisov, Gennady; Fetter, Richard Doty et al. (2016): Competitive Disinhibition Mediates Behavioral Choice and Sequences in Drosophila. In *Cell* 167 (3), 858-870.e19. DOI: 10.1016/j.cell.2016.09.009.

Jovanic, Tihana; Winding, Michael; Cardona, Albert; Truman, James W.; Gershow, Marc; Zlatic, Marta (2019): Neural Substrates of Drosophila Larval Anemotaxis. In *Current biology : CB* 29 (4), 554-566.e4. DOI: 10.1016/j.cub.2019.01.009.

Jürgens, Gerd (1987): Segmental organization of the tail region in the embryo of Drosophila melanogaster : A blastoderm fate map of the cuticle structures of the larval tail region. In *Roux's archives of developmental biology : the official organ of the EDBO* 196 (3), pp. 141–157. DOI: 10.1007/BF00376308.

Kankel, Douglas R. (1980): The structure and Development of the Nervous System.

Keil, Thomas A. (1997): Functional morphology of insect mechanoreceptors. In *Microscopy research and technique* 39 (6), pp. 506–531. DOI: 10.1002/(SICI)1097-0029(19971215)39:6<506::AID-JEMT5>3.0.CO;2-B.

Keilin, D. (1915): Recherches sur les larves de diptères cyclorrhaphes.

Kim, Daeyeon; Alvarez, Mar; Lechuga, Laura M.; Louis, Matthieu (2017): Species-specific modulation of food-search behavior by respiration and chemosensation in Drosophila larvae. In *eLife* 6. DOI: 10.7554/eLife.27057.

Kim, Sung Eun; Coste, Bertrand; Chadha, Abhishek; Cook, Boaz; Patapoutian, Ardem (2012): The role of Drosophila Piezo in mechanical nociception. In *Nature* 483 (7388), pp. 209–212. DOI: 10.1038/nature10801.

Klein, Mason; Afonso, Bruno; Vonner, Ashley J.; Hernandez-Nunez, Luis; Berck, Matthew; Tabone, Christopher J. et al. (2015): Sensory determinants of behavioral dynamics in Drosophila thermotaxis. In *Proceedings of the National Academy of Sciences of the United States of America* 112 (2), E220-9. DOI: 10.1073/pnas.1416212112.

Kreher, Scott A.; Kwon, Jae Young; Carlson, John R. (2005): The molecular basis of odor coding in the Drosophila larva. In *Neuron* 46 (3), pp. 445–456. DOI: 10.1016/j.neuron.2005.04.007.

Kuhn, D. T.; Sawyer, M.; Packert, G.; Turenchalk, G.; Mack, J. A.; Sprey, T. E. et al. (1992): Development of the D. melanogaster caudal segments involves suppression of the ventral regions of A8, A9 and A10. In *Development* 116 (1), pp. 11–20. DOI: 10.1242/dev.116.1.11.

Kwon, Jae Young; Dahanukar, Anupama; Weiss, Linnea A.; Carlson, John R. (2007): The molecular basis of CO2 reception in Drosophila. In *Proceedings of the National Academy of Sciences of the United States of America* 104 (9), pp. 3574–3578. DOI: 10.1073/pnas.0700079104.

Kwon, Jae Young; Dahanukar, Anupama; Weiss, Linnea A.; Carlson, John R. (2011): Molecular and cellular organization of the taste system in the Drosophila larva. In *J. Neurosci.* 31 (43), pp. 15300–15309. DOI: 10.1523/JNEUROSCI.3363-11.2011.

Lai, Sen-Lin; Lee, Tzumin (2006): Genetic mosaic with dual binary transcriptional systems in Drosophila. In *Nature neuroscience* 9 (5), pp. 703–709. DOI: 10.1038/nn1681.

Lakes, R.; Pollack, G. S. (1990): The development of the sensory organs of the legs in the blowfly, Phormia regina. In *Cell and tissue research* 259 (1), pp. 93–103. DOI: 10.1007/BF00571434.

Lakes-Harlan, R.; Pollack, G. S.; Merritt, D. J. (1991): From embryo to adult: anatomy and development of a leg sensory organ in Phormia regina, Meigen (Insecta: Diptera). II. Development and persistence of sensory neurons. In *The Journal of comparative neurology* 308 (2), pp. 200–208. DOI: 10.1002/cne.903080207.

Lanfranchi, Alberto; Belcari, Antonio (1990): Ultrastructure of Keilin's sense organ of Ceratitis capitata (Wiedemann) larva (Diptera : Tephritidae). In *International Journal of Insect Morphology and Embryology* 19 (3-4), pp. 187–194. DOI: 10.1016/0020-7322(90)90004-9.

Larderet, Ivan; Fritsch, Pauline Mj; Gendre, Nanae; Neagu-Maier, G. Larisa; Fetter, Richard D.; Schneider-Mizell, Casey M. et al. (2017): Organization of the Drosophila larval visual circuit. In *eLife* 6. DOI: 10.7554/eLife.28387.

Lewis, E. B. (1978): A gene complex controlling segmentation in Drosophila. In *Nature* 276 (5688), pp. 565–570. DOI: 10.1038/276565a0.

Li, Hsing-Hsi; Kroll, Jason R.; Lennox, Sara M.; Ogundeyi, Omotara; Jeter, Jennifer; Depasquale, Gina; Truman, James W. (2014): A GAL4 driver resource for developmental and behavioral studies on the larval CNS of Drosophila. In *Cell reports* 8 (3), pp. 897–908. DOI: 10.1016/j.celrep.2014.06.065.

Liu, Lei; Yermolaieva, Olena; Johnson, Wayne A.; Abboud, Francois M.; Welsh, Michael J. (2003): Identification and function of thermosensory neurons in Drosophila larvae. In *Nature neuroscience* 6 (3), pp. 267–273. DOI: 10.1038/nn1009.

Lohs-Schardin, M.; Cremer, C.; Nüsslein-Volhard, C. (1979): A fate map for the larval epidermis of Drosophila melanogaster: localized cuticle defects following irradiation of the blastoderm with an ultraviolet laser microbeam. In *Developmental Biology* 73 (2), pp. 239–255. DOI: 10.1016/0012-1606(79)90065-4.

Luan, Haojiang; Peabody, Nathan C.; Vinson, Charles R.; White, Benjamin H. (2006): Refined spatial manipulation of neuronal function by combinatorial restriction of transgene expression. In *Neuron* 52 (3), pp. 425–436. DOI: 10.1016/j.neuron.2006.08.028.

Masson, Jean-Baptiste; Laurent, François; Cardona, Albert; Barré, Chloé; Skatchkovsky, Nicolas; Zlatic, Marta; Jovanic, Tihana (2020): Identifying neural substrates of competitive interactions and sequence transitions during mechanosensory responses in Drosophila. In *PLoS genetics* 16 (2), e1008589. DOI: 10.1371/journal.pgen.1008589.

Mast, Joshua D.; Moraes, Consuelo M. de; Alborn, Hans T.; Lavis, Luke D.; Stern, David L. (2014): Evolved differences in larval social behavior mediated by novel pheromones. In *eLife* 3, e04205. DOI: 10.7554/eLife.04205.

Melcher, Christoph; Bader, Ruediger; Pankratz, Michael J. (2007): Amino acids, taste circuits, and feeding behavior in Drosophila: towards understanding the psychology of feeding in flies and man. In *The Journal of endocrinology* 192 (3), pp. 467–472. DOI: 10.1677/JOE-06-0066.

Miller, Carson J.; Carlson, John R. (2010): Regulation of odor receptor genes in trichoid sensilla of the Drosophila antenna. In *Genetics* 186 (1), pp. 79–95. DOI: 10.1534/genetics.110.117622.

Miroschnikow, Anton; Schlegel, Philipp; Schoofs, Andreas; Hueckesfeld, Sebastian; Li, Feng; Schneider-Mizell, Casey M. et al. (2018): Convergence of monosynaptic and polysynaptic sensory paths onto common motor outputs in a Drosophila feeding connectome. In *eLife* 7. DOI: 10.7554/eLife.40247.

Mishra, Dushyant; Miyamoto, Tetsuya; Rezenom, Yohannes H.; Broussard, Alex; Yavuz, Ahmet; Slone, Jesse et al. (2013): The molecular basis of sugar sensing in Drosophila larvae. In *Current biology : CB* 23 (15), pp. 1466–1471. DOI: 10.1016/j.cub.2013.06.028.

Mishra, Dushyant; Thorne, Natasha; Miyamoto, Chika; Jagge, Christopher; Amrein, Hubert (2018): The taste of ribonucleosides: Novel macronutrients essential for larval growth are sensed by Drosophila gustatory receptor proteins. In *PLoS Biology* 16 (8), e2005570. DOI: 10.1371/journal.pbio.2005570.

Morton, David B.; Stewart, Judith A.; Langlais, Kristofor K.; Clemens-Grisham, Rachel A.; Vermehren, Anke (2008): Synaptic transmission in neurons that express the Drosophila atypical soluble guanylyl cyclases, Gyc-89Da and Gyc-89Db, is necessary for the successful completion of larval and adult ecdysis. In *The Journal of experimental biology* 211 (Pt 10), pp. 1645–1656. DOI: 10.1242/jeb.014472.

Motta, Alessandro; Berning, Manuel; Boergens, Kevin M.; Staffler, Benedikt; Beining, Marcel; Loomba, Sahil et al. (2019): Dense connectomic reconstruction in layer 4 of the somatosensory cortex. In *Science (New York, N.Y.)* 366 (6469). DOI: 10.1126/science.aay3134.

Nava Gonzales, Cesar; McKaughan, Quintyn; Bushong, Eric A.; Cauwenberghs, Kalyani; Ng, Renny; Madany, Matthew et al. (2021): Systematic morphological and morphometric analysis of identified olfactory receptor neurons in Drosophila melanogaster. In *eLife* 10. DOI: 10.7554/eLife.69896.

Ni, Lina; Klein, Mason; Svec, Kathryn V.; Budelli, Gonzalo; Chang, Elaine C.; Ferrer, Anggie J. et al. (2016): The Ionotropic Receptors IR21a and IR25a mediate cool sensing in Drosophila. In *eLife* 5. DOI: 10.7554/eLife.13254.

Ohyama, Tomoko; Schneider-Mizell, Casey M.; Fetter, Richard D.; Aleman, Javier Valdes; Franconville, Romain; Rivera-Alba, Marta et al. (2015): A multilevel multimodal circuit enhances action selection in Drosophila. In *Nature* 520 (7549), pp. 633–639. DOI: 10.1038/nature14297.

Oppliger, F. Y.; M Guerin, P.; Vlimant, M. (2000): Neurophysiological and behavioural evidence for an olfactory function for the dorsal organ and a gustatory one for the terminal organ in Drosophila melanogaster larvae. In *Journal of insect physiology* 46 (2), pp. 135–144. DOI: 10.1016/s0022-1910(99)00109-2.

Park, Jeong-Ho; Kwon, Jae Young (2011): Heterogeneous expression of Drosophila gustatory receptors in enteroendocrine cells. In *PloS one* 6 (12), e29022. DOI: 10.1371/journal.pone.0029022.

Peddie, Christopher J.; Collinson, Lucy M. (2014): Exploring the third dimension: volume electron microscopy comes of age. In *Micron (Oxford, England : 1993)* 61, pp. 9–19. DOI: 10.1016/j.micron.2014.01.009.

Pfeiffer, Barret D.; Ngo, Teri-T B.; Hibbard, Karen L.; Murphy, Christine; Jenett, Arnim; Truman, James W.; Rubin, Gerald M. (2010): Refinement of tools for targeted gene expression in Drosophila. In *Genetics* 186 (2), pp. 735–755. DOI: 10.1534/genetics.110.119917.

Prelic, Sinisa; Pal Mahadevan, Venkatesh; Venkateswaran, Vignesh; Lavista-Llanos, Sofia; Hansson, Bill S.; Wicher, Dieter (2021): Functional Interaction Between Drosophila Olfactory Sensory Neurons and Their Support Cells. In *Front. Cell. Neurosci.* 15, p. 789086. DOI: 10.3389/fncel.2021.789086.

Python, François; Stocker, Reinhard F. (2002): Adult-like complexity of the larval antennal lobe of D. melanogaster despite markedly low numbers of odorant receptor neurons. In *The Journal of comparative neurology* 445 (4), pp. 374–387. DOI: 10.1002/cne.10188.

Rimal, S.; Lee, Y. (2018): The multidimensional ionotropic receptors of Drosophila melanogaster. In *Insect molecular biology* 27 (1), pp. 1–7. DOI: 10.1111/imb.12347.

Rist, Anna; Thum, Andreas S. (2017): A map of sensilla and neurons in the taste system of drosophila larvae. In *The Journal of comparative neurology* 525 (18), pp. 3865–3889. DOI: 10.1002/cne.24308.

Rohwedder, Astrid; Pfitzenmaier, Johanna E.; Ramsperger, Noel; Apostolopoulou, Anthi A.; Widmann, Annekathrin; Thum, Andreas S. (2012): Nutritional value-dependent and nutritional value-independent effects on Drosophila melanogaster larval behavior. In *Chemical senses* 37 (8), pp. 711–721. DOI: 10.1093/chemse/bjs055.

Ryan, Kerrianne; Lu, Zhiyuan; Meinertzhagen, Ian A. (2016): The CNS connectome of a tadpole larva of Ciona intestinalis (L.) highlights sidedness in the brain of a chordate sibling. In *eLife* 5. DOI: 10.7554/eLife.16962.

Sato, T.; Denell, R. E. (1985): Homoeosis in Drosophila: anterior and posterior transformations of Polycomb lethal embryos. In *Developmental Biology* 110 (1), pp. 53–64. DOI: 10.1016/0012-1606(85)90063-6.

Scheffer, Louis K.; Xu, C. Shan; Januszewski, Michal; Lu, Zhiyuan; Takemura, Shin-Ya; Hayworth, Kenneth J. et al. (2020): A connectome and analysis of the adult Drosophila central brain. In *eLife* 9. DOI: 10.7554/eLife.57443.

Schieber, Nicole L.; Machado, Pedro; Markert, Sebastian M.; Stigloher, Christian; Schwab, Yannick; Steyer, Anna M. (2017): Minimal resin embedding of multicellular specimens for targeted FIB-SEM imaging. In *Methods in cell biology* 140, pp. 69–83. DOI: 10.1016/bs.mcb.2017.03.005.

Schindelin, Johannes; Arganda-Carreras, Ignacio; Frise, Erwin; Kaynig, Verena; Longair, Mark; Pietzsch, Tobias et al. (2012): Fiji: an open-source platform for biological-image analysis. In *Nature methods* 9 (7), pp. 676–682. DOI: 10.1038/nmeth.2019.

Schlegel, Philipp; Texada, Michael J.; Miroschnikow, Anton; Schoofs, Andreas; Hückesfeld, Sebastian; Peters, Marc et al. (2016): Synaptic transmission parallels neuromodulation in a central food-intake circuit. In *eLife* 5. DOI: 10.7554/eLife.16799.

Schlegel, Philipp; Yin, Yijie; Bates, Alexander Shakeel; Dorkenwald, Sven; Eichler, Katharina; Brooks, Paul et al. (2023): Whole-brain annotation and multi-connectome cell typing quantifies circuit stereotypy in Drosophila. In *bioRxiv : the preprint server for biology*. DOI: 10.1101/2023.06.27.546055.

Schmidt-Ott, U.; González-Gaitán, M.; Jäckle, H.; Technau, G. M. (1994): Number, identity, and sequence of the Drosophila head segments as revealed by neural elements and their deletion patterns in mutants. In *Proceedings of the National Academy of Sciences of the United States of America* 91 (18), pp. 8363–8367. DOI: 10.1073/pnas.91.18.8363.

Scholz, Nicole; Gehring, Jennifer; Guan, Chonglin; Ljaschenko, Dmitrij; Fischer, Robin; Lakshmanan, Vetrivel et al. (2015): The adhesion GPCR latrophilin/CIRL shapes mechanosensation. In *Cell reports* 11 (6), pp. 866–874. DOI: 10.1016/j.celrep.2015.04.008.

Scholz, Nicole; Guan, Chonglin; Nieberler, Matthias; Grotemeyer, Alexander; Maiellaro, Isabella; Gao, Shiqiang et al. (2017): Mechano-dependent signaling by Latrophilin/CIRL quenches cAMP in proprioceptive neurons. In *eLife* 6. DOI: 10.7554/eLife.28360.

Schoofs, Andreas; Miroschnikow, Anton; Schlegel, Philipp; Zinke, Ingo; Schneider-Mizell, Casey M.; Cardona, Albert; Pankratz, Michael J. (2023): Serotonergic reinforcement of a complete swallowing circuit. DOI: 10.1101/2023.05.26.542464.

Selcho, Mareike; Pauls, Dennis; Han, Kyung-An; Stocker, Reinhard F.; Thum, Andreas S. (2009): The role of dopamine in Drosophila larval classical olfactory conditioning. In *PloS one* 4 (6), e5897. DOI: 10.1371/journal.pone.0005897.

Shanbhag, S. R.; Müller, B.; Steinbrecht, R. A. (2000): Atlas of olfactory organs of Drosophila melanogaster 2. Internal organization and cellular architecture of olfactory sensilla. In *Arthropod structure & development* 29 (3), pp. 211–229. DOI: 10.1016/s1467-8039(00)00028-1.

Singh, R. N. (1997): Neurobiology of the gustatory systems of Drosophila and some terrestrial insects. In *Microscopy research and technique* 39 (6), pp. 547–563. DOI: 10.1002/(SICI)1097-0029(19971215)39:6<547::AID-JEMT7>3.0.CO;2-A.

Singh, R.Naresh; Singh, Kusum (1984): Fine structure of the sensory organs of Drosophila melanogaster Meigen larva (Diptera : Drosophilidae). In *International Journal of Insect Morphology and Embryology* 13 (4), pp. 255–273. DOI: 10.1016/0020-7322(84)90001-1.

Steinbrecht, Rudolf Alexander (1984): Chemo-, Hygro-, and Thermoreceptors, pp. 523–553. DOI: 10.1007/978-3-642-51593-4_28.

Takagi, Suguru; Cocanougher, Benjamin Thomas; Niki, Sawako; Miyamoto, Dohjin; Kohsaka, Hiroshi; Kazama, Hokto et al. (2017): Divergent Connectivity of Homologous Command-like Neurons Mediates Segment-Specific Touch Responses in Drosophila. In *Neuron* 96 (6), 1373-1387.e6. DOI: 10.1016/j.neuron.2017.10.030.

Tastekin, Ibrahim; Riedl, Julia; Schilling-Kurz, Verena; Gomez-Marin, Alex; Truman, James W.; Louis, Matthieu (2015): Role of the subesophageal zone in sensorimotor control of orientation in Drosophila larva. In *Current biology : CB* 25 (11), pp. 1448–1460. DOI: 10.1016/j.cub.2015.04.016.

Thorne, Natasha; Amrein, Hubert (2008): Atypical expression of Drosophila gustatory receptor genes in sensory and central neurons. In *The Journal of comparative neurology* 506 (4), pp. 548–568. DOI: 10.1002/cne.21547.

Thum, Andreas S.; Gerber, Bertram (2019): Connectomics and function of a memory network: the mushroom body of larval Drosophila. In *Current opinion in neurobiology* 54, pp. 146–154. DOI: 10.1016/j.conb.2018.10.007.

Thurm, U. (1964): MECHANORECEPTORS IN THE CUTICLE OF THE HONEY BEE: FINE STRUCTURE AND STIMULUS MECHANISM. In *Science (New York, N.Y.)* 145 (3636), pp. 1063–1065. DOI: 10.1126/science.145.3636.1063.

Tichy, H.; Kallina, W. (2010): Insect hygroreceptor responses to continuous changes in humidity and air pressure. In *Journal of neurophysiology* 103 (6), pp. 3274–3286. DOI: 10.1152/jn.01043.2009.

Tirian, Laszlo; Dickson, Barry J. (2017): The VT GAL4, LexA, and split-GAL4 driver line collections for targeted expression in the Drosophila nervous system. DOI: 10.1101/198648.

Titze, Benjamin; Genoud, Christel (2016): Volume scanning electron microscopy for imaging biological ultrastructure. In *Biology of the cell* 108 (11), pp. 307–323. DOI: 10.1111/boc.201600024.

Tracey, W. Daniel; Wilson, Rachel I.; Laurent, Gilles; Benzer, Seymour (2003): painless, a Drosophila gene essential for nociception. In *Cell* 113 (2), pp. 261–273. DOI: 10.1016/s0092-8674(03)00272-1.

van Giesen, Lena; Hernandez-Nunez, Luis; Delasoie-Baranek, Sophie; Colombo, Martino; Renaud, Philippe; Bruggmann, Rémy et al. (2016): Multimodal stimulus coding by a gustatory sensory neuron in Drosophila larvae. In *Nature communications* 7, p. 10687. DOI: 10.1038/ncomms10687.

van Goes Naters, Wynand; Carlson, John R. (2007): Receptors and neurons for fly odors in Drosophila. In *Current biology : CB* 17 (7), pp. 606–612. DOI: 10.1016/j.cub.2007.02.043.

Verasztó, Csaba; Jasek, Sanja; Gühmann, Martin; Shahidi, Réza; Ueda, Nobuo; Beard, James David et al. (2020): Whole-animal connectome and cell-type complement of the three-segmented Platynereis dumerilii larva. DOI: 10.1101/2020.08.21.260984.

Vermehren-Schmaedick, Anke; Ainsley, Joshua A.; Johnson, Wayne A.; Davies, Shireen-A; Morton, David B. (2010): Behavioral responses to hypoxia in Drosophila larvae are mediated by atypical soluble guanylyl cyclases. In *Genetics* 186 (1), pp. 183–196. DOI: 10.1534/genetics.110.118166.

White, J. G.; Southgate, E.; Thomson, J. N.; Brenner, S. (1986): The structure of the nervous system of the nematode Caenorhabditis elegans. In *Philosophical transactions of the Royal Society of London. Series B, Biological sciences* 314 (1165), pp. 1–340. DOI: 10.1098/rstb.1986.0056.

Whittle, J. R.; Tiong, S. Y.; Sunkel, C. E. (1986): The effect of lethal mutations and deletions within the bithorax complex upon the identity of caudal metameres in the Drosophila embryo. In *Journal of embryology and experimental morphology* 93, pp. 153–166. PubmedID: 3090188

Widmann, Annekathrin; Eichler, Katharina; Selcho, Mareike; Thum, Andreas S.; Pauls, Dennis (2018): Odor-taste learning in Drosophila larvae. In *Journal of insect physiology* 106 (Pt 1), pp. 47–54. DOI: 10.1016/j.jinsphys.2017.08.004.

Winding, Michael; Pedigo, Benjamin D.; Barnes, Christopher L.; Patsolic, Heather G.; Park, Youngser; Kazimiers, Tom et al. (2022): The connectome of an insect brain. DOI: 10.1101/2022.11.28.516756.

Wipfler, Benjamin; Schneeberg, Katharina; Löffler, Andreas; Hünefeld, Frank; Meier, Rudolf; Beutel, Rolf G. (2013): The skeletomuscular system of the larva of Drosophila melanogaster (Drosophilidae, Diptera): a contribution to the morphology of a model organism. In *Arthropod structure & development* 42 (1), pp. 47–68. DOI: 10.1016/j.asd.2012.09.005.

Yack, Jayne E. (2004): The structure and function of auditory chordotonal organs in insects. In *Microscopy research and technique* 63 (6), pp. 315–337. DOI: 10.1002/jemt.20051.

Yan, Zhiqiang; Zhang, Wei; He, Ye; Gorczyca, David; Xiang, Yang; Cheng, Li E. et al. (2013): Drosophila NOMPC is a mechanotransduction channel subunit for gentle-touch sensation. In *Nature* 493 (7431), pp. 221–225. DOI: 10.1038/nature11685.

Zacharuk, R. Y. (1972): Fine structure of the cuticle, epidermis, and fat body of larval Elateridae (Coleoptera) and changes associated with molting. In *Can. J. Zool.* 50 (11), pp. 1463–1487. DOI: 10.1139/z72-195.

Zheng, Zhihao; Lauritzen, J. Scott; Perlman, Eric; Robinson, Camenzind G.; Nichols, Matthew; Milkie, Daniel et al. (2018): A Complete Electron Microscopy Volume of the Brain of Adult Drosophila melanogaster. In *Cell* 174 (3), 730-743.e22. DOI: 10.1016/j.cell.2018.06.019.

Zhong, Lixian; Hwang, Richard Y.; Tracey, W. Daniel (2010): Pickpocket is a DEG/ENaC protein required for mechanical nociception in Drosophila larvae. In *Current biology : CB* 20 (5), pp. 429–434. DOI: 10.1016/j.cub.2009.12.057.

TABLE LEGENDS

Table 1: Summary of morphological features of head sensory organs of third instar *Drosophila* larvae

* Singh & Singh (1984) report the VO to consist of five sensilla

** adopted from Rist & Thum (2017)

Table 2: Summary of morphological findings of this study for sensilla of thoracic and abdominal segments of first (L1) and third (L3) instar larvae.

[1] Hertweck (1931); [2] Lewis et al. (1978); [3] Lohs-Shardin et al. (1979); [4] Kankel et al. (1980); [5] Singh & Singh (1984); [6] Sato et al. (1985); [7] Campos-Ortega & Hartenstain (1985); [8] Dambly-Chaudiere & Ghysen (1986); [9] Hartenstein (1988); [10] Green & Hartenstein (1997); [11] Jürgens (1987); abbreviations: t - terminal sensory cones, tb - tubular body.

FIGURE LEGENDS

Figure 1: Larval body organization and a spatial map of external and chordotonal sense organs. A) Ventral view of an L3 Drosophila larva. The larval body is divided into the pseudocephalon (pce), three thoracic (T1-T3), and nine abdominal (A1-A9) segments. A') Latero-frontal view of the pce. Major sensory organs of the head are bilaterally organized and consist of several sensilla: the dorsal organ (DO) and terminal organ (TO) on the tip of the head lobes; the ventral organ (VO) located between rows of cuticle hairs; the labial organ (LO) below the mouth opening. A'') Lateral view of the last fused abdominal segments A8 and A9, called the anal division. Sensilla in this region are organized in terminal sensory cones (t1-t7). On the ventral side, the anal plate (ap) is visible; towards the posterior end, the posterior spiracles are located. B) Map of sensilla on pseudocephalon, thoracic and abdominal segments. We categorized types of sensilla as papilla (p)-, knob (k)- and hair (h) sensilla. The major head organs, the keilin's organ (KO), the terminal sensory cones and the spiracle sense organ (sp) are formed by several sensilla. The organization of sensilla is bilateral. Sensilla have fixed positions on hemisegments; therefore, all segments exhibit a fixed sensillar pattern. We noticed varying arrangements for T1, T2-T3, and A1-A7, with a consistent sequence of sensilla in each configuration. The pseudocephalon and the anal division display a structural organization very different from the other segments. The schematic summarizes the result of our investigation and includes results from previous studies (Dambly-Chaudière and Ghysen, 1986; Green and Hartenstein, 1997). C) Map of neurons innervating the external sense organs and the chordotonal organs. Again, the results and names from previous studies (Dambly-Chaudière and Ghysen 1986; Green and Hartenstein 1997) were used but slightly modified to create a standardized nomenclature (see discussion). Scale bars: A) 500 µm. Abbreviations: TOG – terminal organ ganglion; DOG – dorsal organ ganglion; VOG – ventral organ ganglion; LOG – labial organ ganglion. For the nomenclature of neurons in (C), see discussion.

Figure 2: Ultrastructure of the dorsal organ – an overview. A) 3D reconstruction of a representative dorsal organ of an L1 larva highlighting its position at the larval body (top) and its cell type organization. Color scheme: yellow- olfactory receptor neuron (ORN); –

purple – chordotonal organ (ChO); blue – $DO_{p3/5/6}$ cooling cell; orange – $DO_{p3/5/6}$ warming cell; turquoise – $DO_{p1/2/4}$ mechanosensory cell; red – $DO_{p2/4}$ unknown sensory cell. Color code in (A) applies to all micrographs in Figures 2-6 **B)** SEM image depicting the outer morphology of the dorsal organ in an L3 larva. The dome is covered by multiple tiny perforations (pf). Three of the seven molting pores, which are traces of ecdysis, are visible. **C)** Reconstruction of the peripheral and olfactory sensilla of the DO from their sensory tip to their cell body in the DOG. **D)** L3: Cross section of the dome with tiny perforations and molting pores. The olfactory triplets are still visible, but dendritic branching is already present at this level. **E)** L1: longitudinal section of the dome with tiny perforations but absent molting pores, as ecdysis has not occurred yet. The olfactory dendrites are branched and spread throughout the dome. **F)** L3: ganglion of the dorsal organ, showing exemplary peripheral (p) and olfactory (asterisks) cell bodies **G)** L1: ganglion of the dorsal organ, showing exemplary peripheral (p) and olfactory (asterisks) cell bodies. Scale bars: (B) 2 µm; (D) 5 µm; (E) 2 µm; (F) 5 µm; (G) 10 µm. Abbreviations: d - dendritic branches; mp - molting pores; p –peripheral cell bodies; pf – perforations.

Figure 3: Ultrastructure of the dorsal organ – olfactory sensilla A) 3D reconstruction of a dorsal organ of an L1 larva showing its position at the larval body (top) and one exemplary triplet of olfactory receptor neurons (ORNs) (yellow, bottom). The color code in A applies to all micrographs in this Figure. **B)** L1: A longitudinal section through the base of the dorsal organ showing seven olfactory triplets bathed in the outer sensillum lymph (osl). Peripheral sensilla (DO_p) 1, 2 and 6 are visible **C)** L3: A cross section through the base of the dorsal organ showing seven olfactory triplets and all peripheral sensilla 1 to 6. **D)** L1: olfactory triplet at the level of the inner sensillum lymph (isl) cavity. **E)** L3: olfactory triplets further proximal than in C. **F)** L1: dendritic inner segments of the olfactory triplet bathed in the isl. The thecogen support cell is highly lamellated (lm). **G)** L1: longitudinal section through an olfactory sensillum from dendritic branching (b) in the dome through osl where the dendrite is enclosed by a dendritic sheath (ds) to the ciliary constriction (cc) at the transition from the outer to the inner dendritic segment inside the isl cavity. Scale bars: (B) 2 µm; (C) 5 µm; (D) 1 µm; (E) 5 µm; (F) 1 µm; (G) 5 µm. Abbreviations: $DO_{p1\text{-}p6}$ – peripheral sensilla 1 to 6; b – (dendritic) branching; cc - ciliary constriction; d - dendrite; ds - dendritic sheath; inner sensillum lymph – isl; lc - lymph cavity; lm – lamellation; osl – outer sensillum lymph; ORN – olfactory receptor neuron.

Figure 4: Ultrastructure of the dorsal organ – peripheral sensilla 1, 2 and 4. A) 3D reconstruction of a dorsal organ of an L1 larva showing its position at the larval body (top) and the peripheral sensilla $DO_{p1/2/4}$ and their innervating neurons $DO_{p1/2/4\text{-}A}$ and $DO_{p2/4\text{-}B}$ (bottom). The color code in A applies to all micrographs in this Figure. **B)** DOp1 at the sensory tip with the sensory dendrite Dop1A containing a tubular body (tb). The dendrite is enclosed by a dendritic sheath (ds). **C)** DO_{p1A} at the level of the ciliary constriction (cc) inside the inner sensillum lymph (isl) cavity. **D)** DO_{p2} at the sensory tip with ds, the dendrite of DO_{p2B} does not contain a tb in contrast to DO_{p2A}. **D')** DO_{p2A} at the sensory tip with tb. **E)** DO_{p2A}

and DO_{p2B} at the level of the cc inside the isl cavity. **F)** DO_{p4} at the sensory tip with ds. DO_{p4A} contains a tb, whereas DO_{p4B} does not. **G)** DO_{p4A} and DO_{p4B} at the level of cc bathed in the isl. Scale bars: (B) 1 µm; (C) 1 µm (D) 1 µm; (E) 1 µm; (F) 1 µm; (G) 1 µm. Abbreviations: tb - tubular body; ds - dendritic sheath; cc - ciliary construction; isl - inner sensillum lymph.

Figure 5: Ultrastructure of the dorsal organ – peripheral sensilla 3, 5 and 6. A) 3D reconstruction of a dorsal organ of an L1 larva showing its position at the larval body (top) and the peripheral sensilla $DO_{p3/5/6}$, which exhibit the same morphology (bottom). $DO_{p3/5/6}$ are innervated by their corresponding neurons $DO_{p3/5/6\text{-}A}$ and $DO_{p3/5/6\text{-}B}$. The color code in A applies to all micrographs in this Figure. **B)** DO_{p3B} is enclosed by a dendritic sheath (ds), which is connected to the epicuticle. **C)** DO_{p3} further proximal with DO_{p3A} enclosed by a dendritic sheath and a thecogen cell. **D-G)** DO_{p3A} enters the inner sensillum lymph (isl) cavity formed by the thecogen cell; the ds is no longer visible. The dendrite is transforming from the outer to the inner dendritic segment through a ciliary constriction (cc). The same is true for the dendrite of DO_{p3B}, but it is not projecting through the ds towards the cuticle. Instead, it forms a lamellated bulbous structure within the lymph cavity, the dendritic bulb (db). **D)** longitudinal section of peripheral sensillum DO_{p5} at the level of the isl cavity, which is formed by thecogen cell. **E)** Longitudinal section of DO_{p3} at the level of the isl cavity. DO_{p3B} is enters the cavity proximally, where it transforms from an enlarged inner dendritic segment (ids) to a ciliary outer dendritic segment (ods). The cilium forms a lamellated db inside the cavity. DO_{p3A} appears rather inconspicuously but protrudes towards the cuticle in contrast to DO_{p3B}. **F)** Close-up view of the isl cavity in D), the db of DO_{p5B} is visible. DO_{p5A} is projecting inside the ds towards the cuticle. **G)** L3: peripheral sensillum DO_{p3} at the ciliary constriction. Both ids are heavily swollen. Scale bars: (B) 0.5 µm; (C) 0.5 µm; (D) 5 µm; (E) 2 µm; (F) 1 µm; (G) 2 µm. Abbreviations: db - dendritic bulb; ds - dendritic sheath; cc - ciliary constriction; isl - inner sensillum lymph.

Figure 6: Ultrastructure of the dorsal organ – the chordotonal organ. A) 3D reconstruction of a dorsal organ of an L1 larva showing the position of the chordotonal organ dCh_{1A} at the larval body (top) and its cellular organization (bottom). The color code in A applies to all micrographs in this Figure. **B)** Longitudinal section of dCh_{1A} at left DO (white box) within the whole larval volume. **C)** Cross section of dCh_{1A} at right DO (white box) within the whole larval volume. **D)** Presentation of the white box shown in B at higher magnification. The dendrite (purple) is inserted into the scolopale made of the scolopale rods (sr). The dendritic inner segment (dis) and the cilium with a ciliary dilation (cd) are visible. The cilium is inserted into a cap at the distal end. **E)** Presentation of the white box shown in C at higher magnification. The sr enclose the inner sensillum lymph (isl), in which the cilium is bathed. **F)** Dis of dCh_{1A} with striated ciliary rootlet (ro). **G)** The dCh_{1A} is also present in L3 larvae (white arrow). Scale bars: (B) 5 µm; (C) 5 µm; (D) 2 µm; (E) 1 µm; (F) 1 µm; (G) 5 µm. Abbreviations: cd – ciliary dilation; ChO – chordotonal organ; dis – dendritic inner segment; isl - inner sensillum lymph; ro - ciliary rootlet; sr - scolopale rods.

Figure 7: Ultrastructure of the dorsal organ – the sensilla and associated support cells. A) Overview of the dorsal organ proximal to the sensory dome (to the upper left corner). **B)**

Schematic drawing of A) defining all olfactory and peripheral sensilla and their associated support cells. All sensilla possess their individual set of support cells. The thecogen cells form an inner sensillum lymph space for each individual sensillum. The trichogen and tormogen cells wrap around the thecogen cell and contribute to the sensillar integrity. In addition, the olfactory support cells build up a common outer sensillum lymph space (asterisk). Abbreviations: DO_{p1-p6} – dorsal organ peripheral sensilla 1 to 6; Scale bar: 2 µm.

Figure 8: Ultrastructure of the ventral organ. A) 3D reconstruction of the ventral organ of an L1 larva (bottom). The outline shows the position of this organ on the larval head (top). B, D, E: (FIB)-SEM images of L3 larvae; C, F, G, H: ssTEM images of L1 larvae. The color code in A applies to all micrographs in this Figure. **B)** Electron micrograph of the ventral organ in L3 larva consisting of four sensilla, which were named VO_1-VO_4. VO_1 is arched outwards like a dome, whereas VO_{2-4} lie in small depressions. **C)** Cross section of the ventral organ in an L1 larva. $VO_{1/3/4}$ possess a tubular body each (tb; white arrowheads). VO_2 consists of a cuticle tube (ct) with a terminal pore. C') tubular body of VO_3. C'') tubular body of VO_1. **D)** Cross section through the base of VO_4 in an L3 larva. The dendrite with tb and dendritic sheath (ds) is anchored in the cuticle by electron-dense material. A putative molting pore (mp) can be observed. **E)** VO_2 in an L3 larva. The pore channel is streaked by fine dendritic branches (b). **F)** Cross section through the ventral organ further proximal than in C). **G)** Schematic drawing of F), showing the associated sensory and support cells. **H and I)** Micrograph (I) and schematic drawing (H) of the ventral organ further proximal than F) at the level of the ganglion, defining the sensory cells and the associated support cells. The two dendrites of VO_2 become clearly visible when the pore enters a greater cavity formed by the thecogen cell. The dendrites then penetrate the thecogen cell, which exhibits a particular appearance like the support cells of the pit sensilla of the terminal organ (not shown). Those cells appear to be electron-lucent (asterisks), and their mitochondria exhibit a tubular (white arrowhead) instead of a cristae type (black arrowhead). Scale bars: (B) 1 µm; (C) 1 µm, inlets 0.5 µm; (D) 0.5 µm; (E) 0.5 µm; (F) 1 µm; (G) 2 µm; (H) 2 µm. Abbreviations: b – dendritic branches; ds - dendritic sheath; ct - cuticle tube; mp – molting pore; tb - tubular body.

Figure 9: Ultrastructure of the labial organ. A) 3D reconstruction of the labial organ of an L1 larva (bottom). The outline shows the position of this organ on the larval head (top). B, C, D: (FIB)-SEM images of L3 larvae; E, F, G, H: ssTEM images of L1 larvae**.** The color code in A applies to all micrographs in this Figure. **B)** SEM image of the lower larval head with left and right labial organ (LO). C) SEM image of the LO in an L3 larva. The LO is composed of two sensilla, here named LO_1 and LO_2. LO1 forms a pore in the center of a small socket on the bottom of a cylindrical cuticle depression. LO_2 protrudes peg-shaped from the cuticle; its outer cuticle structure appears rough. **D)** Cross section through the base of LO_1 and LO_2. Here, putative molting pores (mp) are visible. LO_2 is enclosed by a socket septum (ss). **E)** Cross section of the base of LO_1 and LO_2. LO_1 contains a tubular body and is enclosed by a dendritic sheath. The knob of LO_2 is mainly formed by the epicuticle and partially by the exocuticle at the base (asterisk). **F)** Cross section proximal of E). LO_1 and LO_2 are enclosed by a dendritic sheath. In LO_2, the tubular body is visible. The whole knob-shaped structure is

held in place by the socket septum. **G)** Cross section proximal of F). Dendrite of LO_1 has entered the inner sensillum lymph (isl) cavity. The ciliary constriction (cc) is visible at the transition between the inner and outer segment. LO_2 is still enclosed by the dendritic sheath. **H)** Cross section through the labial organ showing the enveloping support cells. **I)** Schematic drawing of (H): The dendrites are surrounded by their sensillar support cells, the thecogen (which forms the dendritic sheath), the trichogen and the tormogen cell. Scale bars: (B) 10 µm; (C) 1 µm; (D) 1 µm; (E) 1 µm; (F) 1 µm; (G) 1 µm; (H) 2 µm. Abbreviations: cc - ciliary constriction; ds - dendritic sheath; isl – inner sensillum lymph; mp – molting pore; ss - socket septum; tb - tubular body.

Figure 10: Ultrastructure of the papilla sensillum. **A)** 3D reconstruction of a papilla sensillum of an L1 larva (bottom). The outline shows the distribution of this sensillum type on the thoracic and abdominal hemisegments (top). B, D, F: (FIB)-SEM images of L3 larvae; C, E, G, H: ssTEM images of L1 larvae. The color code in A applies to all micrographs in this Figure. **B)** Electron micrographs of a papilla sensillum in an L3 larva. The sensillum lays in a cuticular depression with a visible molting pore (mp). **C)** Longitudinal section through a papilla sensillum showing typical features of a mechanoreceptive sensillum. The base is formed by the dendrite, and the tubular body (tb) is enclosed by a dendritic sheath (ds), which is formed by the thecogen cell. The dendrite tip is anchored in the cuticle by the socket septum (ss). Further proximal, the dendrite enters the inner sensillum lymph (isl) cavity and transitions from the outer to the inner dendritic segment at the ciliary constriction (cc). **D and E)** Longitudinal section through the base of a papilla sensillum in third (D) and L1 larva (E). A molting pore is visible in (D), whereas it is missing in (E). **F)** Untypical papilla sensillum, with a short hair-like protuberance. **G)** Sensory tip of abdominal papilla sensillum p_6 with two dendrites, one without a tubular body (white arrowhead). **G')** Sensory tip of abdominal papilla sensillum p_5, also called slit papilla sensillum. The tubular body is oval-shaped and appears more electron-lucent than canonical tubular bodies. **G'')** Sensory tip of thoracic papilla sensillum p_x with an electron-lucent and oval-shaped tubular body. **G''')** Sensory tip of thoracic papilla sensillum p_y with very electron-dense tubular body. **H)** Electron micrograph of sensory and support cells at the level of ciliary constriction. **I)** Schematic drawing of (H) highlighting the sensillar support cells: the thecogen, the trichogen and the tormogen cell. Scale bars: (B) 1 µm; (C) 0.5 µm; (D) 1 µm; (E) 1 µm; (F) 0.5 µm; (G) 0.5 µm; (H) 1 µm. Abbreviations: cc - ciliary constriction; ds - dendritic sheath; isl – inner sensillum lymph; mp – molting pore; ss - socket septum; tb - tubular body.

Figure 11: Ultrastructure of the hair sensillum. **A)** 3D reconstruction of a hair sensillum of an L1 larva (bottom). The outline shows the distribution of this sensillum type on the thoracic and abdominal hemisegments (top). B, D, F: (FIB)-SEM images of L3 larvae; C, E, G, H: ssTEM images of L1 larvae. The color code in A applies to all micrographs in this Figure. **B/B')** Electron micrographs of hair sensilla in L3 larvae. Hair sensilla can be branched (B') or unbranched (B). A molting pore is visible on the hair in B. **C)** Longitudinal section through a hair sensillum showing typical features of a mechanoreceptive sensillum (see (E) for details). The base is formed by the dendrite (green), and the tubular body (tb) is enclosed by

a dendritic sheath (ds), which is formed by the thecogen cell. The dendrite tip is anchored in the cuticle by the socket septum (ss). The hair is devoid of dendrites. **D)** Longitudinal section through the base of a hair with a putative molting pore (mp). **E) and G)** Longitudinal section through the sensory dendrite. The dendritic outer segment enters the lymph cavity and tapers off, reaching the ciliary constriction from where the inner dendritic segment begins. The dendrite is enclosed by the thecogen cell (the), trichogen cell (tri) and tormogen cell (tor). **F)** Mechanoreceptive region of the dendrite with a tubular body surrounded by a dendritic sheath and enclosed by a septum socket. **H)** Electron micrograph of sensory and support cells at the level of ciliary constriction. **I)** schematic drawing of (H) highlighting the sensillar support cells: the thecogen, the trichogen and the tormogen cell. Scale bars: (B) 2 and (B') 1 µm, respectively; (C) 1 µm; (D) 1 µm; (E) 1 µm; (F) 1 µm; (G) 1 µm; (H) 1 µm. Abbreviations: cc - ciliary constriction; ds - dendritic sheath; isl – inner sensillum lymph; mp – molting pore; ss - socket septum; tb - tubular body; the – thecogen cell; to – tormogen cell; tri – trichogen cell.

Figure 12: Ultrastructure of the double hair organ. A) 3D reconstruction of a double hair organ of an L1 larva (bottom). The outline shows the distribution of this organ on the abdominal hemisegments (top). B: SEM image of an L3 larva; C-H: ssTEM images of L1 larvae. The color code in A applies to all micrographs in this Figure. **B)** SEM image of a double hair organ, which consists of a long hair and a short bristle. **C)** Longitudinal section through a double hair organ showing a dendrite at the base of the hair and a dendrite with a tubular body at the base of the bristle. **D)** Dendrites at the base of the hair and bristle, both enclosed by a dendritic sheath (ds), and both containing a tubular body but of different appearance. The dendrite at the hair is surrounded by a socket septum. **E)** ssTEM further proximal of D: the dendrite of the hair is enclosed by a dendritic sheath and support cells. The dendrites of the bristle are entering an inner sensillum lymph (isl) cavity and are in the transition from outer to inner segment with associated ciliary constrictions (cc). **F)** ssTEM further proximal of E): The dendrite of the hair is entering a lymph cavity and is in the transition from outer to inner segment with an associated ciliary constriction. The outer dendritic segments of the bristle-associated sensory cells are visible. **G)** The dendrites of a double hair organ at the level of the isl cavity: individual variations within one animal can occur; in this case, all three dendrites share the same set of support cells, forming one united sensillum. **H)** Section through a double hair organ at the level of isl cavity. The enveloping tormogen, trichogen and thecogen cells can be seen. **I)** Schematic drawing of H, defining the sensory cells and the associated tormogen, trichogen and thecogen cells. Scale bars: (B) 1 µm; (C) 1 µm; (D) 1 µm; (E) 2 µm; (F) 2 µm; (G) 0.5 µm; (H) 1 µm. Abbreviations: cc - ciliary constriction; ds – dendritic sheath; isl – inner sensillum lymph; tb – tubular body; ss - socket septum

Figure 13: Ultrastructure of the knob sensillum. A) 3D reconstruction of a knob sensillum of an L1 larva (bottom). The outline shows the distribution of this sensillum type on the thoracic hemisegments (top). B, D, F: (FIB)-SEM images of L3 larvae; C, E, G, H: ssTEM images of L1 larvae. The color code in A applies to all micrographs in this Figure. **B)** SEM image of a knob sensillum. Externally, a knob-shaped sensillum shaft is visible that is sunken into a deep

and steep cavity. **C)** Longitudinal section through the knob sensillum. The dendrite of one sensory cell protrudes into the knob (orange) and bulges out at the end. Two other dendrites, one with (green) and one without (red) a tubular body (tb), end at the base of the shaft. **D) and E)** Close-up view of a cross section through all three dendrites at the base of the shaft in third (D) and L1 (E) larvae, respectively. The dendrites are enclosed by a common dendritic sheath (ds). In L3, we see a putative molting pore (mp). **F)** Cross section through the three dendrites at the level of the ciliary constriction (cc). The common thecogen cell forms an inner sensillum lymph (isl) cavity. **G)** Longitudinal section showing all three dendrites from the base of the shaft to their transition from dendritic outer to dendritic inner segment at the cc inside the isl. **H)** Cross section with all three dendrites bathed in the isl cavity and enclosed by the tormogen, trichogen and thecogen cell. **I)** Schematic drawing of (H), defining the sensory cells and the associated tormogen, trichogen and thecogen cells. Scale bars: (B) 0.5 µm; (C) 1 µm; (D) 1 µm; (E) 1 µm; (F) 1 µm; (G) 1 µm; (H) 1 µm. Abbreviations: cc - ciliary constriction; ds - dendritic sheath; isl – inner sensillum lymph; mp – molting pore; tb – tubular body.

Figure 14: Ultrastructure of the keilin's organ. A) 3D reconstruction of a keilin's organ of an L1 larva (bottom). The outline shows the distribution of this sensillum type on the thoracic hemisegments (top). B, D, F: (FIB)-SEM images of L3 larvae; C, E, G, H: ssTEM images of L1 larvae. The color code in A applies to all micrographs in this Figure. **B)** SEM image of a keilin's organ consisting of three external hairs. **C)** Cross section of keilin's organ with three hairs of hair-like sensilla and one dendrite of a papilla-like sensillum without a hair. **D)** A dendrite with a tubular body (tb) and a putative molting pore (mp) is visible at the base of the left hair. The dendrite is surrounded by a dendritic sheath and enclosed by a septum socket (ss). **E)** The keilin's organ dendrites have visible tubular bodies but absent molting pores. The dendrites are surrounded by a dendritic sheath and enclosed by a septum socket. Three hair-like and two papilla-like sensilla can be observed. **F)** Keilin's organ dendrites with visible tubular bodies. In L3 larvae, only one papilla-like sensillum is abundant. **G)** The dendrite of the keilin's organ further proximal than E), with ciliary constrictions (cc) at the transition from dendritic outer to dendritic inner segment. Dendrites are surrounded by thecogen cells, which form an inner sensillum lymph (isl) cavity in this region. **H)** Cross section further proximal than G). The enveloping tormogen, trichogen and thecogen cells can be seen. **I)** Schematic drawing of (H), defining the sensory cells and the associated tormogen, trichogen and thecogen cells. Scale bars: (B) 1 µm; (C) 1 µm; (D) 1 µm; (E) 1 µm; (F) 1 µm; (G) 2 µm; (H) 2 µm. Abbreviations: cc - ciliary constriction; dd – dendritic degeneration; ds - dendritic sheath; isl – inner sensillum lymph; mp – molting pore; ss - socket septum; tb – tubular body.

Figure 15: Ultrastructure of the hair sensillum at the terminal sensory cones. A) 3D reconstruction of a hair sensillum at the terminal segment of an L1 larva (bottom). The outline shows the distribution of this sensillum type on the last fused hemisegments (top). B, C: ssTEM images of an L1 larva. The color code in A applies to all micrographs in this Figure. **B)** Longitudinal section through the hair sensillum. A sensory hair is sitting on top of

a cone-like structure with more (non-innervated) hairs and bristles. A dendrite with a tubular body (tb) ends at the base of the sensory hair. It is surrounded by a dendritic sheath (ds) and anchored in the cuticle by a septum socket (ss). **C)** Longitudinal section further proximal than B) at the level of the ciliary constriction (cc). The inner sensillum lymph (isl) cavity and the support cells can be observed. **D)**Schematic drawing of (C), defining the sensory cell and the associated tormogen, trichogen and thecogen cells. Scale bars: B) 2 µm; (C) 1 µm. Abbreviations: cc - ciliary constriction; ds - dendritic sheath; isl – inner sensillum lymph; ss - socket septum; tb – tubular body.

Figure 16: Ultrastructure of the knob sensillum at the terminal sensory cones. A) 3D reconstruction of a knob sensillum at the terminal sensory cone t_3 in an L1 larva (bottom). The outline shows the distribution of knob sensilla on the last fused hemisegments (top). C-H: ssTEM images of an L1 larva. The color code in A applies to all micrographs in this Figure. **B)** 3D reconstruction of the outer appearance of t_3. Inside the cone, a knob-shaped sensillum shaft is visible that is sunken into a deep and steep cavity. The cone is surrounded by (non-sensory) hairs and bristles. **C) and D)** Longitudinal section through the knob in the cone t_3. The dendrite of one sensory cell protrudes into the shaft and bulges out at the end (orange). Two other dendrites end at the base of the shaft, one containing a tubular body (green), the other not (red, arrowhead). All dendrites are enclosed by a dendritic sheath (ds). Knob sensilla innervated by three sensory cells are found in t_2 and t_3. **E)** Longitudinal section through the knob sensillum of cone t_5. Only two dendrites are abundant, one protruding into the sensillum shaft (orange) and the other containing a tubular body (green). Further proximal, the dendrites are bathed inside the inner sensillum lymph (isl) at the level of the ciliary constriction (cc). Knob sensilla innervated by only two sensory cells are found in cones t_1, t_5 and t_7. **F)** Longitudinal section through the three dendrites of t_3 at the level of the ciliary constriction. The common thecogen cell (the) forms an isl cavity. The thecogen cell is enclosed by the trichogen cell (tri) and the tormogen (tor) cell. **G)** Knob sensillum of the terminal organ with only one abundant dendrite (orange) that protrudes into the knob. **H)** Longitudinal section of t_3 proximal of D) with all three dendrites sharing a common dendritic sheath, enclosed by the tormogen, trichogen and thecogen cell. **I)** Schematic drawing of (H), defining the sensory cells and the associated tormogen, trichogen and thecogen cells. Scale bars: (C) 2 µm; (D) 2 µm; (E) 2 µm; (F) 1 µm; (G) 1 µm; (H) 1 µm. Abbreviations: cc - ciliary constriction; ds - dendritic sheath; isl – inner sensillum lymph; tb – tubular body; the – thecogen cell; to – tormogen cell; tri – trichogen cell.

Figure 17: Ultrastructure of the spiracle sense organ. A) 3D reconstruction of the spiracle sense organ (sp) at the terminal segment of an L1 larva (bottom). The outline shows the position of this organ on the last fused hemisegments (top). B, C: ssTEM images of an L1 larva. The color code in A applies to all micrographs in this Figure. **B)** Longitudinal section through a posterior spiracle. The main tracheal tube (tr) and two spiracular glands (sg) are visible. **C**) Longitudinal section of the tip of the spiracle. Two sensilla of the spiracle sense organ can be observed. Furthermore, a spiracular gland and a wax pore (wp) associated with another spiracular gland are visible. The glands secrete wax around the tracheal valve to prevent moisture ingress. **D)** Close-up view of the mechanoreceptive region of a spiracle sensillum near the tracheal valve. The dendrite contains a tubular body (tb) at the tip and is

enclosed by a typical dendritic sheath (ds). **E)**, Longitudinal section of the tip of the spiracle further proximal than (B) showing the two sensilla inside the inner sensillum lymph (isl) with their associated support cells. The ciliary constriction (cc) is visible for one sensillum. **F)** schematic drawing of (E), defining the sensory cells and the associated tormogen, trichogen and thecogen cells. Furthermore, the tracheal and gland cells are shown. Scale bars: (B) 10 µm; (C) 5 µm; (D) 2 µm; (E) 5 µm. Abbreviations: cc - ciliary constriction; ds - dendritic sheath; isl – inner sensillum lymph; sg – spiracular glands; sp – spiracle; tb – tubular body; tr – trachea.

SUPPLEMENTARY FIGURE LEGENDS

Figure S1: Block embedding versus minimal embedding technique. A) In conventional block-embedding, the sample is embedded in a bulk of resin. **A')** Block-embedded larval head: Frontal view of the block surface imaged with a stereomicroscope. The contours of the cuticle are complex to identify. Therefore, the block leads to extensive processing prior to FIB-SEM: excessive resin must be cut away to expose the region of interest to the ion and the electron beam. **A'')** Block surface seen through the SEM. Visible are the trenches left by FIB slicing of the regions of interest. **B)** In contrast, minimal embedding preserves the topology of the sample because only a thin layer of resin covers the sample (**B'**). Samples can be glued directly to a SEM stub without prior cutting. Body parts and sensilla are visible by SEM (**B''**) and can be directly targeted by the FIB. Scale bars: A'), A''): 200 µm; B'): 100 µm B''): 20 µm.

Figure S2: SEM image of the larval head seen from above. The terminal organ (TO) and the dorsal organ (DO) are visible. Numbers define the peripheral DO sensilla which lie in a circle around the dome structure.

Figure S3: 3D reconstruction of terminal sensory cone 1 (t1). The reconstruction shows the outer appearance of t_1 in an L1 larva. Inside the cone, we find a knob sensillum and a hair sensillum. In addition, one papilla sensillum sits at the base of the cone. The hair and the papilla sensillum are both innervated by one sensory cell containing a tubular body (tb). The knob sensillum is innervated by two sensory cells, one containing a tb that ends at the base of the knob and one without a tb that protrudes into the knob (asterisk).

Figure S4: Mechanotransduction in a hair sensillum. Shown is a ssTEM image of a typical hair sensillum in an L1 larva. When force (F) is applied to either side of the hair, it is transmitted to the tubular body (tb) by the hair base and the dendritic sheath. Inside the tb body, specialized channels ensure mechanotransduction.

TABLES

Table 1

sensillum	external structure	pores	dendrites	hypothesized function
DO				
dome	round, dome-shaped cuticle shaft	multiple pores	21 arranged in seven triplets one with	olfaction
DO_{p1}	cuticle bulge with pore in center at dome-base	terminal pore (molting)	a tubular body	mechanosensation
DO_{p2}, DO_{p4}	cuticle bulge with pore in center at dome-base	terminal pore (molting)	two; one with a tubular body	mechanosensation + unknown
DO_{p3}, DO_{p5}, DO_{p6}	cuticle bulge with pore in center at dome-base	terminal pore (molting)	two; "dendritic bulbs"	thermosensation
VO *				
VO_1	shallow dome	terminal pore (molting)	one with a tubular body	mechanosensation
VO_2	steep pore in cuticle surface	terminsal pore	two	contact chemosensation
VO_3, VO_4	steep pore in cuticle surface	terminal pore (molting)	one with a tubular body	mechanosensation
LO				
LO_1	cuticle cavity with pore in center	terminal pore (molting)	one with a tubular body	mechanosensation
LO_2	peg-shaped shaft, rough surface	basal pore (molting)	one with a tubular body	mechanosensation
TO**				
$P_{1/3}$	bud-shaped shaft with pore in the center	terminal pore	three; one with a tubular body	gustation + mechanosensation
P_2	bud-shaped shaft with pore in the center	terminal pore	five; one with a tubular body	gustation + mechanosensation
P_{do}	bud-shaped shaft with pore in the center	terminal pore	three	gustation
P_{mod}	bud-shaped shaft	lateral pore (molting)	one with a tubular body	mechanosensation
$T_{1/5}$	cuticle cavity with pore in center	terminal pore	three; one with a tubular body	gustation + mechanosensation
T_2	cuticle cavity with pore in center	terminal pore	four	gustation
$T_{3/4}$	cuticle cavity with pore in center	terminal pore	two	gustation
$S_{di/do}$	pore in cuticle	terminal pore (molting)	one with a tubular body	mechanosensation
K_1	knob-shaped shaft	lateral pore (molting)	one	chemosensation (oxygen)
K_2	knob-shaped shaft	lateral pore (molting)	one (slightly lammelated)	osmosensation + chemosensation (oxygen)

Table 2

sensillum	number, location *(per hemisegment)*	external structure	pores	dendrites	hypothesized function	Other names/ classifications
hair sensillum (h) single double	**total: 41** 27 T1-3: 3 dorsal and lateral A1-7: 2 lateral A8: 4 at t1-2, t4, t6 7x2 hairs A1-7: 1 dorsal	hair-shaped smooth cuticle shaft, different sizes: short, intermediate, long; shaft might be bifurcated long, no bifurcation short and long; no bifurcation	L1: none L3: basal pore (molting)	**one**: terminates at base shaft with tb h3: **two**, one with and one w/o tb h4: **one** with tb	mechanosensation mechanosensation unknown function mechanosensation	hair-types C, D, E [4] trichoid [8, 9, 10]
knob sensillum (k)	**total: 11** T1: 2, one dorsal; one ventral T2-3: 2, one lateral, one ventral A8/9: 5 at t1-3, t5, t7	knob-shaped cuticle shaft in cavity; smooth surface long; shaft protrudes out of cavity; smooth surface	L1: none L3: basal pore (molting)	T1-3: **three**: one innervates peg, one at base with tb, one at base w/o tb A8/9: **three** or **two** (one w/o tb is missing)	chemosensation (oxygen) mechanosensation unknown function	koelbchen [1, 8] knob-in-pit [5] hair-type B [4] basiconic [9] sensory papillae [6] dorsal/ ventral pit [2] black sensory organ [3] black dot [7]
papilla sensillum (p)	**total: 94,5** head: 6 T1: 10 T2-3: 7 A1-7: 9 dorsal , lateral, ventral A8: 1 at t1 + 1 unpaired at anus (vas)	shallow cuticle depression (with pore in center in L3)	L1: none L3: terminal pore (molting)	**one**: one at base with tb **two**: p6 (A1-A7) one at base with tb, one w/o tb	mechanosensation mechanosensation unknown function	papilla [8, 9, 10] campaniform [5, 9] pit [10]
keilin's organ (KO)	**total: 3** T1-3: 1 ventral	three hair sensilla: hair-shaped shaft of similar length two papilla sensilla: pore in cuticle surface in L3	L1: none L3: basal pore (molting) L1: none L3: terminal pore (molting)	**five (**four in L3**)**: one at base of each hair (3) one below each papilla (2) all with tb	mechanosensation mechanosensation	hair-type A [4] Fussstummelsinnesorgan [1]
spiracle sense organ (sp)	**total: 1** at posterior spiracle	four sensilla at base of the spiracular hairs	L1: none	**four:** one at base with tb	mechanosensation	spiracular hairs [11] hair tufts [6]

FIGURES

Figure 1

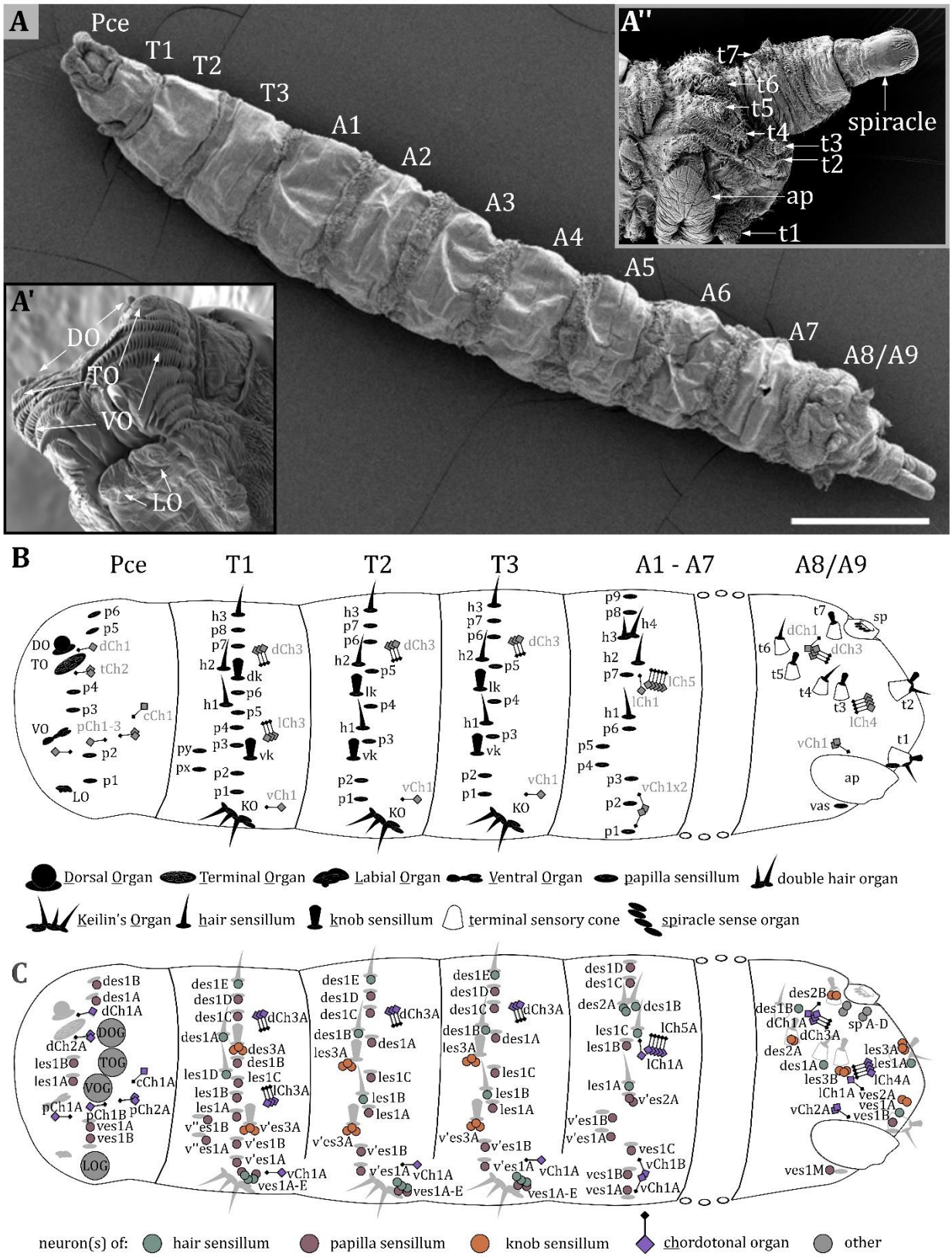

Figure 2

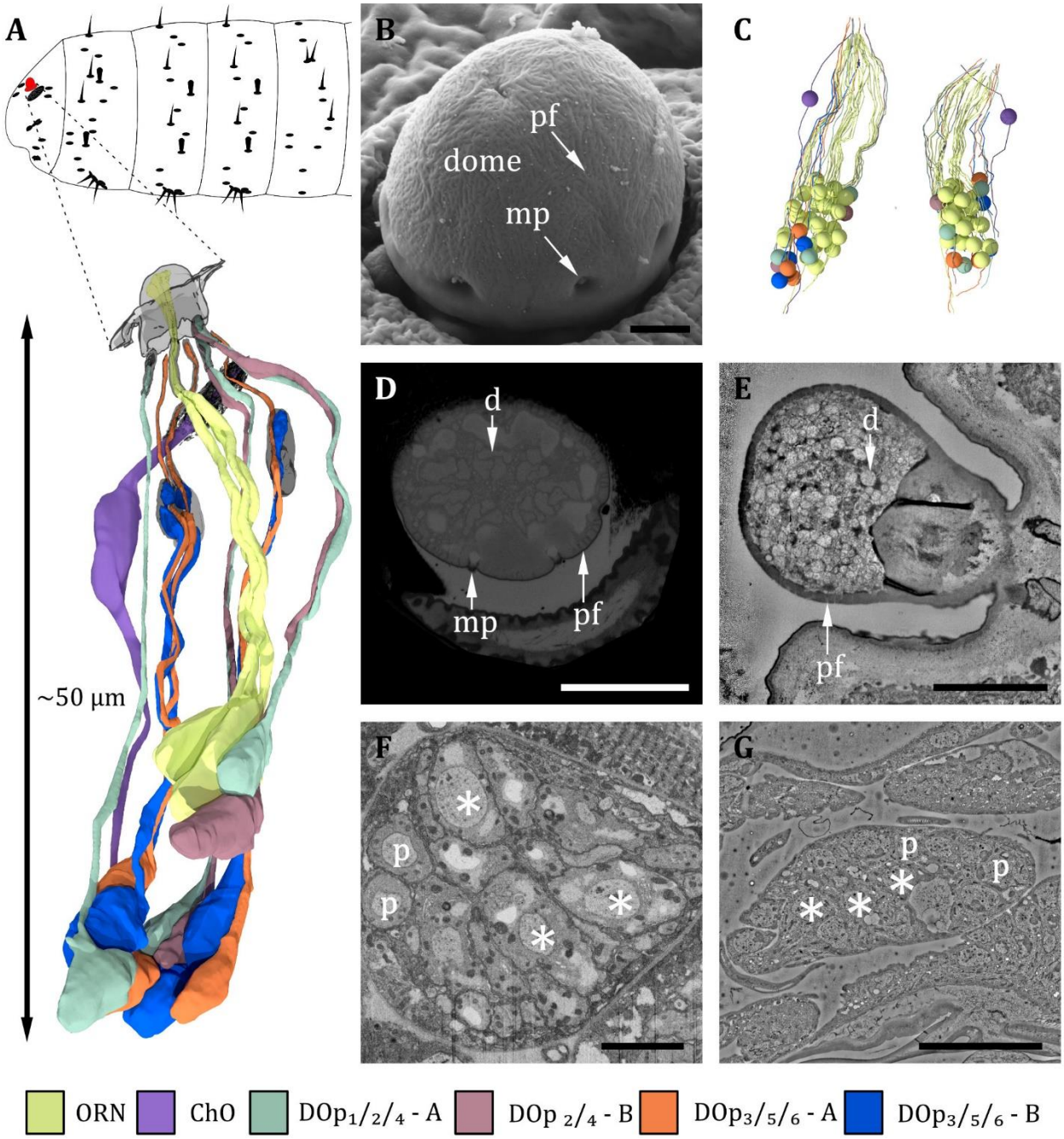
A
B
C
pf
dome
mp
D
d
mp
pf
E
d
pf
~50 µm
F
p
p
G
p
p
ORN
ChO
DOp1/2/4 - A
DOp 2/4 - B
DOp3/5/6 - A
DOp3/5/6 - B

Figure 3

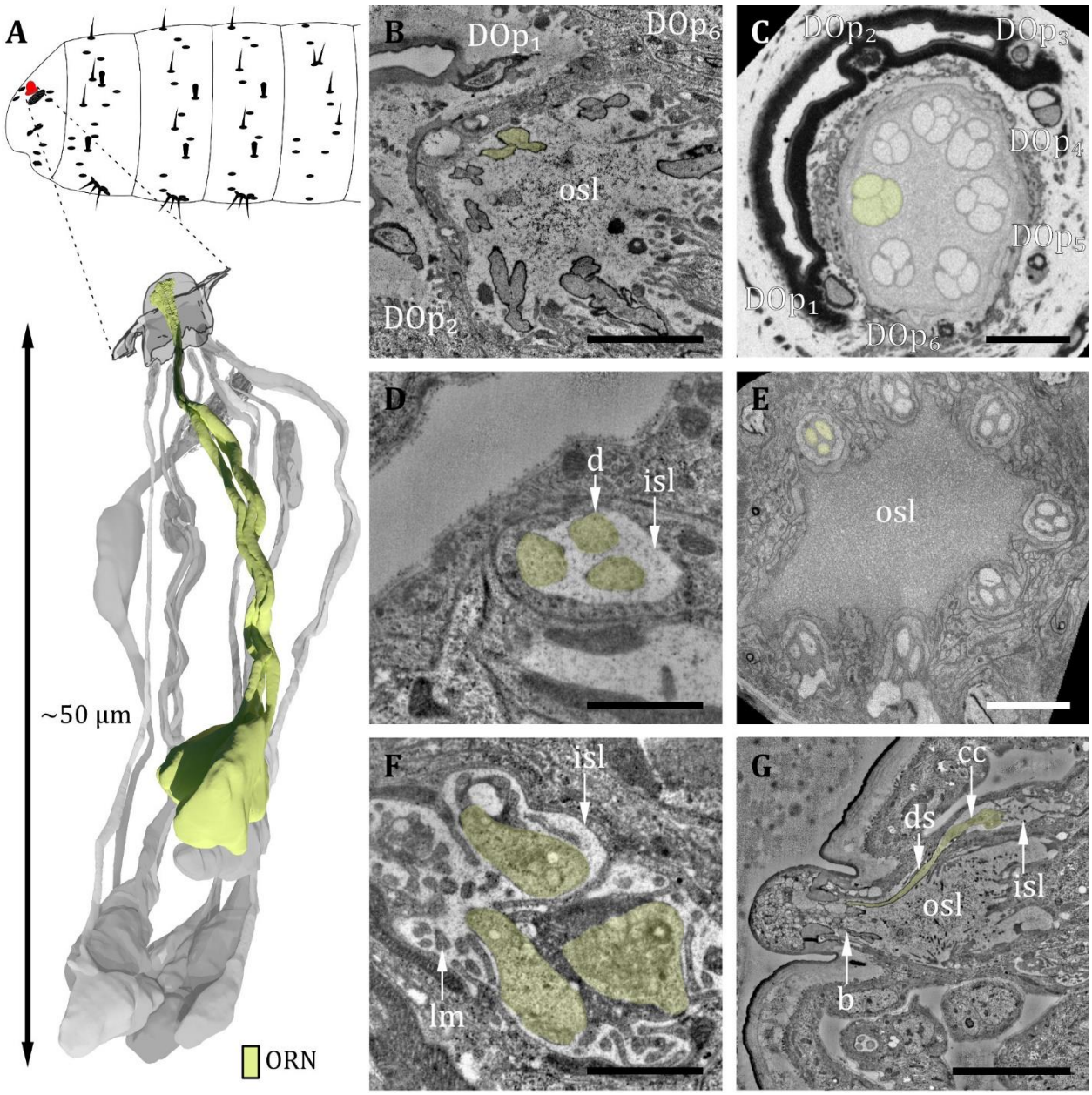
A
~50 µm
ORN
B
DOp1
DOp6
osl
DOp2
C
DOp2
DOp3
DOp4
DOp5
DOp1
DOp6
D
d
isl
E
osl
F
isl
lm
G
cc
ds
isl
osl
b

Figure 4

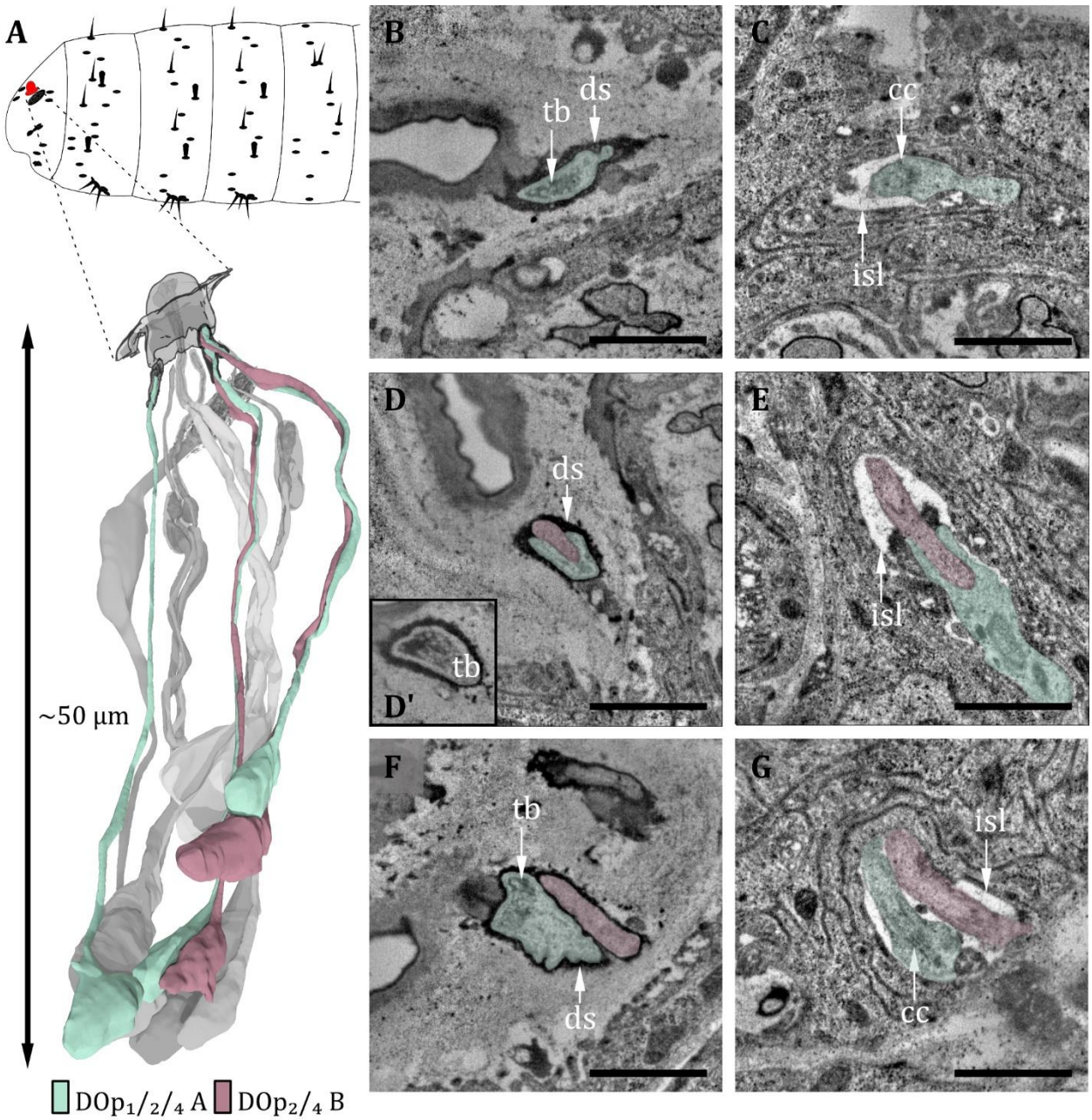
A
B
tb
ds
C
cc
isl
D
ds
tb
D'
E
isl
F
tb
ds
G
isl
cc
~50 µm
DOp1/2/4 A
DOp2/4 B

Figure 5

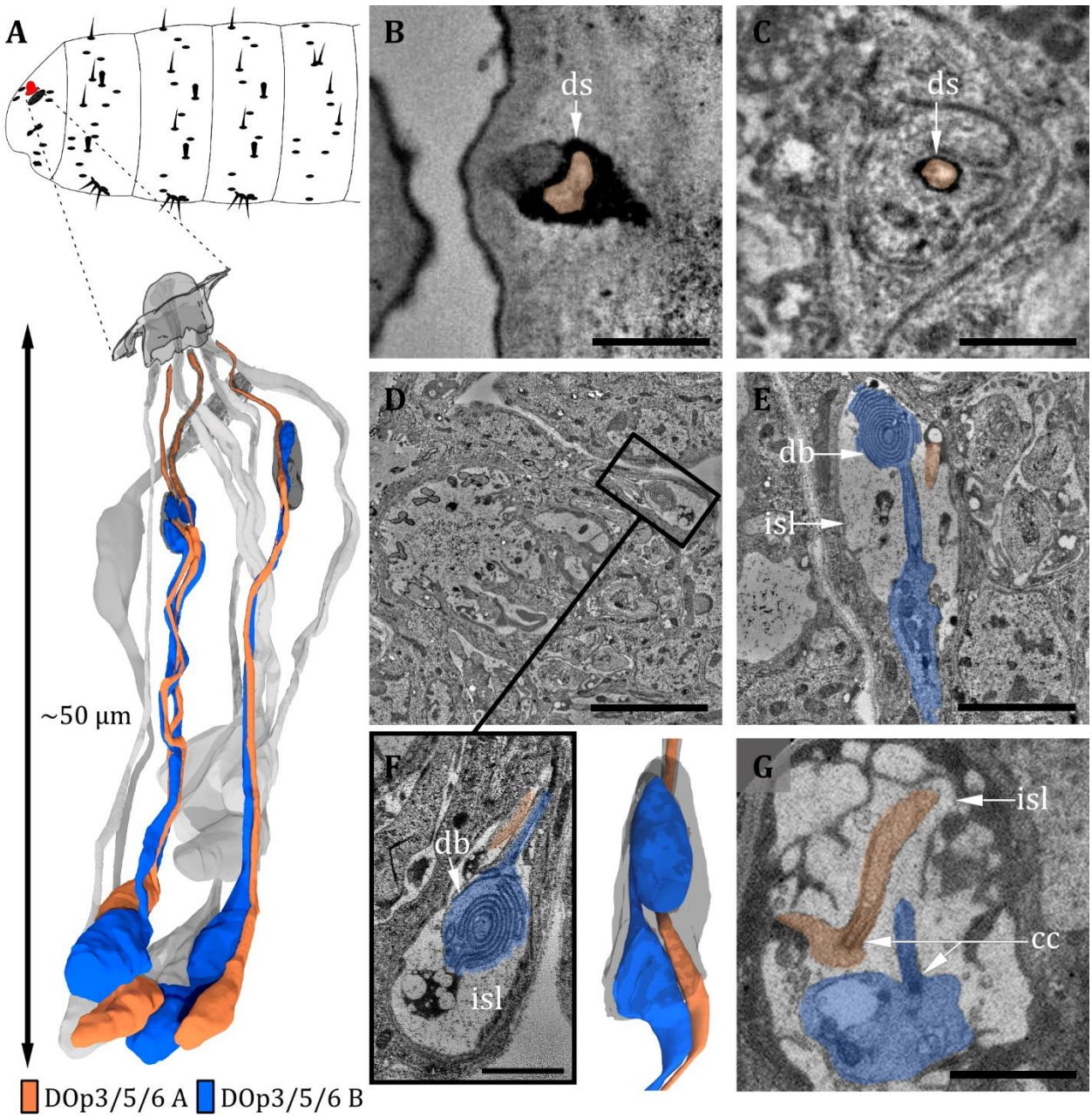

Figure 6

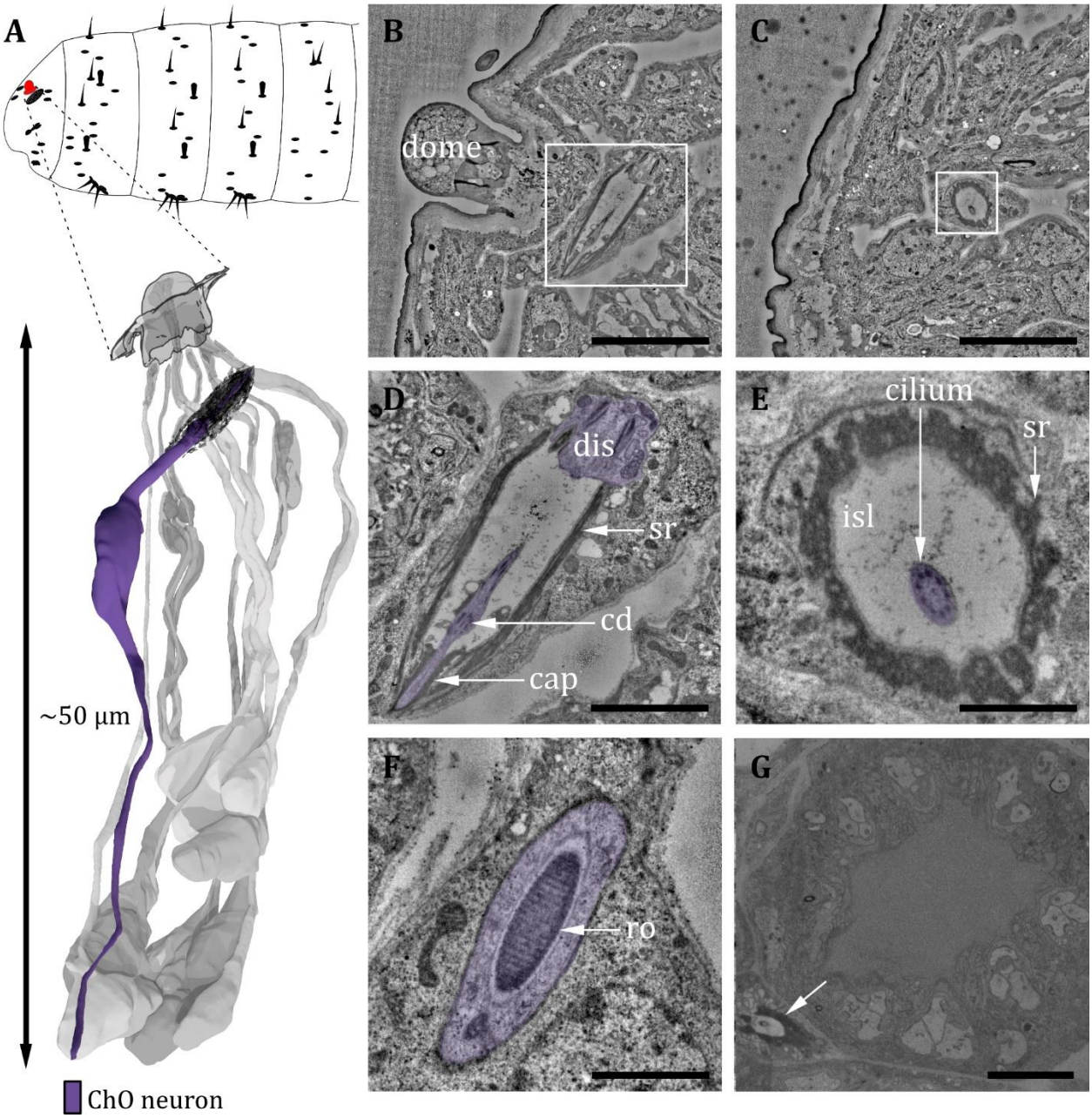

Figure 7

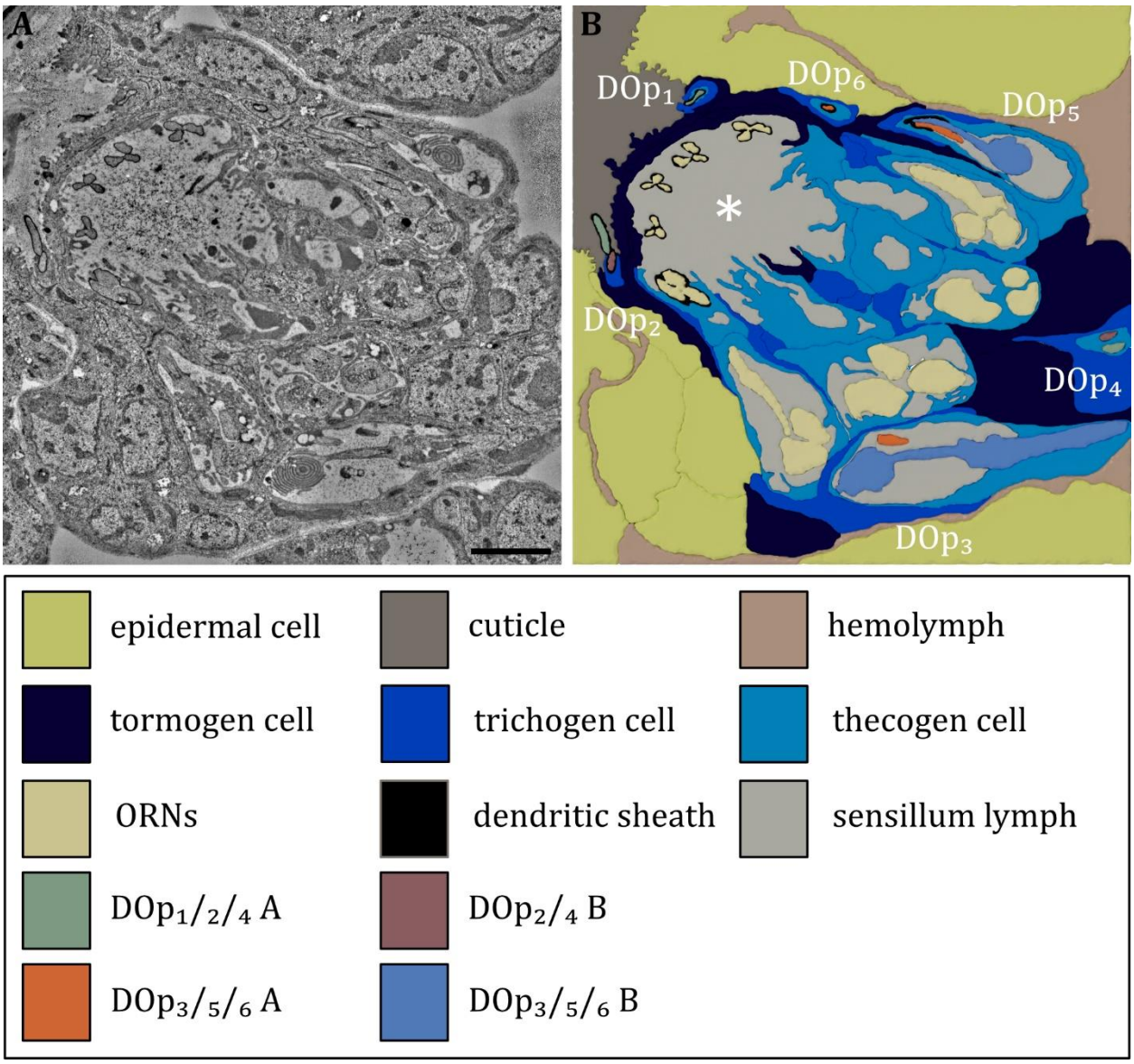
A
B
DOp1
DOp6
DOp5
*
DOp2
DOp4
DOp3
epidermal cell
cuticle
hemolymph
tormogen cell
trichogen cell
thecogen cell
ORNs
dendritic sheath
sensillum lymph
DOp1/2/4 A
DOp2/4 B
DOp3/5/6 A
DOp3/5/6 B

Figure 8

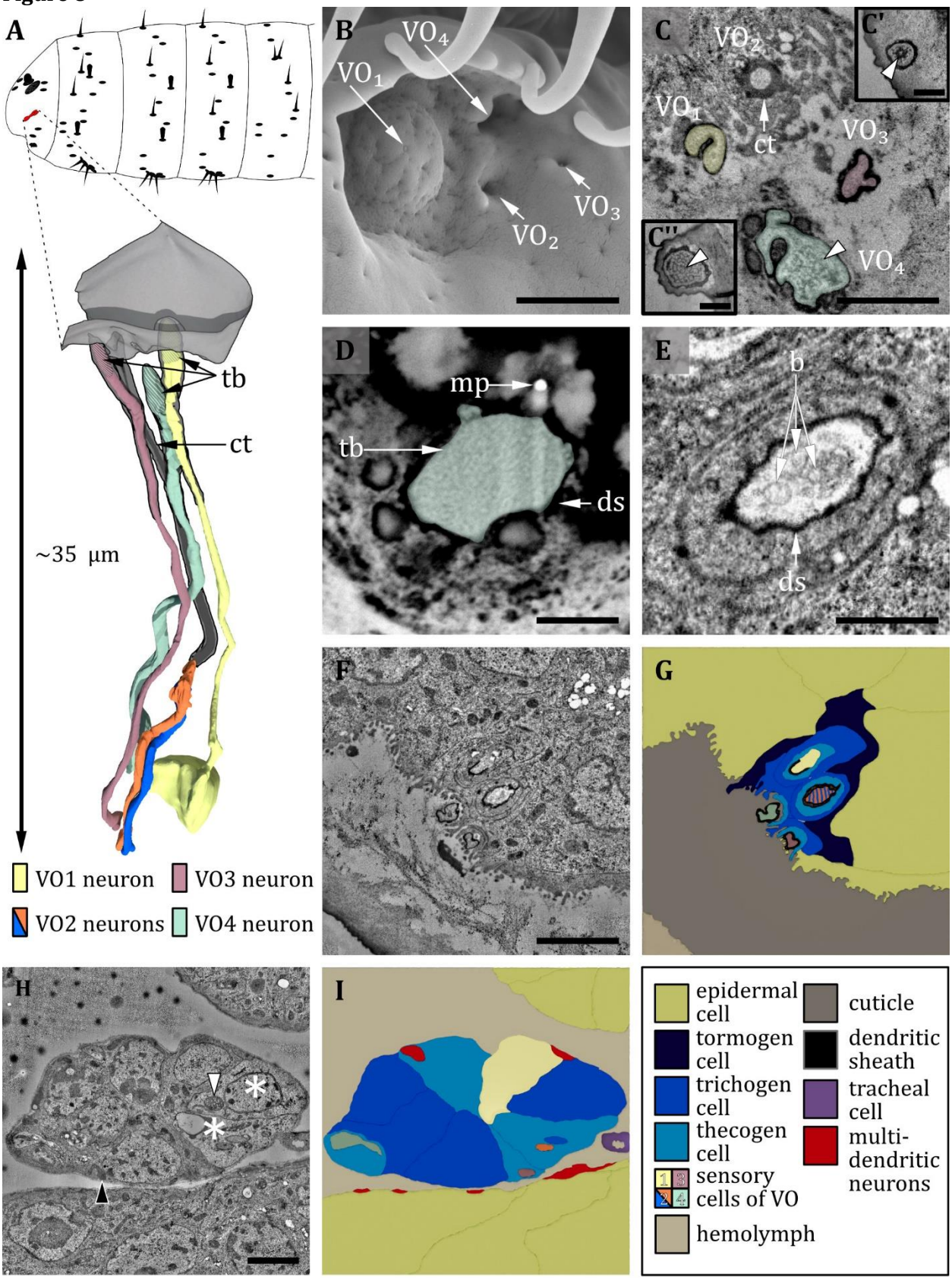
A
tb
ct
~35 µm
VO1 neuron
VO3 neuron
VO2 neurons
VO4 neuron
B
VO4
VO1
VO3
VO2
C
VO2
C'
VO1
ct
VO3
C''
VO4
D
mp
tb
ds
E
b
ds
F
G
H
I
epidermal cell
cuticle
tormogen cell
dendritic sheath
trichogen cell
tracheal cell
thecogen cell
multi-dendritic neurons
sensory cells of VO
hemolymph

Figure 9

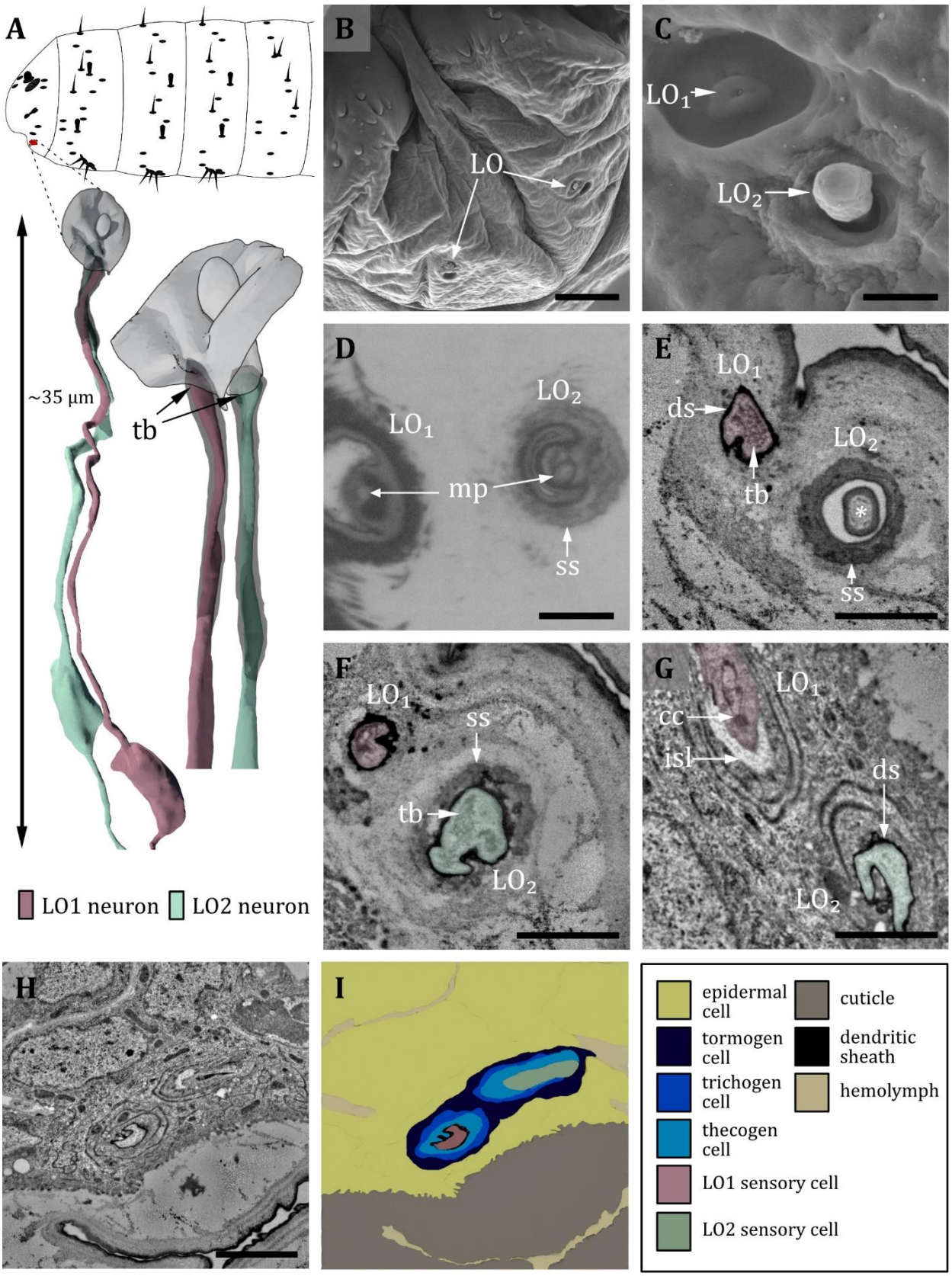
A
~35 µm
tb
LO1 neuron
LO2 neuron
B
LO
C
LO1
LO2
D
LO1
LO2
mp
ss
E
LO1
ds
LO2
tb
*
ss
F
LO1
ss
tb
LO2
G
LO1
cc
isl
ds
LO2
H
I
epidermal cell
cuticle
tormogen cell
dendritic sheath
trichogen cell
hemolymph
thecogen cell
LO1 sensory cell
LO2 sensory cell

Figure 10

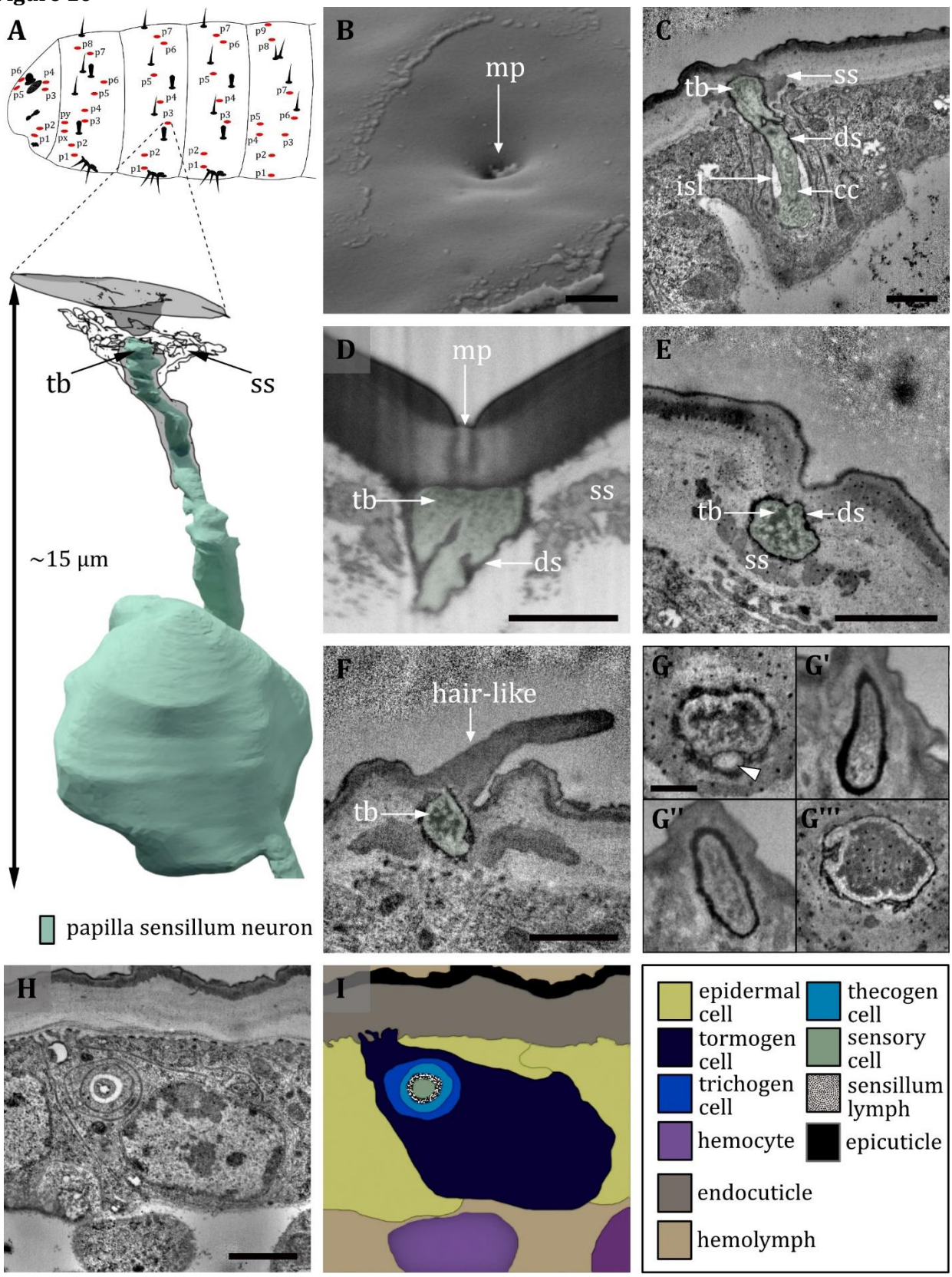
A
B
mp
C
tb
ss
ds
isl
cc
tb
ss
~15 µm
papilla sensillum neuron
D
mp
tb
ss
ds
E
tb
ds
ss
F
hair-like
tb
G
G'
G''
G'''
H
I
epidermal cell
thecogen cell
tormogen cell
sensory cell
trichogen cell
sensillum lymph
hemocyte
epicuticle
endocuticle
hemolymph

Figure 11

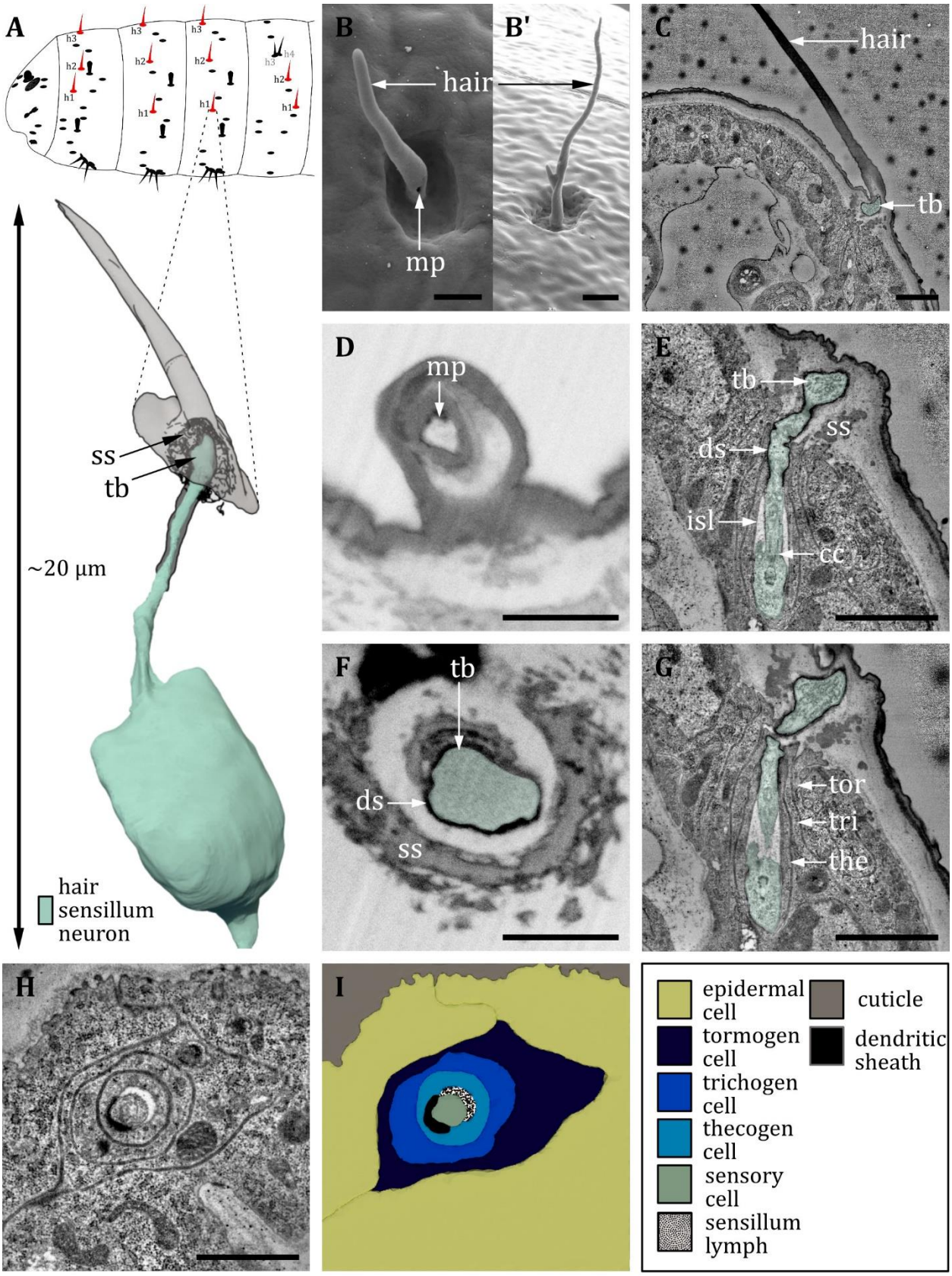
A
h1
h2
h3
h4
ss
tb
~20 µm
hair
sensillum
neuron
B
hair
mp
B'
C
hair
tb
D
mp
E
tb
ss
ds
isl
cc
F
tb
ds
ss
G
tor
tri
the
H
I
epidermal cell
tormogen cell
trichogen cell
thecogen cell
sensory cell
sensillum lymph
cuticle
dendritic sheath

Figure 12

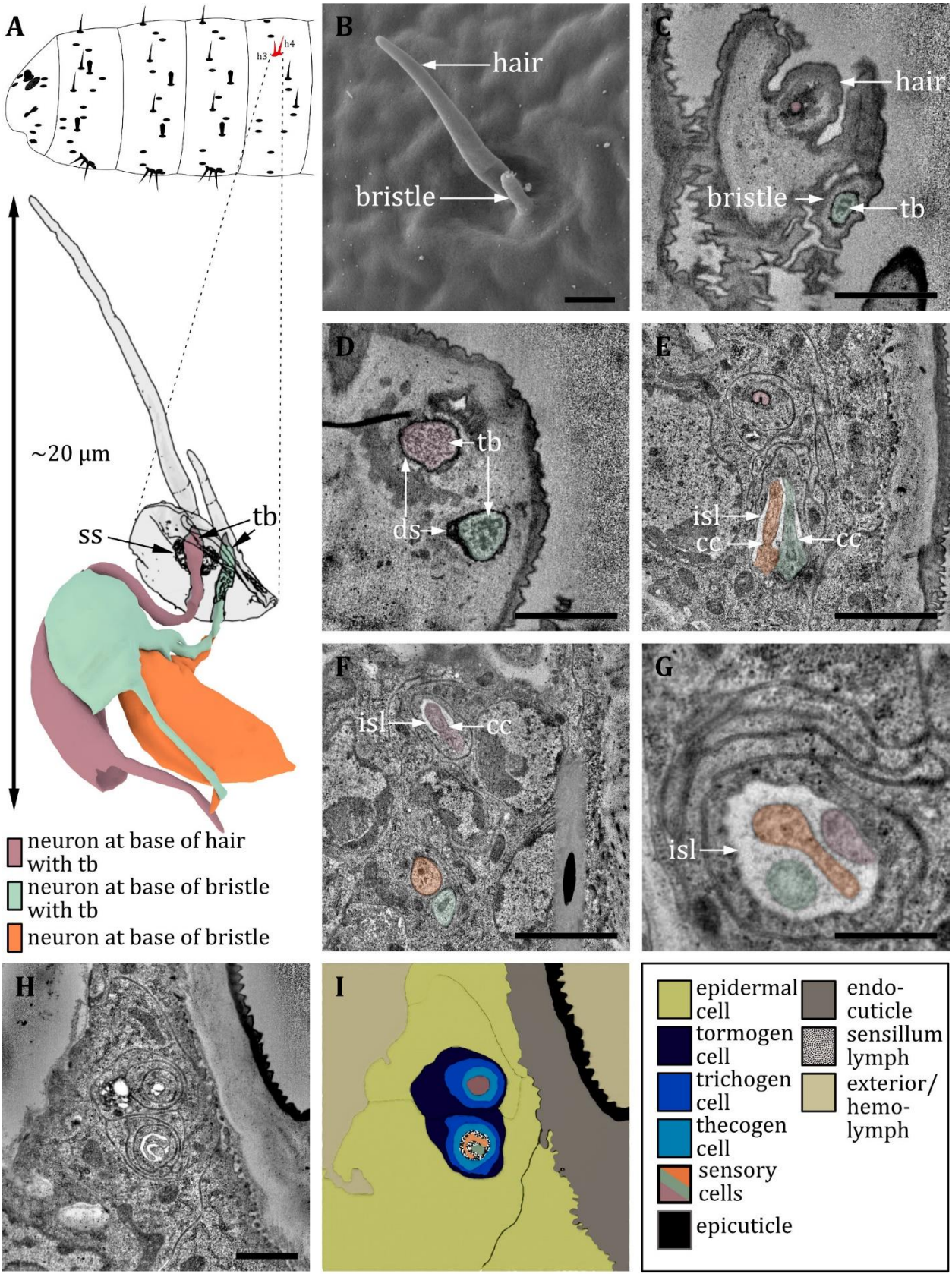
A
h3
h4
~20 µm
ss
tb
neuron at base of hair with tb
neuron at base of bristle with tb
neuron at base of bristle
B
hair
bristle
C
hair
bristle
tb
D
tb
ds
E
isl
cc
cc
F
isl
cc
G
isl
H
I
epidermal cell
tormogen cell
trichogen cell
thecogen cell
sensory cells
epicuticle
endo-cuticle
sensillum lymph
exterior/ hemo-lymph

Figure 13

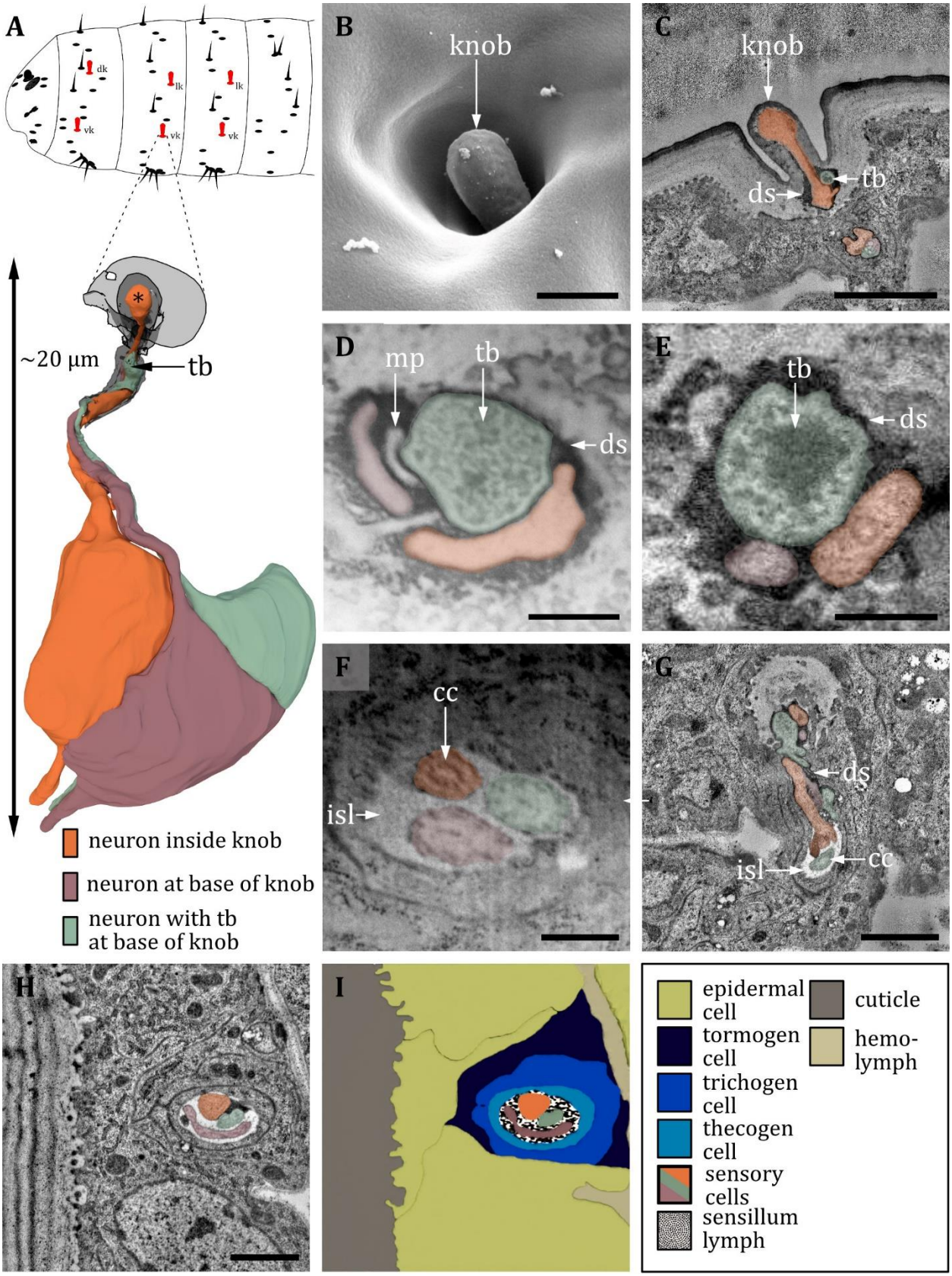
A
dk
lk
lk
vk
vk
vk
~20 µm
tb
neuron inside knob
neuron at base of knob
neuron with tb
at base of knob
B
knob
C
knob
ds
tb
D
mp
tb
ds
E
tb
ds
F
cc
isl
G
ds
isl
cc
H
I
epidermal cell
tormogen cell
trichogen cell
thecogen cell
sensory cells
sensillum lymph
cuticle
hemo-lymph

Figure 14

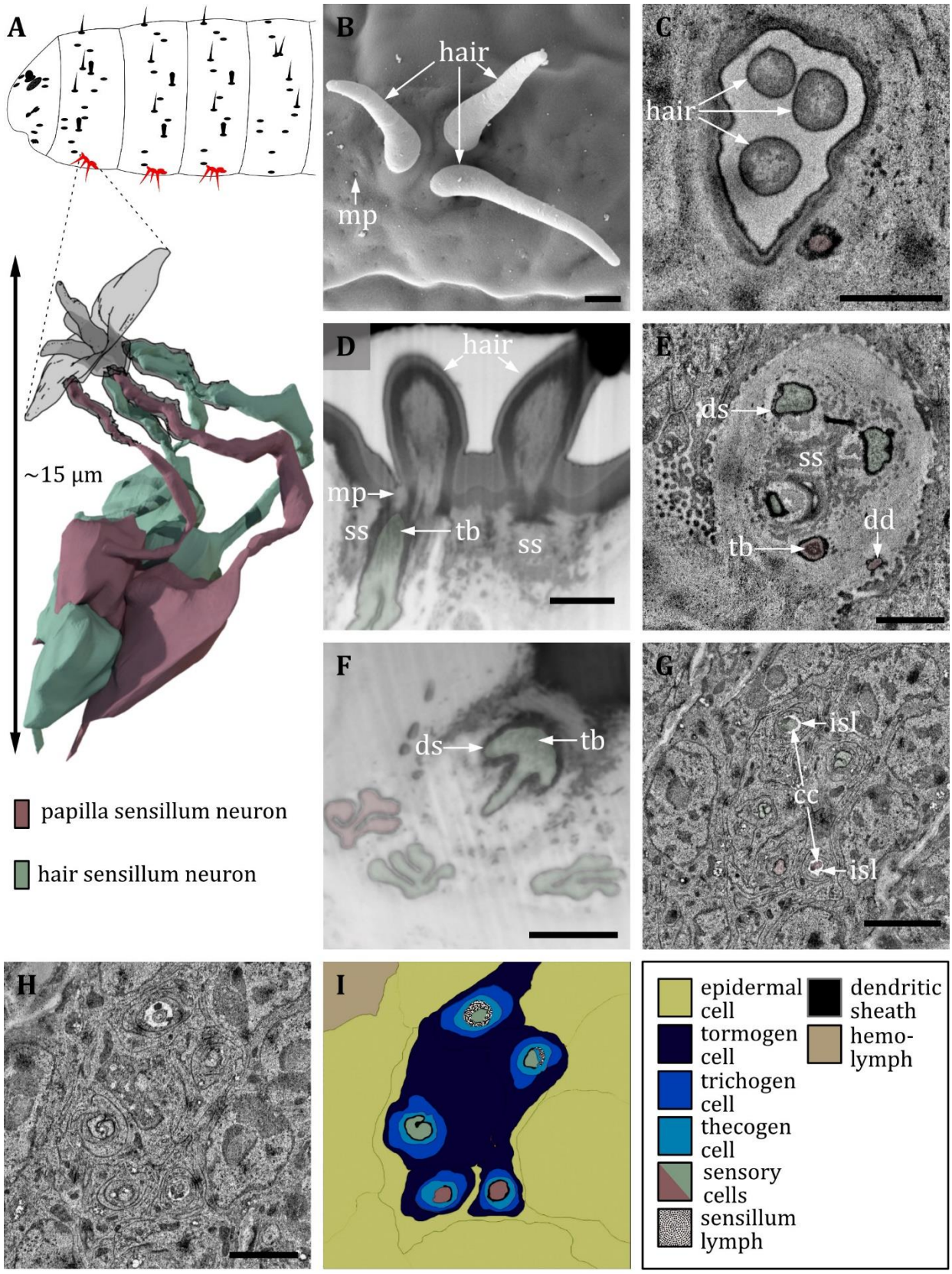
A
~15 µm
papilla sensillum neuron
hair sensillum neuron
B
hair
mp
C
hair
D
hair
mp
ss
tb
ss
E
ds
ss
dd
tb
F
ds
tb
G
isl
cc
isl
H
I
epidermal cell
tormogen cell
trichogen cell
thecogen cell
sensory cells
sensillum lymph
dendritic sheath
hemo-lymph

Figure 15

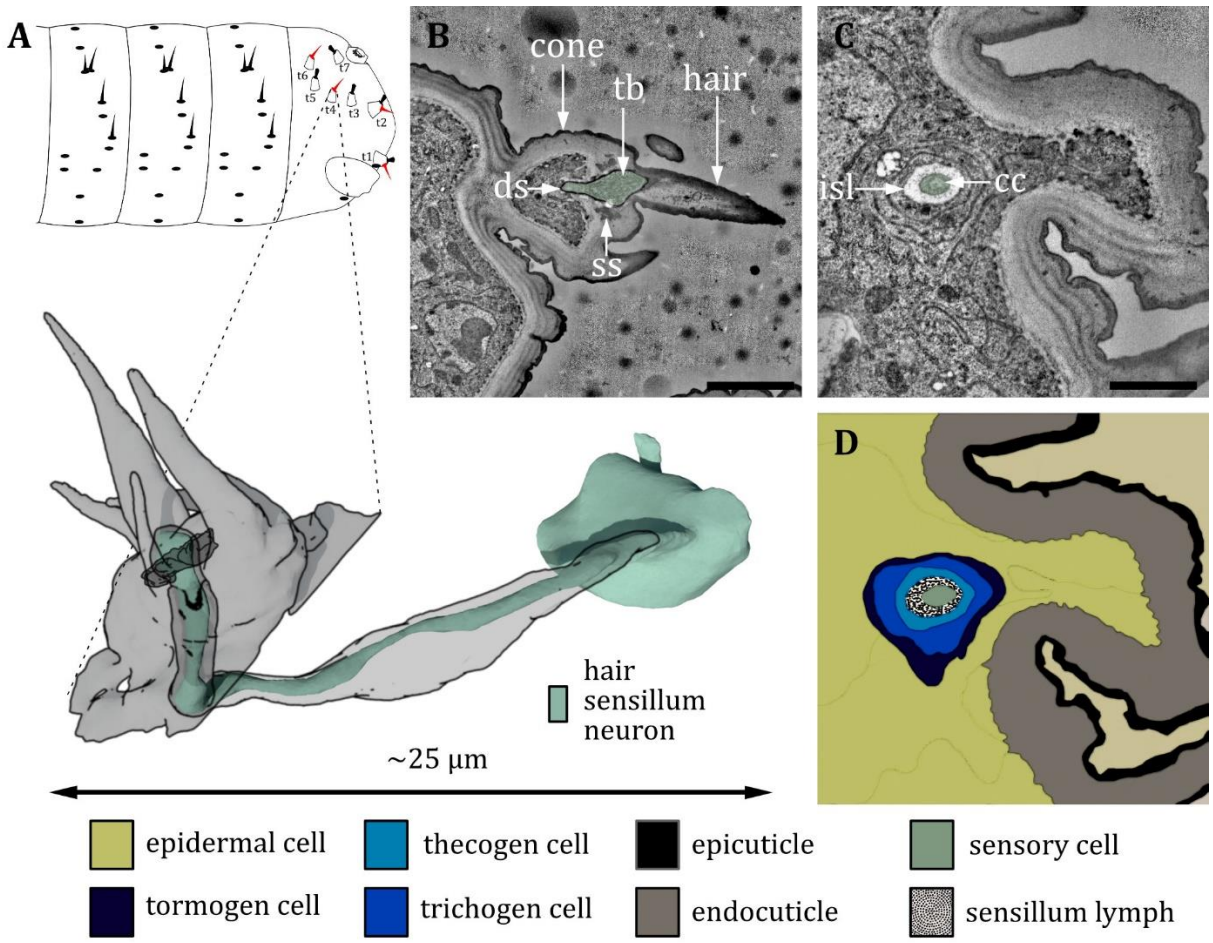
A
t1
t2
t3
t4
t5
t6
t7
B
cone
tb
hair
ds
ss
C
isl
cc
D
hair
sensillum
neuron
~25 µm
epidermal cell
thecogen cell
epicuticle
sensory cell
tormogen cell
trichogen cell
endocuticle
sensillum lymph

Figure 16

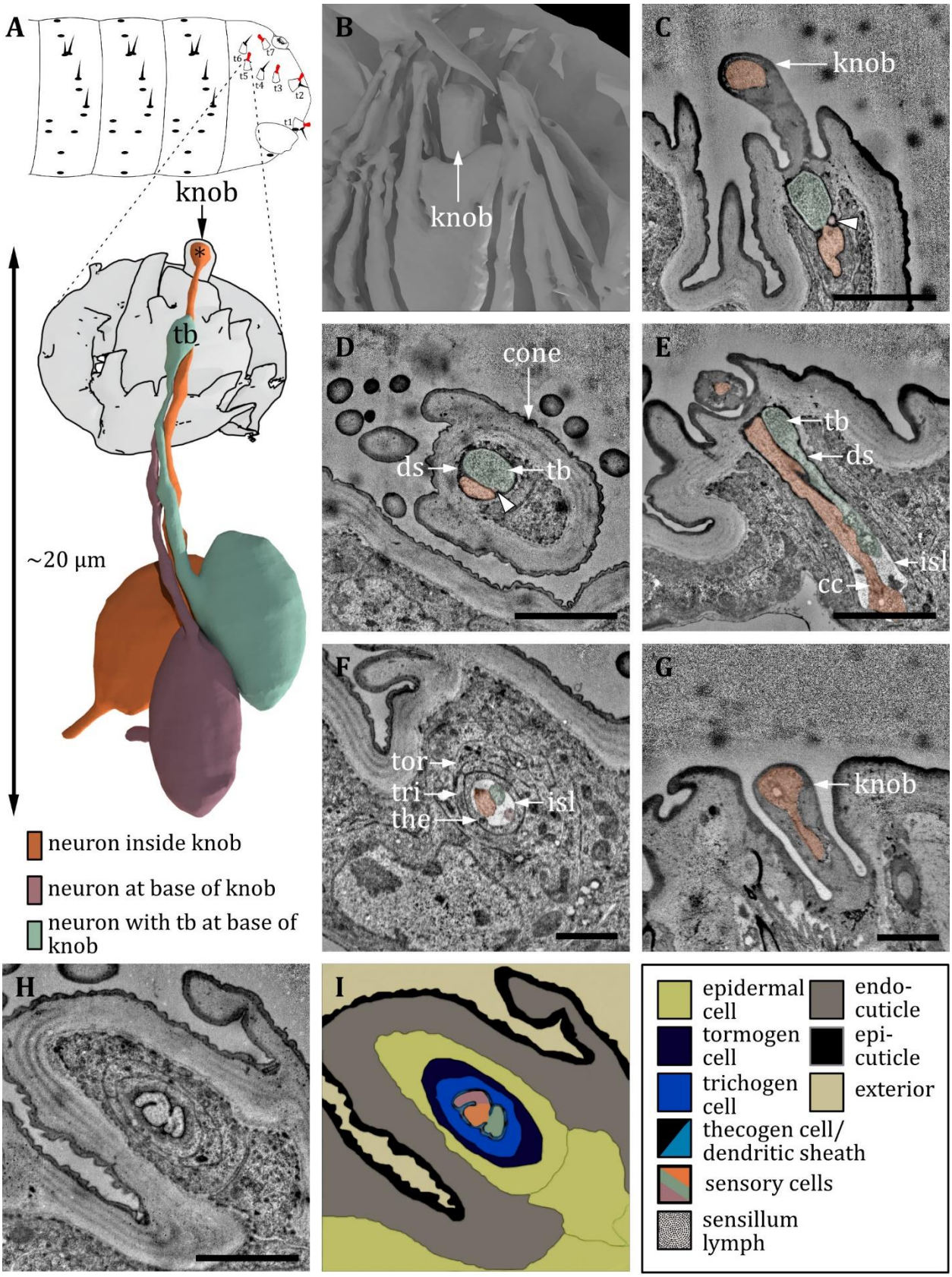
A
t1
t2
t3
t4
t5
t6
t7
knob
tb
~20 µm
neuron inside knob
neuron at base of knob
neuron with tb at base of knob
B
knob
C
knob
D
cone
ds
tb
E
tb
ds
isl
cc
F
tor
tri
the
isl
G
knob
H
I
epidermal cell
endo-cuticle
tormogen cell
epi-cuticle
trichogen cell
exterior
thecogen cell/ dendritic sheath
sensory cells
sensillum lymph

Figure 17

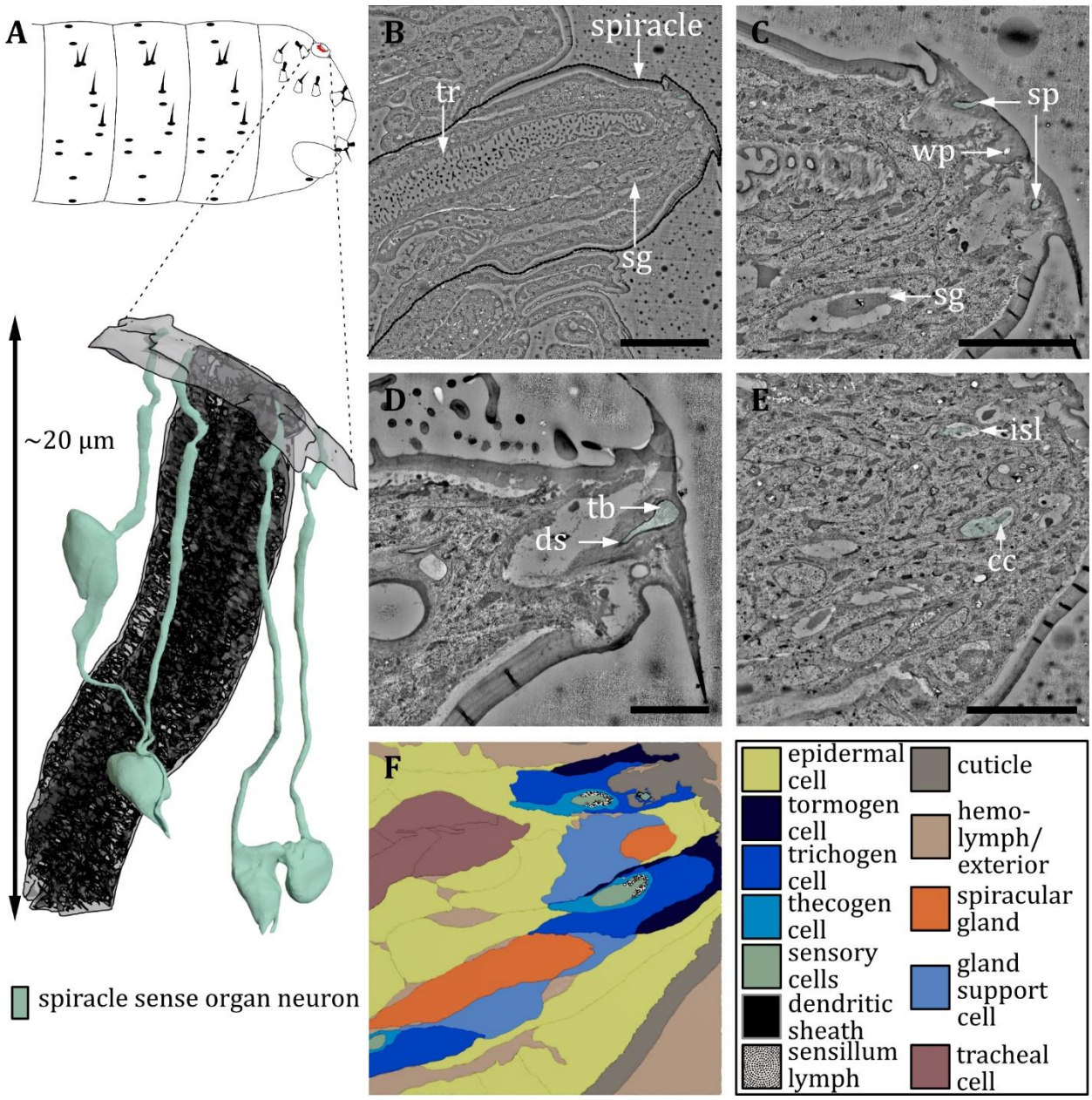
A
B
spiracle
tr
sg
C
sp
wp
sg
~20 µm
D
tb
ds
E
isl
cc
F
spiracle sense organ neuron
epidermal cell
tormogen cell
trichogen cell
thecogen cell
sensory cells
dendritic sheath
sensillum lymph
cuticle
hemo-lymph/ exterior
spiracular gland
gland support cell
tracheal cell

SUPPLEMENTARY FIGURES

Figure S1

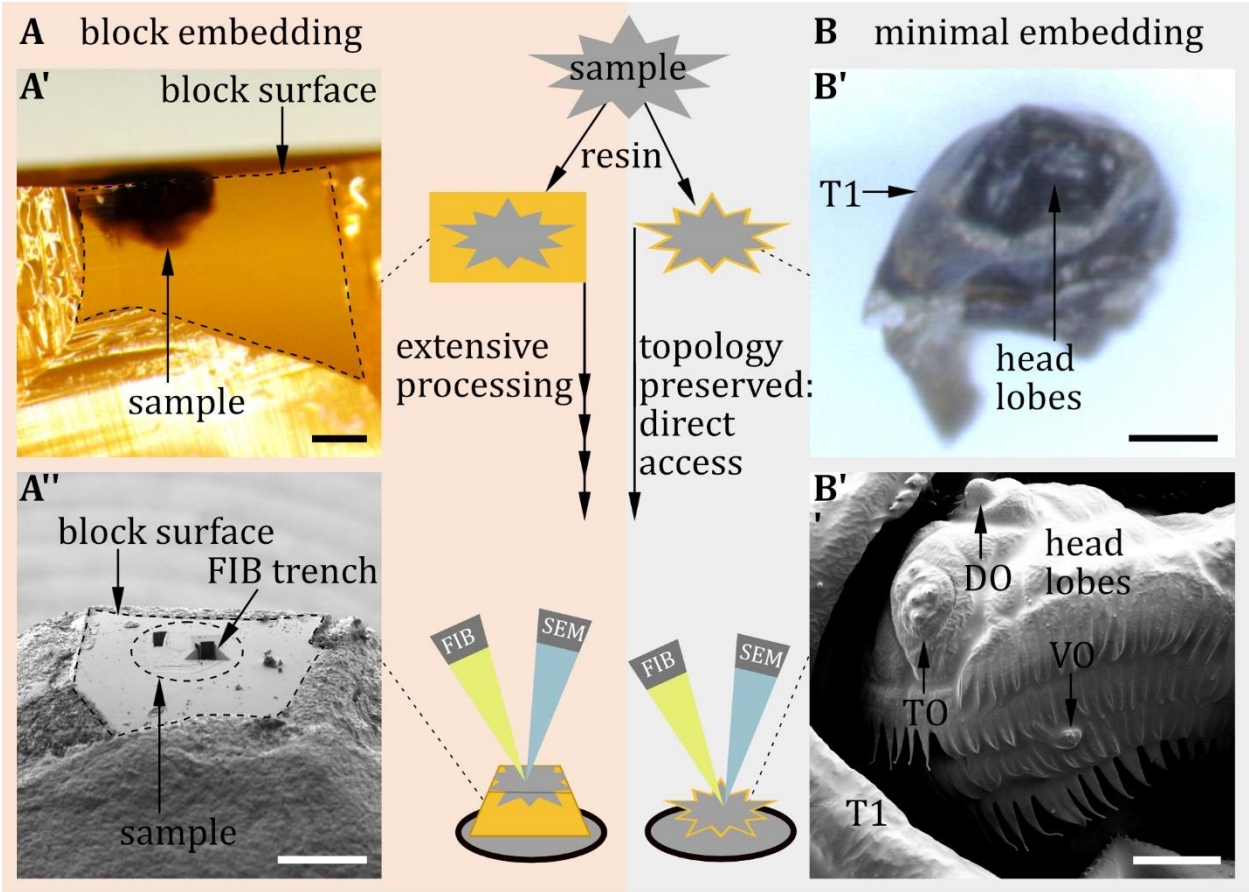

Figure S2

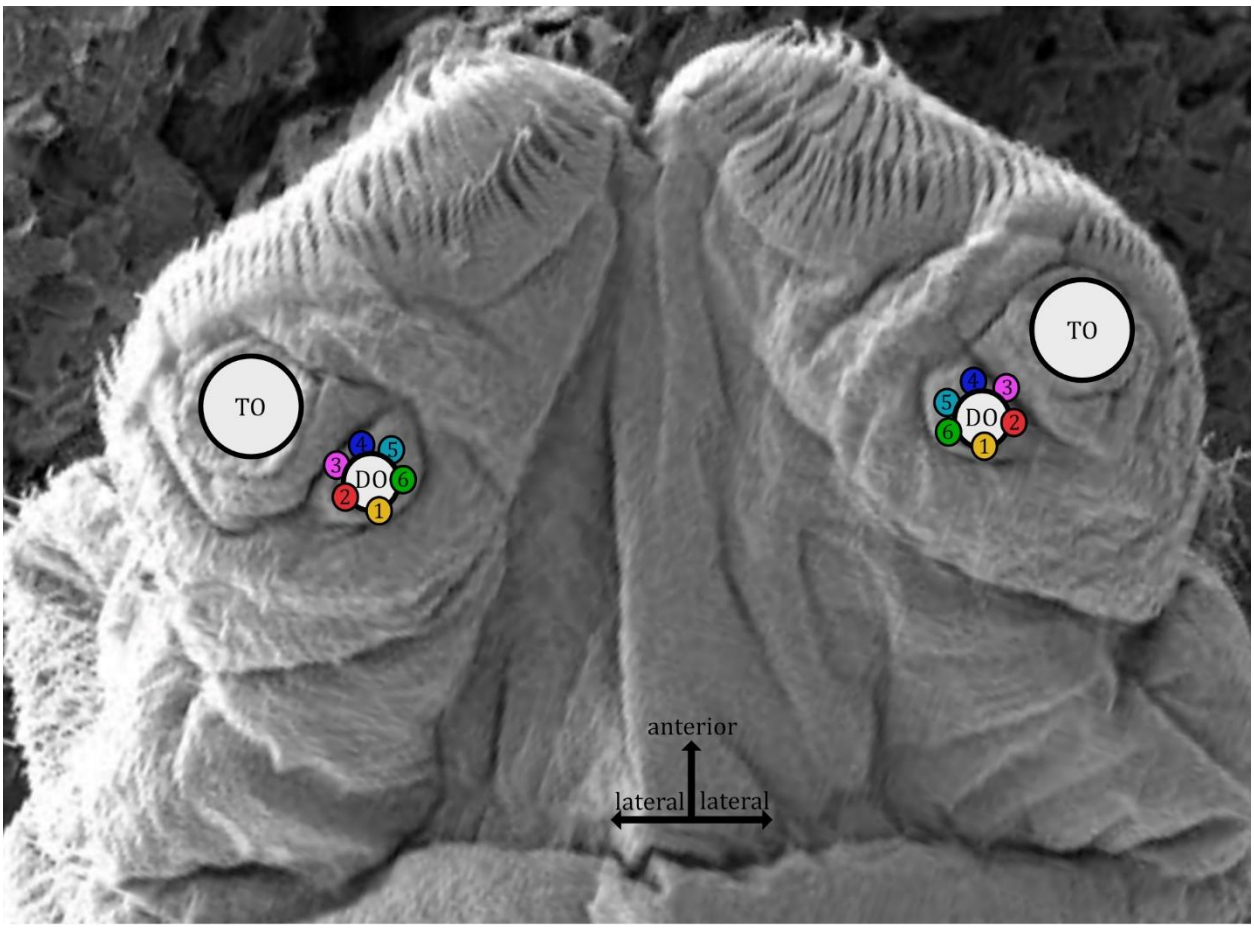

Figure S3

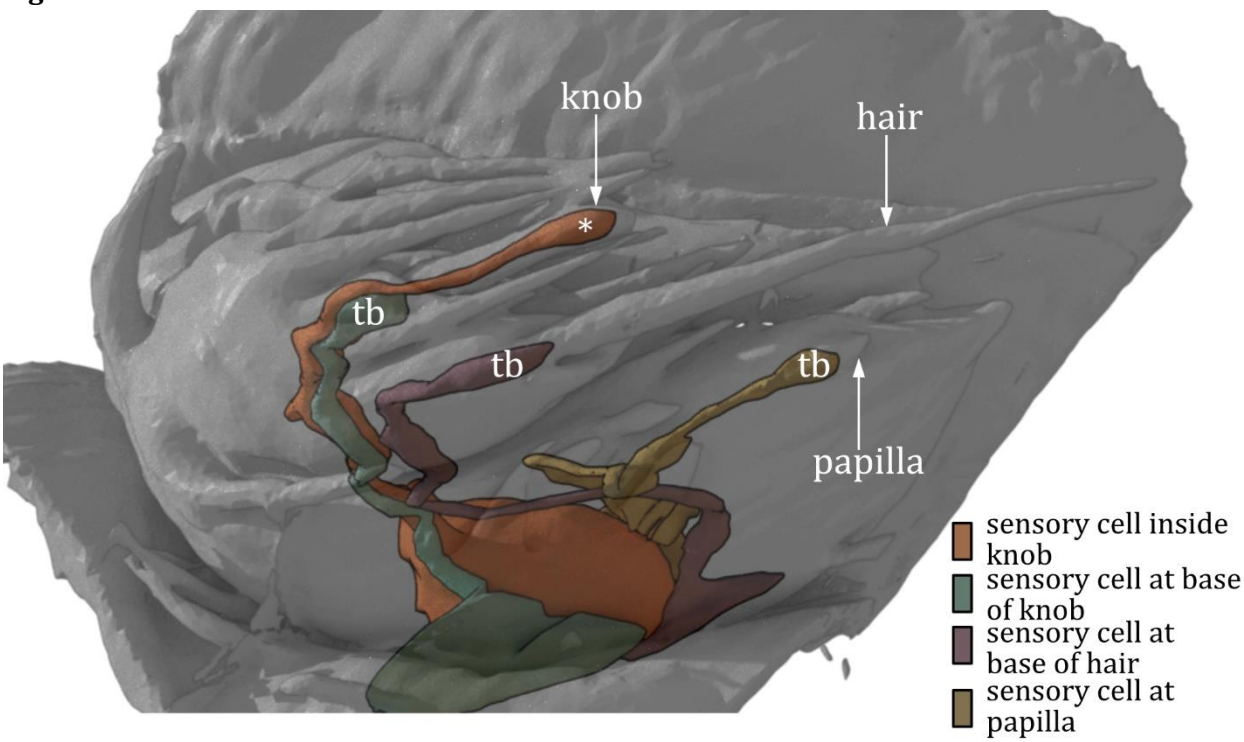
knob
hair
*
tb
tb
tb
papilla
sensory cell inside knob
sensory cell at base of knob
sensory cell at base of hair
sensory cell at papilla
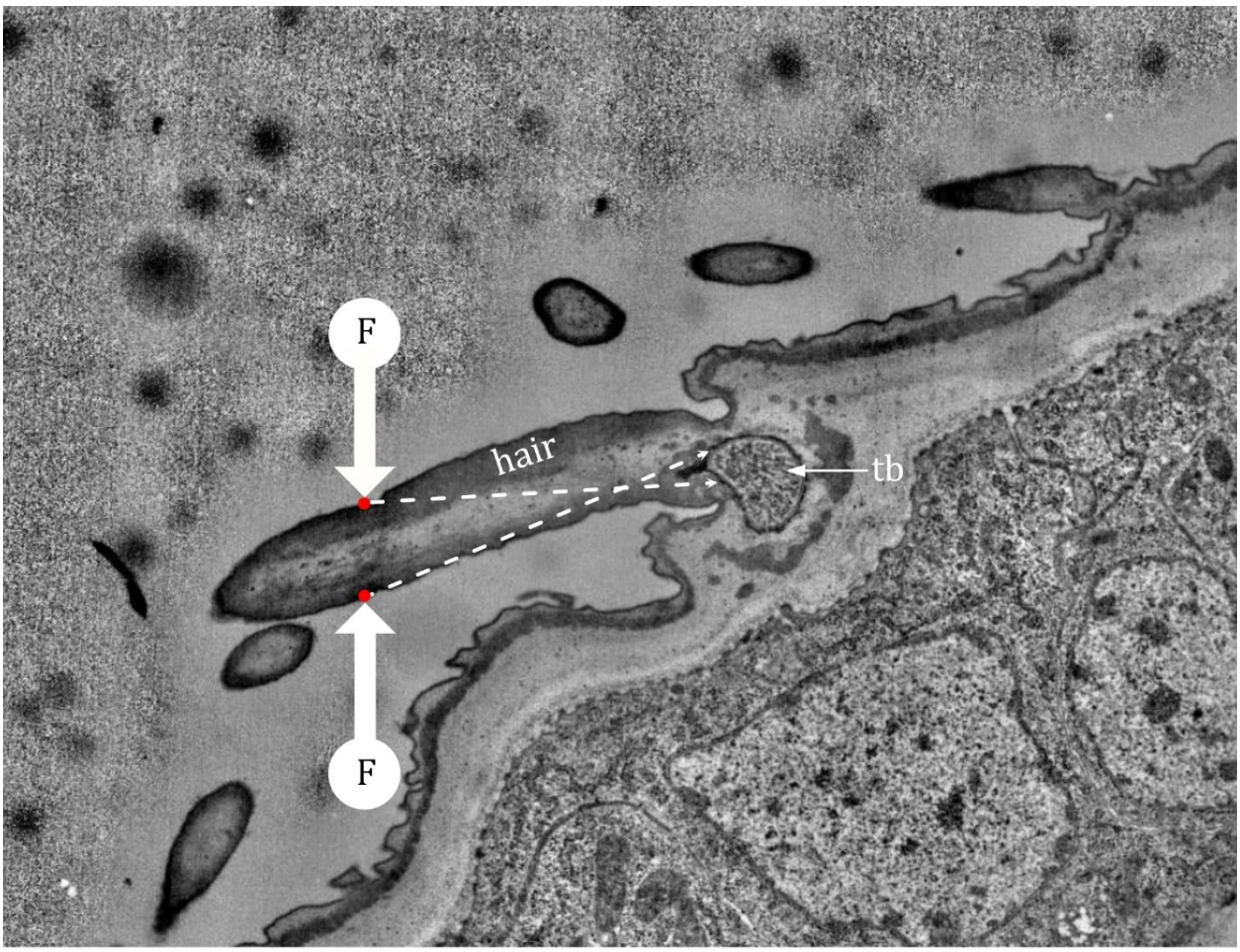
Figure S4